Julia Cancola, BSc

Hydromorphological assessment applied on a stretch on river Sulm

MASTERARBEIT

zur Erlangung des akademischen Grades

Diplom-Ingenieurin

Masterstudium Bauingenieurwissenschaften - Geotechnik und Wasserbau

eingereicht an der

Technischen Universität Graz

Betreuer

Ass.Prof. Dipl.-Ing. Dr.techn. Helmut KNOBLAUCH
Univ.-Prof. Dipl.-Ing. Dr.techn. Gerald ZENZ

Institut für Wasserbau und Wasserwirtschaft

Dipl-Ing. Clemens Dorfmann

Graz, Oktober 2016

EIDESSTATTLICHE ERKLÄRUNG

Ich erkläre an Eides statt, dass ich die vorliegende Arbeit selbstständig verfasst, andere als die angegebenen Quellen/Hilfsmittel nicht benutzt, und die den benutzten Quellen wörtlich und inhaltlich entnommenen Stellen als solche kenntlich gemacht habe. Das in TUGRAZonline hochgeladene Textdokument ist mit der vorliegenden Masterarbeit identisch.

Datum

Unterschrift

Acknowledgement

I am using this opportunity to express my great gratitude to everyone who encouraged me during this master thesis.

I would like to give special thanks to my supervisor Ass.Prof. Dipl.-Ing. Dr.techn. Knoblauch Helmut for guiding and supporting me throughout this master thesis. I also wish to express my gratitude to Dipl.-Ing. Dorfmann Clemens for his great support in numerical modelling.
Special appreciation to the staff of Department of Water Management, Resources and Sustainability of Land Steiermark in particular to Dipl.-Ing. Hornich Rudolf who kindly provided documents and made the treated case study possible.
Moreover, I want to thank all my colleagues, who have accompanied me and the staff of the Institute of Hydraulic Engineering and Water Resource Management for supporting me during my master thesis and in all matters through this master course.

I am very grateful to my family and specially to my parents who enabled my education and all the valuable experiences.
Moreover, I want to thank my three sisters and Stefan who motivated me and supported me in all aspects of life.

Finally, I am grateful to all my friends who were always there for me.

Abstract

The aim of this work is to identify hydromorphological conditions and trends of rivers by applying numerical modelling software. Special focus is set to the preparation processes of the hydrodynamic numerical model (HN-model). It includes calibration and validation of the HN-model and a sensitivity analysis. Lack of time is the reason that in projects little attention is given to these processes. Therefor this master thesis has a special emphasis on this processes. An hydomorphological survey is performed at a river stretch on the river Sulm in south of Styria. In 2000 by order of Land Steiermark a flood protection project downstream of Heimschuh was implemented and several river engineering measurements were applied. Supported by a numerical software called TELEMAC-2d, shear stresses are determined along this stretch and zones are identified according to the predominate dynamic processes. This is done for several discharges with different recurrence intervals. Numerical results together with current conditions determined in several field visits allow a qualitative assessment of hydromorphological conditions and trends.

Contents

1. Introduction

Economic aspects were given a high significance in former river engineering projects. Many rivers in Europe got a tight and hard corset to restrict its natural behaviors in order to support land reclamation or produce energy. The tight and hard corset, usually made of concrete, fulfilled the desire of flood protection. Instead they lead to straight rivers which are poor in vegetation and do not follow natural stream courses anymore. At the time the negative impacts on biological variety, chemical conditions and the rivers dynamic were not predictable.
Nowadays, ecological aspects gain more and more importance and river engineering projects aim for an integrated system that includes flood protection, water ecology and multifunctional use. Many different groups of interest are involved in river engineering projects and promote sustainable riverine zones. [1]
To ensure satisfying conditions of water bodies, the European Water Framework Directive (WFD) was published. The WFD was adopted in 2000 and implemented into national law in 2003 (water rights amendment 2003). The main objectives of the WFD are achieving good chemical and ecological state of water bodies. An ecological state of a water body is mainly described by biological and chemical quality components. Beside these, hydromorphological are non-negligible and have to be considered as well. Especially to achieve high ecological status, chemical, biological and hydromorphological components have to be rated high. Since hydromorphological conditions are a decisive factor for aquatic habitats, hydromorphology plays an indirect role for reaching a good ecological status. [2]

The foundation of this work was laid during a student exchange in 2015 in Portugal where I got the opportunity to deal intensively with bioengineering methods and river hydromorphology.
Additionally, a lecture, held by the institute of Hydraulic Engineering and Water Resources Management of TU Graz, arouses interest in working with numerical models.
This has led to the present master thesis where a numerical model is applied to examine hydromorphological river conditions.

The institute of Hydraulic Engineering and Water Resource Management performs research work in physical and numerical modelling and hence, provides profound knowledge in working with 2d models. In the present work a focus is set in developing and working with a numerical model therefor the department of Water Management, Resources and Sustainability of Land Steiermark kindly supported this work and provided several documents for a case study.

The case study treated in the following document is located in Styria on the river Sulm where a flood protection project was implemented in 2000 and several bio-engineering measures were applied. After completion, a monitoring program performed between 2000 and 2003 by the University of Natural Resources and Life Sciences in Vienna examined hydromorphological changes. This present master thesis presents a resumption of the previous examination by using a 2d numerical model.

2. Principles of river morphology

The following chapter treats the basics of this master thesis. Hydrodynamic numerical models require the input of data. This data and its acquisition is described. Topographical and hydrological data are included as well as surface roughness of the model area. Moreover, sediments and its meaning in river systems are highlighted.

2.1 Hydrology

Hydrology is the science of water, its occurrence, properties and behavior on and underneath the earth surface. Part of water appearing on the surface occurs as discharge. Water is forced by gravity and flows on or beneath the surface. The location of the flow is a matter of infiltration. Different methodologies to measure discharge and its graphical representation are presented below. [1]
In Austria hydrological data is released by the hydrographical service of the federal and the provinces. More than 950 gauging stations are maintained in Austria which supply discharges. In Styria 157 gauging stations are installed, 99 are maintained by the federal and 57 by the province of Styria. Data collection is done by writing stripes, data logger or periodical reading of water level gauges. [3]

2.1.1 Discharge measurement

- Indirect methodology

Indirect methodologies describe measurements of parameters which enable determination of the discharge due to linear relation. Commonly measured parameters are water level and velocity.
Water level measurements are done at installed gauging stations. Therefore, a well accessible location is chosen where measuring of very low up to very high water levels is possible. Preferred locations are natural straight sections where the water level is not influenced by hydropower stations, dam structures or any discharge regulating constructions. Additionally, the measurement profile must not be exposed to erosion or deposition.

In former times gauging stations were usually equipped with periodically reading water level gauges. Nowadays water level gauges are replaced by continuously measuring devices like pneumatic gauges or swimmer gauges. The periodical reading ones are still used as additional device for manual reading.

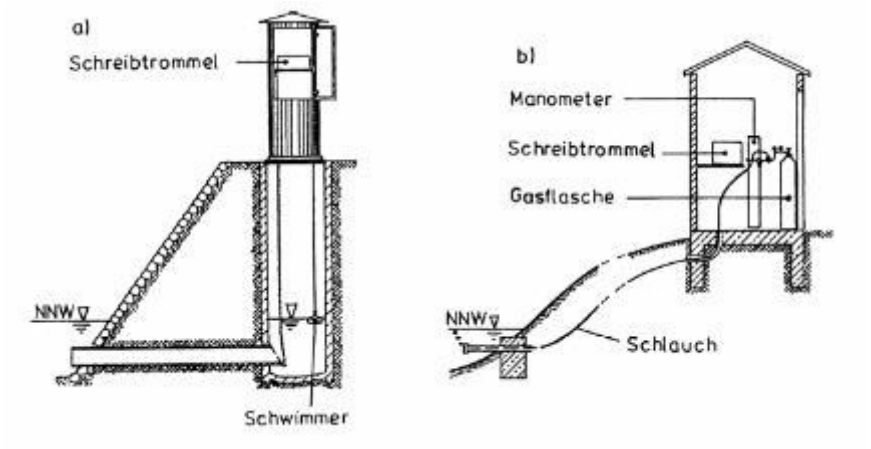

Figure 1 Continuous measuring with (a) swimmer and (b) compressed air [4]

The velocity and discharge area enable the determination of discharge. Therefore, the profile is divided into subareas and a velocity is measured for each of it. A common device to measure velocity is the vane measurement device. An adjustable propeller fixed on a stick is oriented perpendicular to the stream. Measurements may be performed in different water depths. Rotations per second are recorded to determine the velocity. Another method to measure velocity is the Acoustic Doppler Velocimetry (ADV). The measuring principle is based on the Doppler Effect: an acoustic signal is send from the center of the measuring probe, is reflected on particles and absorbed by acoustic receivers (Figure 2). Duration and particle displacement let assume the flow velocity. [5]

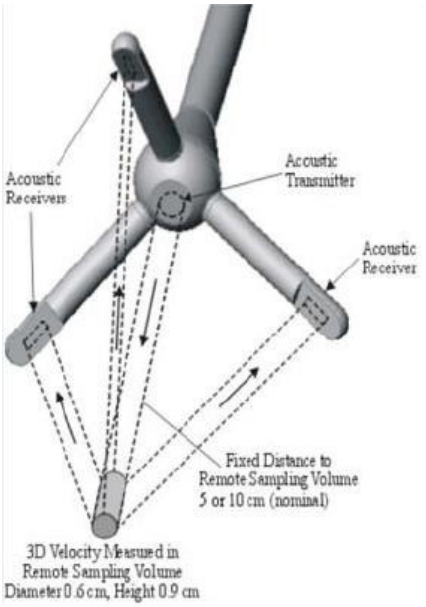

Figure 2 Principle of an Acoustic Doppler Velocimetry [5]

- Direct methodology

Discharge is measured at specific measuring constructions where a defined relation between discharge and water level is known. The upstream water level is measured at artificial profiles. Therefor a calibrated profile like a measuring wire or Venturi flume is used. Volumetric measurement is a seldom-used method mainly used for laboratory applications since it is restricted to small discharges. [6]

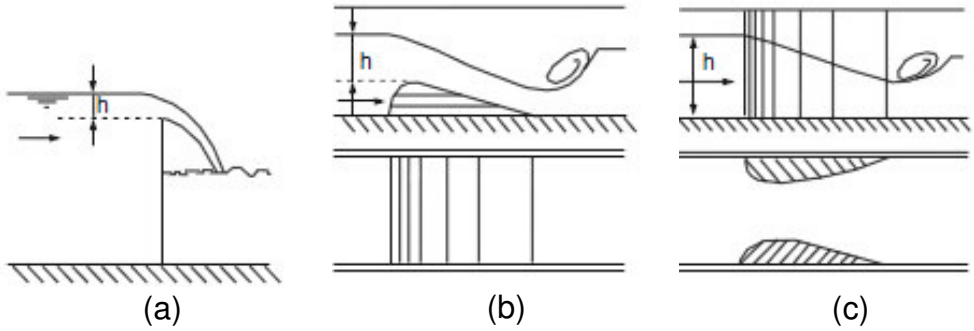

Figure 3 Direct discharge measurement (a) measuring wire (b) Venturi sill (c) Venturi flume [6]

2.1.2 Graphic representation of discharge

- Hydrographs represent the measured discharge at a certain location in its chronological order.

- Flow duration curve represents the discharge sorted by the frequency of occurrence. It shows the time which a flow is equal or exceeds a specified value.
- Rating curves present the relation of water level and discharge at a certain profile. It is an important input data for numerical calculations therefore, it is commonly set as boundary conditions.

Figure 4 presents a hydrograph and its derived duration curve.

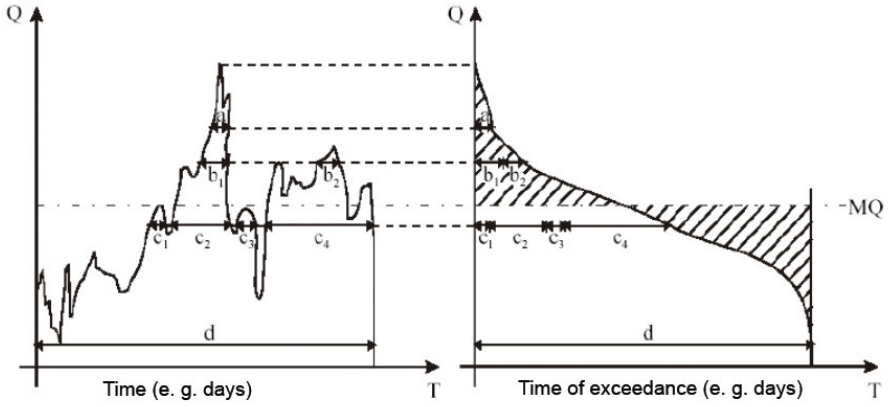

Figure 4 Hydrograph (left) and duration curve (right) [6]

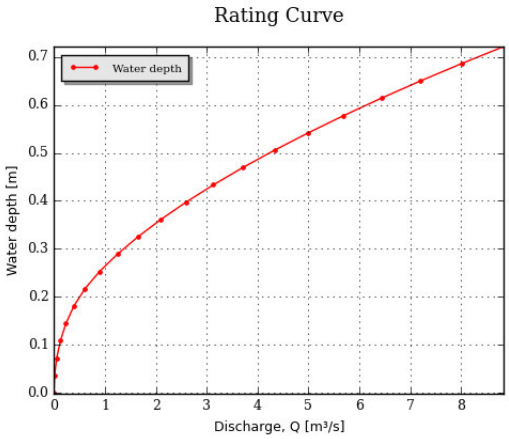

Figure 5 Rating curve in a profile at the river Sulm

- Hydrological main values

Due to constant observation of hydrological parameters, events with certain frequencies are defined. The determination of extreme events is based on statistic

evaluations. Therefore, the observation period should be at least one third of the design time scale. For hydraulic engineers extreme events are of particular importance since they may present the significant load case for hydraulic design. Extreme flow events with its standardized terms are listed in Table 1.

Table 1 Standardized terms for extreme flow events

Shortcut	Notation	Calculation
MQ	Medium flow rate	Mean average of the flow rate in a period
NQ	Low flow rate	Lowest value of the flow rate in a period
HQ	Storm water flow	Highest value of the flow rate in a period
MNQ	Medium low flow rate	Mean average of the lowest values from several similar periods (months, years)
MHQ	Medium storm water flow	Mean average of the highest values from several similar periods (months, years)
NNQ	Lowest low flow rate	Lowest known value (minimum of the low flow)
HHQ	Highest storm water flow	Highest known value (maximum of the high flow)

- Channel forming discharge

Alluvial rivers alter their shape continuously. It is obvious that a higher discharge transports a bigger amount of bed load. This might cause big changes in the channel but occurs too infrequently and thus is not mandatorily the significant event for form changing processes. Decisive for the extent of change are the amount of discharge and its duration. Information about the sequences of discharges is gathered in a hydrograph. However, considering natural sequences of discharges over a long period requires a huge amount of data and would be an enormous computational effort. This is the reason why a steady discharge was defined which produces the same change in a channel as the natural sequence of discharges does. This so-called channel forming discharge makes it easier to determine the sediment transport over a long period.

There are three common methodologies to determine the channel forming discharge:

- Bank full discharge describes the discharge, which fills the channel to the top of its banks.
- Flow of a given recurrence interval. Hence, a recurrence interval between two and five years is usually assumed.
- Effective discharge mobilizes the largest amount of sediments over its time of occurrence.

[7]

2.2 Morphologic channel characteristics

A channel in equilibrium over the decadal time scale is typically defined as a dynamic channel whose morphologic characteristics do not significantly change despite possible alterations in channel position. [8]
Morphological characteristics depend on dynamic processes and change with time and space. Sediment transport on a certain location is the result of catchment wide processes. From the temporal point one distinguishes short-term changings due to extreme events and long-term trends. For an overall assessment of sediment balance in a river system different spatial scales are distinguished. Each of them have characteristic processes and form of appearance.

2.2.1 Dynamic channel- processes

The processes, which are erosion, transportation and deposition are driven by the channel slope. They vary their intensity along the channel. The destructive process which solves small particles and sediments from the surface is called erosion and can be evoked due to chemical, physical and biological impacts. Erosion is followed by transportation and furthermore by deposition. A resting particle is prone to another deformation; hence, it can be transported again. Erosion leads to a sinking water level and ground water level in the adjacent area of the channel, while sedimentation does the opposite. [1]

2.2.2 Physical appearance of channels

The shape of a channel is formed by dynamic processes and alters from its spring to the river mouth. Profile shapes, longitudinal and plan view shapes are related to each other.

Three zones can be observed in longitudinal direction. These zones differ mainly in steepness and in morphological processes. The zone of headwater is the most up situated and steepest part along a longitudinal cut of a channel. In this case the channel is more or less straight. The capacity for sediment transport is higher than the sediment support, which leads to deep and narrow valleys. The adjacent and flatter zone is called transfer zone. In this zone deposit and erosion are almost equilibrated. The channel starts to meander, the deposition zone is situated in the lowland. Since the slope is minimal, the current tractive force decreases and causes deposition. The channel start branching.

Two characteristic profiles occur along the channel: profiles with constant water depth which are in straight sections and between bends, and unsymmetrical profiles which primarily appear in bends. The shallow zones in the transition area between bends are called fords. The unsymmetrical profile shows a deeper part in the outer side of the bend and shallow zones in the inner side. Deep zones are named scour and arise as a result of secondary currents. Erosion forms cut banks at the outside of the bend and point bars at the inside of the bend. Figure 6 and Figure 7 show the connection between the physical characteristics in a channel. [1]

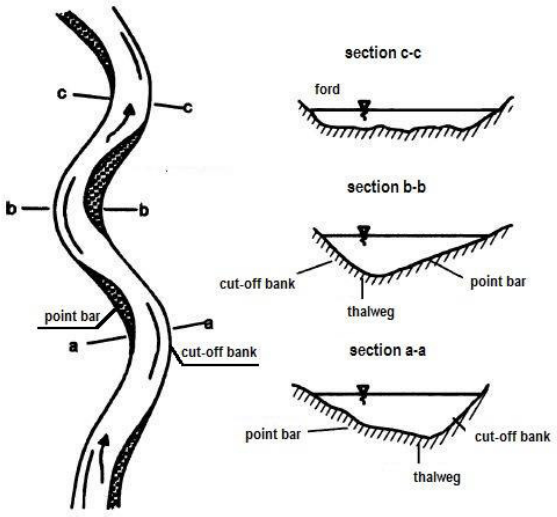

Figure 6 Plan view linked with cross section [6]

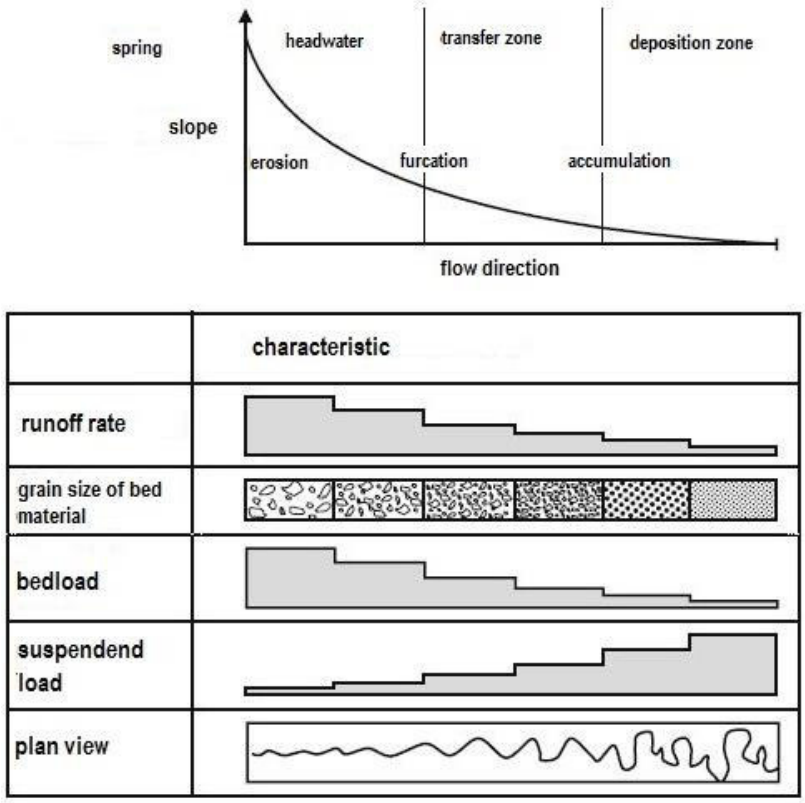

Figure 7 Altering abiotic features along a river [6]

2.2.3 Measure topography

Terrestrial surveys, laser scan or photogrammetric surveys are the common methods to acquire the visual appearance of data. Laser scan surveys provide a dense data mesh and large scale measurements can be easily made. Additional terrestrial supplements are not necessary. Terrestrial surveys usually do not deliver detailed information. Their data volume is less than the one of laser scan surveys since only required objects are measured, where large-scale surveys are more cost and time intensive. Terrestrial surveys can be combined with Hydro acoustic methods. Hydro acoustic surveys measure profiles within the channel while additional terrestrial surveys acquire foreland and bank topography. Photogrammetric surveys are no that common anymore.

2.2.4 Resistance of channel

The channel presents resistance against the acting forces of flowing water. Resistance is displayed by a resistance coefficient. The coefficient has to be chosen

carefully since it has an enormous influence on the precision of a calculation. The resistance of a channel is the summation of different partial resistances including bank resistance, bed resistance and resistance due to other factors as curvature or vegetation. The influences of the latter one is relatively unexplored. Bed resistance is subdivided in form drag, grain resistance and resistance due to scour or sedimentation and vegetation. (Figure 8)

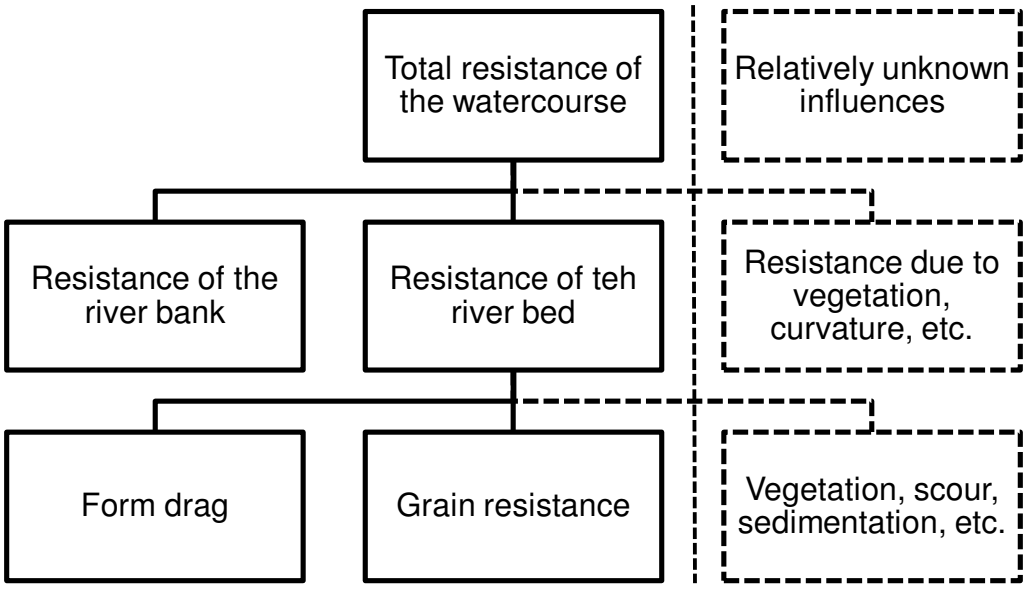

Figure 8 Resistance of a channel [1]

Assessment of the resistance requires field visits or orthophotos. It has to be considered that resistance may alter due to vegetation periods and is expressed as roughness.

A commonly used value is the Strickler value k_{st}. It is used in the empirical flow equation of Manning-Strickler and describes the resistance of the whole cross section. [1] Beside k_{st} other empirical values as de Chézy coefficient C or Mannings value n ($k_{st}=1/n$) exist. [9]

Another value is the resistance coefficient λ which is used in the formula of Darcy-Weißbach. It is derived from the Colebrook-White formula which is originally used for rough pipe flow. The advantage of λ is the possibility of interaction of several partial resistances. This is now used in case of k_{st}. [1]

$$\frac{1}{\lambda} = -2\log\left(\frac{2{,}51}{Re\sqrt{\lambda}} + \frac{k_s}{3{,}71R_{hy}}\right) \quad (1)$$

Where

ks is the equivalent sand grain roughness

Re is the Reynolds Number

R_{hy} is the hydraulic diameter

The equivalent sand roughness k_S is a function of characteristic grain size diameter and considers the bedding of the sediments as well. According to GARBRECHT k_{St} is obtained from k_S as followed. [9]

$$k_{St} = \frac{26}{k_s^{1/6}} \tag{2}$$

Some standard values are given in Table 2.

Table 2 Roughness coefficients [9]

Type of surface	$\boldsymbol{k_{St} = \frac{1}{n}}$ $[\boldsymbol{m^{\frac{1}{3}}/s}]$	$\boldsymbol{k_S}$ $[\boldsymbol{mm}]$
Flat bottom, sand, gravel	30-45	5-20
Flat bottom, rough gravel	25-30	60-200
Bottom with ripple	20-30	h_{ripple}
Field of groynes	10	
Mounted river bank	20-35	15-300
Smooth channel wall	40-70	1-10
Rough channel wall	30-40	20-100
Foreland, acre	20-30	20-250
Foreland, grassland	15-25	100-350
Foreland, vegetation	5-15	130-400
Built-up areas	5-10	
Sealed areas	40-70	1-10
Water surfaces	40-70	(1-5)

2.2.5 Sediments

The transported sediments in the channel are called the total bed load. It is divided in material, which stems from the river bed (bed material load) and from the catchment area (wash load). Bed material is the result of river erosion, while wash load is the result of land erosion in the catchment. The amount of bed material load increases rapidly with increased velocity. Bed material load occurs as bed load or suspended load. However, there is no significant passage between these two types of transport. Figure 9 gives an overview of the mentioned parts of total bed load.

Bed load presents the total load, which is transported on or directly above the channel bed. Depending on the particle size and weight it is transported by traction or saltation on the bottom. Bed load is not continuously in suspension or solution. [10]

Suspended load is carried within the water by turbulent flow. Usually the particles size is very small, comparable with the size of silt or clay. The transport velocity is more or less equal to the flow velocity. [11]

<table>
<tr><th rowspan="2">Grain size [mm]</th><th rowspan="2">Component of sediment</th><th colspan="3">Type of load</th></tr>
<tr><th>general</th><th>special</th><th>total</th></tr>
<tr><td>Clay and silt
< 0.063</td><td>Fine suspended load</td><td rowspan="2">Suspended load</td><td>Wash load</td><td rowspan="4">Total sediment load</td></tr>
<tr><td>Sand
0.063 - 2</td><td>Suspended sand</td><td rowspan="3">Channel forming load</td></tr>
<tr><td>Gravel
2 - 63</td><td rowspan="2">Bed load</td><td rowspan="2">Bed load</td></tr>
<tr><td>Stone
> 63</td></tr>
</table>

Figure 9 Total bed load and its classifications [11]

- Sediment determination

Determination of grain size distribution requires extraction of a sample. The sampling point is either the substratum or the top layer or a combination of both. The

sampling material can be taken in a line or from one point. Moreover, the material can be extracted according to its volume or distributed over an area.
A common method to determine the grain size distribution is sieving. Several sieves with a standardized mesh sizes are placed above each other. The sieves are shaken over a certain time and the remaining amount of material on each sieve is weighted. The process of sieving is standardized in DIN 18123.
Another method is the so-called line pebble counting. It enables the characterization of the top layer. Stones with a diameter bigger than 1cm are measured. Therefor a string is stretched on the bank parallel to the river bed and stones underneath this string are collected and measured on its b-length. The b-length is the width of a stone. The graphic representation for it is given in Figure 10.

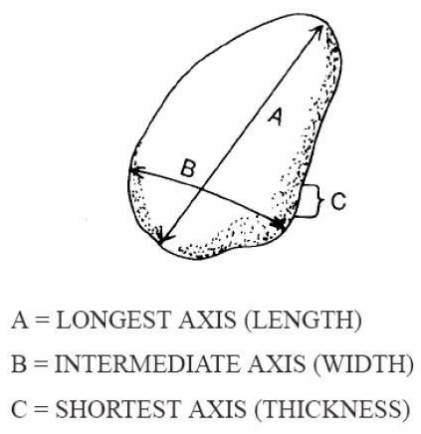

Figure 10 Dimension of a stone [12]

Stones are assigned to grain-size classes and their number counted. For a representative result a minimum of 150 stones with a minimum of 30 stones in the middle class has to be measured. Afterwards the obtained grain size distribution is converted to a weight volume analysis, which is required to subsequently determine the fine part of the bed load. The combination with the Fuller line makes it possible to gain information about the substratum. Other methods are the random walk method or the evaluation by photographs. [11] [12]

2.2.6 Incipient motion

The incipient motion describes the moment when particles of soil material start to move. Incipient motion can be expressed mathematically therefore different empirical theories are used. The following parameters describe initial motion.

- Critical velocity u_{cr}
- Critical shear stress τ_{crit}
- Critical water depth h_{cr}
- Critical slope I_{cr}
- Critical discharge Q_{cr}

Basic data for determining this value are the grain size of the soil, which is exposed to the current. A characteristic grain diameter d_{ch} is taken, which corresponds to d_{90}, the 90-percent-through diameter.

- Critical velocity u_{cr}

HJULSTRÖM (1935) did an empirical approach and described incipient motion with critical velocity. The HJULSTRÖM diagram (Figure 11) considers average flow velocity u_m and particle size d_m and presents the transition between resting particles and particles in motion. The HJULSTRÖM curve is valid for streams with a flat slope as well as for a water depth bigger than $1.0m$. Viscosity, water depth and surface roughness are not taken into account thus it is more used to work with Shields approach of a critical shear stress. Since incipient motion is afflicted with some uncertainties, the HJULSTRÖM curve presents a range of possible critical velocities. [1]

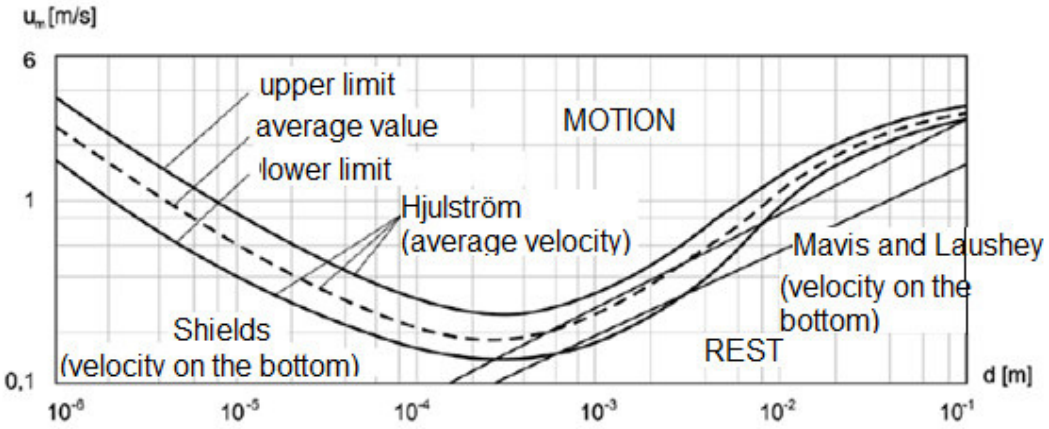

Figure 11 Incipient motion according to HJULSTRÖM [13]

ZANKE (2002) shows an empirical approach which brings values close to HJULSTRÖM. The formula is valid for water depths ranges between $0.7m$ and $2.0m$.

$$v_{cr} = \alpha \left[\sqrt{\rho' g d} + 5{,}25 \frac{v}{d} c \right] \tag{3}$$

Where

v_{cr} is the critical velocity when a particle starts to move [m/s]

α is a coefficient which considers the upper and lower level of the range and is between 1,5 and 2,8

ρ' is the relative sediment density [-]

g is the force of gravity [m/s^2]

v is the viscosity of water [m^2/s]

d is the characteristic grain size diameter [m]

c is a coefficient that considers the cohesion of the soil (for sand it is 1.0)

- Critical shear-stress τ_{crit} according to SHIELDS (1936)

The SHIELDS approach is based on several laboratory tests and is valid for different grain size diameters, shape and density of uniform grain size distribution and flat channel bed. It considers water depth, roughness of the surface but does not include the uplift forces. SHIELDS established a relation of a sediment Froude number Fr^* and a sediment Reynolds number Re^*. Re^* is the relation between grain diameter and thickness of the laminar sublayer. ZANKE (1990) extended

the so-called SHIELDS curve by R which describes the probability of motion. Input data for the diagram depicted in Figure 12 are Re^*, Fr^* and the sedimentological grain size diameter D^*. [1]

$$Re^* = \frac{d_{ch}}{\nu} u_0^* \tag{4}$$

$$\mathrm{Fr}^* = \frac{\mathrm{u}_0^{*2}}{\rho' g d_{\mathrm{m}}} \tag{5}$$

$$D^* = \left(\frac{\rho' g}{\nu^2}\right)^{1/3} d_{ch} = \left(\frac{Re^{*2}}{Fr^*}\right)^{1/3} \tag{6}$$

$$\rho' = \frac{\rho_S - \rho_W}{\rho_W} \tag{7}$$

$$u_0^* = \sqrt{\frac{\tau_0}{\rho_W}} \tag{8}$$

$$\tau_0 = \rho_W g R I \tag{9}$$

Where:

Fr^* is the sediment Froude number [-]

Re^* is the sediment Reynolds number [-]

d_{m} is the characteristic grain size diameter [m]

ν is the kinematic viscosity [m^2/s]

ρ' is the relative sediment density [-]

ρ_W is the water density [kg/m^3]

ρ_S is the sediment density [kg/m^3]

u_0^* is the friction velocity [m/s]

τ_0 is the shear stress [m^2/s]

g is the acceleration due to gravity [m^2/s^2]

R is the hydraulic radius [m]

I is the energy gradient [-]

Friction velocity is not a real velocity since it presents the resistance of the channel bed. The SHIELDS curve is valid starting from $d_m \sim 0.05mm$. For hydraulically rough conditions (Re^*>300) only compressive forces are relevant and Fr^* and Re^* do not depend on each other. In this case incipient motion is a matter of shape resistance. In hydraulic smooth conditions (Re^*<2) forces due to viscosity dominate (Fr^*~0,1/Re^*). In practice one is talking about rough conditions if $Re^*$is bigger than 70.

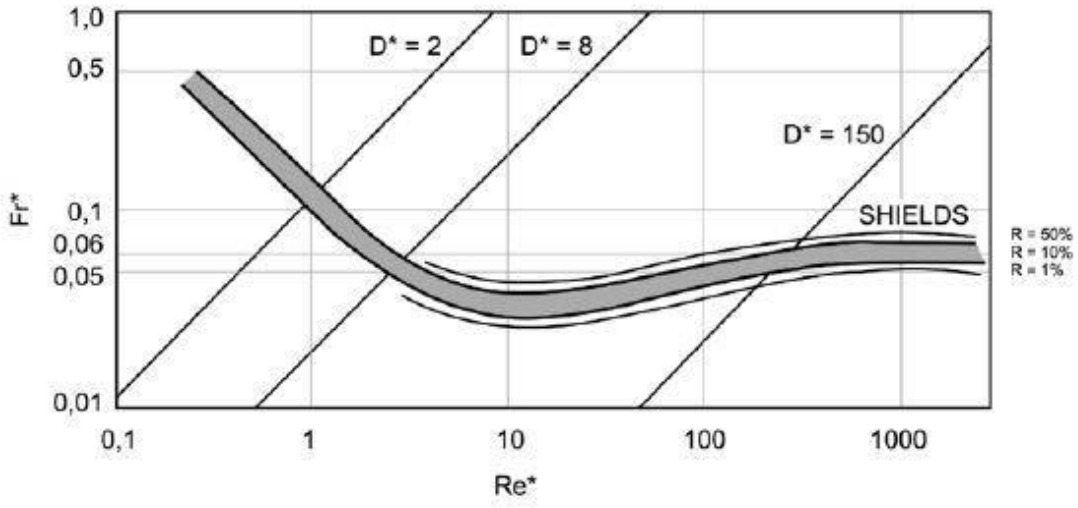

Figure 12 Shields curve including the possibility of motion (R) [1]

Furthermore, SHIELDS defines the critical shear stress τ_{crit}. It describes the necessary shear stress to move a particle which was not in motion before. According to SHIELDS τ_{crit} is given as followed.

$$\tau_{crit} = \theta_{crit}(\rho_s - \rho_W)gd_m \tag{10}$$

θ_{crit} is the non-dimensional critical Shields-parameter which is a function of sediment Reynolds number *Re** and thus considers the influence of smooth or rough turbulent flow conditions. Usual values for θ_{crit} are between 0.05 and 0.06. MEYER-PETER-MÜLLER recommends a value of 0.047. [11] The effective grain size diameter d_m defines the arithmetic average and is obtained as follows. [14]

$$d_m = \frac{\sum d_k p_{b,k}}{\sum p_{b,k}} \tag{11}$$

Where

d_k is the grains size diameter

$p_{b,k}$ is the fraction of a particle size group in percentage

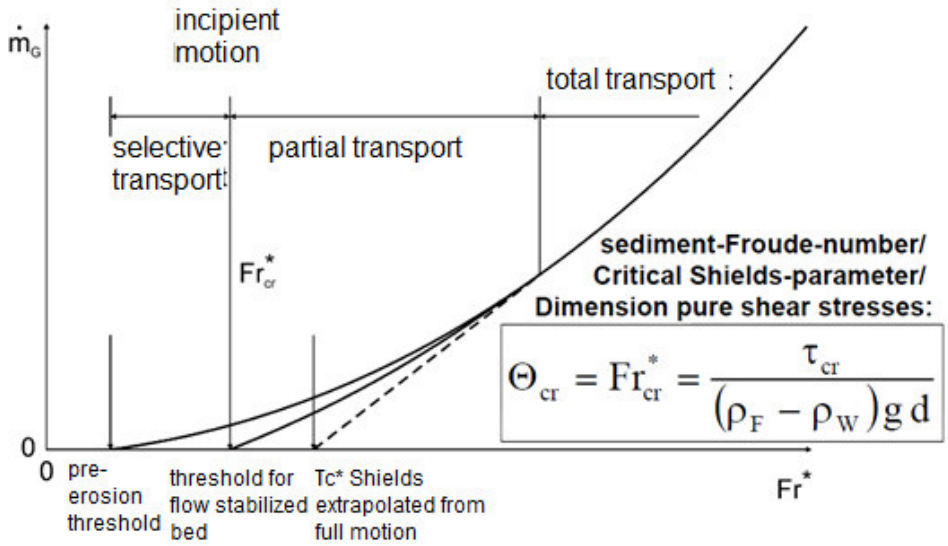

Figure 13 Critical Shields parameter for hydraulically rough conditions [11]

2.2.7 Suspended load and bed load

Although several approaches are existing, there are no strict delimitations of suspended load and bed load. Especially close to the surface it is difficult to make a clear distinction.

- BURZ (1964) made several samplings on Bavarian rivers and found out that 90% of the suspended load is smaller than $0.2mm$.
- KRESSER (1964) determined a Froude number for a critical grain size diameter d_{ch} and an average velocity v_m.

$$Fr^2 = \frac{v_m^2}{d_{ch}\, g} = 360 \tag{12}$$

- ROUSE developed the so-called suspended load number z, also known as Rouse number.

$$z = \frac{v_s}{\beta\, \kappa\, v_0^*} \tag{13}$$

Where

v_0^* is the friction velocity

v_s is the sinking velocity

β is a constant parameter which considers eddy viscosity and eddy diffusivity

κ is the Kármán´s constant which describes the velocity profile

Assuming the product of the parameter κ and β is 0.4 , RAUDKIVI (1982) defined three characteristic areas:

$\mathbf{15 > z > 5}$ → bed load

$5 > z > 1{,}5$ → transition zone

$2 > z > 0$ →suspension

- ENGELUND (1965) did similar analysis and found out that a particle is transported suspended as long as the friction velocity is at least 25% of the sinking velocity ($v_0^* = 0{,}25\ v_s$). This gives a Rouse number of $z < 10$.
- ZANKE (1982) defines $z < 6.25$ as the threshold for suspended transport. [11]

2.2.8 Bed load transport

For determining the bed load transport rate many approaches exist. The engineer´s task is applying an appropriate formula, which describes present conditions as good as possible. The following approach is commonly used in central Europe.

MEYER-PETER AND MÜLLER (1948) developed a formula to describe the bed load transport rate M_G considering the channel roughness. For the critical shear stress Meyer-Peter and Müller assume $\theta_{crit} =$ 0.047.

$$M_G = \frac{\rho_S}{\rho_S - \rho_W}\frac{8}{g}\sqrt{\frac{1}{\rho_W}}\ (\rho_W g \mu I R - 0{,}047\rho' \rho_W g d_m)^{3/2} \qquad (14)$$

It is based on experimental data and is used for coarse sediments and rough riverbeds. It is valid for slopes up to 2%, grain size diameter between 0.4mm and 29mm and an average velocity between 0.37 m/s and 2.87 m/s. The transport rate is a function of a constant and the difference of the current shear stress τ_0 and the critical shear stress τ_{crit}. If the current shear stress is below the critical shear stress, no bed load transport occurs. [1]

$\boldsymbol{\tau_0 \leq \tau_{crit}}$ → no transport

$\tau_0 = \tau_{crit}$ → Incipient motion

$\tau_0 \leq \tau_{crit}$ → transport

3. River training measures

The following chapter treats which measures applied by river engineers. Moreover, their field of application and hydraulically effects are mentioned.

3.1 Channel protection techniques

River training measures are applied to protect riverbanks and -beds against erosion and support or avoid sedimentation. Therefor two types of materials are distinguished: Living materials includes seeds, plants, seedlings and shoot forming woody plants. While dead materials are for example stones, concrete, steel or geotextiles

Living and dead materials are used in several techniques in combination or by itself.

From the ecological point of view dead material should be avoided, but especially in urban areas where space is limited hard installations are preferred.

Techniques with living materials have a positive effect on ecological conditions but are less resistant than hard installations. Especially shortly after installation living materials are not reliable since they need time to develop. This is why a combination of hard installations and living materials often cannot be prevented. Bioengineering methods combine the advantages of both materials and present a close-to-nature construction method.

3.1.1 Longitudinal structures

The techniques listed below usually come in combination with sowing, planting of reeds or wooden plants. The roots of plants present a planar erosion protection of banks.

- Tree spur

Tree spur consists of felling conifers, which are located along the river bank to protect affected banks. Conifers with quite dense needles are fixed to the trunk with help of a steel rope, pile anchors the rope to the river bank. The top of the

tree points downstream. The rough surface of the tree creates decreased velocity and deposition of sediments.

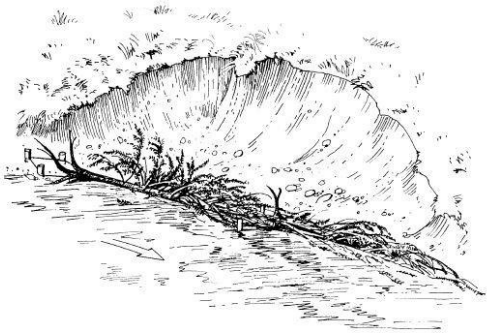

Figure 14 Affected river bank protected by a tree spur [1]

- Fascines

Fascines are bundles made of willow twigs or stones. They are linear elements placed parallel to the riverbank behind each other. They are mainly used to protect the bank against erosion or support the toe of the bank.

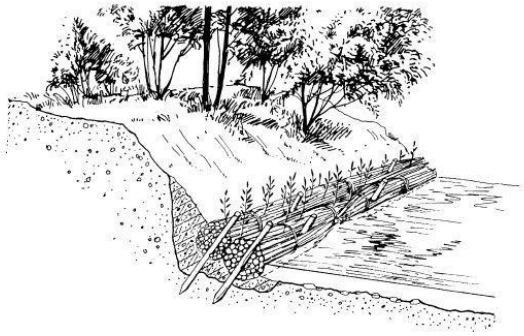

Figure 15 Willow fascine [1]

- Wattle fences

Wattle fences are used to support deposition close to the river bank. Moreover, they are used to protect the toe of a riverbank and are usually applied in shallow depths and rivers with low bed load discharge.

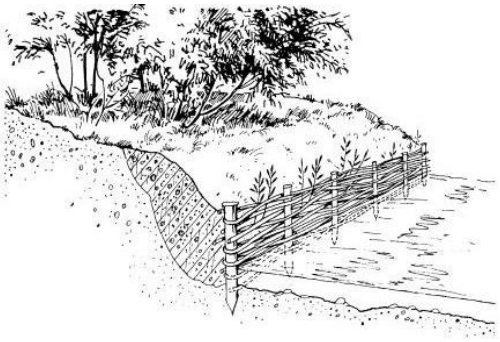

Figure 16 - Backfilled wattle fence [1]

- Willow brush layer

Willow brush layers are a common technique to stabilize steep slopes. They are also applicable for slopes made of coarse material.

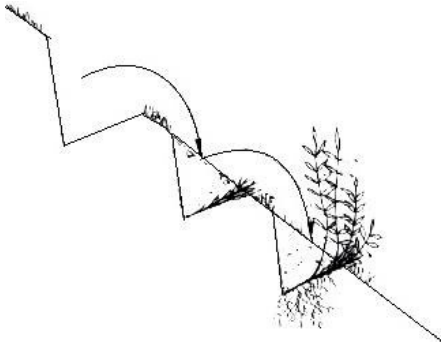

Figure 17 Willow brush layers [1]

- Rip-rap

Stones are the most important representatives of dead material or hard supporting techniques. Usually they are used when living material does not withstand occurring stresses or space is limited. Attention should be paid on the way stones are embedded in the bank. Moreover, washing out of the bed must be prohibited.

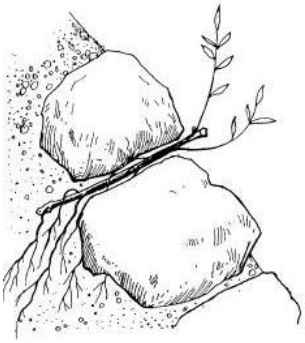

Figure 18 Willow cuttings combined with rip-rap [1]

- Wooden crib wall

Round timber is placed alternatingly parallel and normal to the channel. The space between is filled and may get planted. Wooden crib walls are used for steep banks.

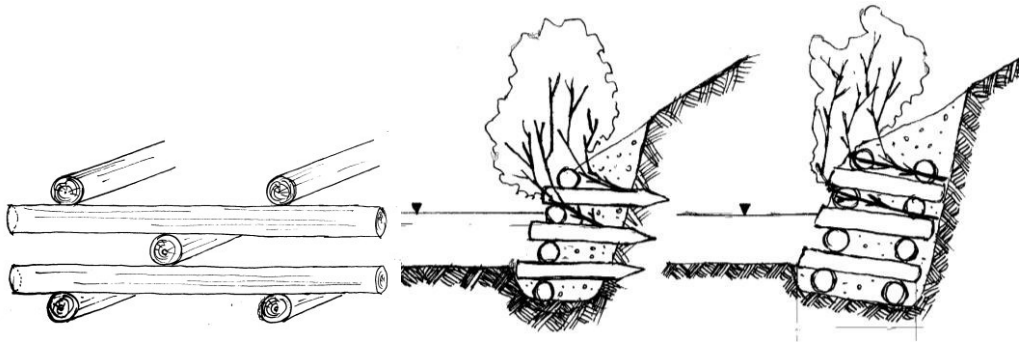

Figure 19 Wooden crib wall [15]

3.1.2 Transversal structures

- Groynes

In order to protect river banks against erosion groynes are used. They are installed at the river bank point to the center of the river hence, redirect the stream. They are used to protect the riverbank against erosion. Due to narrowing the channel, water depth increases and thus shear stresses increases too. The effect differs according to their orientation and the amount of overflowing water.

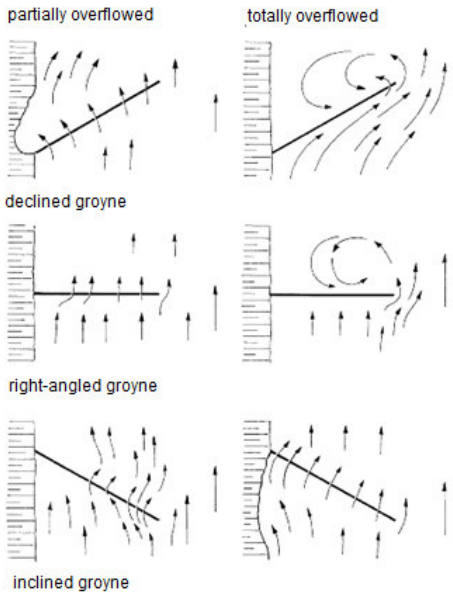

Figure 20 Groynes and their spatial arrangement in the channel [1]

– Bottom structures

Bottom structures prevent degradation of the channel bed. Energy dissipation occurs in the zone of flow transition, ideally on the mounted channel bed or downstream of the structure in a stilling basin. Degradation mainly occurs in straight sections with steep slopes where widening of the channel is restricted. High shear stresses occur and the channel is getting deeper. Depending on the hydraulic behavior of the structure sills and bed steps can be distinguished. If the transition of flow occurs at the construction one is talking about a bed step otherwise it is names sill.

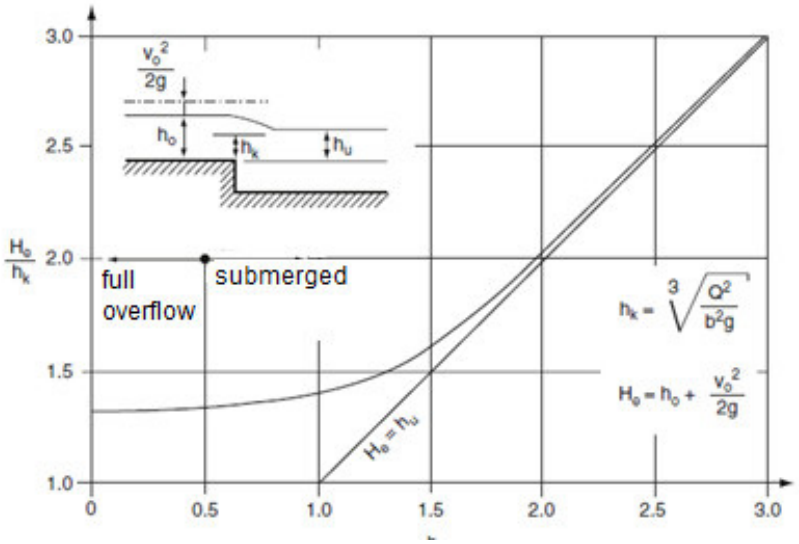

Figure 21 Influence of tail water to head water – relation between relative tail water height h_u/h_k and relative energy height H_e/h_k [6]

Figure 21 presents the influence of tail water to the water level in head water in an rectangular cross section in case of an incomplete overflow. The index u stands for tail water, o for head water and k for the critical value.. If the relative tail water height h_u/h_k is below the threshold, head water gets influenced due to increased relative energy height H_e/h_k. An increasing tail water is influencing more and more the head water. This might be caused by an increased discharge, alteration of roughness or channel slope. To ensure a structure is hydraulically effective, the relative tail water height should be below 1.0. Another possibility for energy dissipation is using river bottom ramps or or block ramps. For dimensioning of river bottom ramps and block ramps the slope and the discharge are decisive. [6]

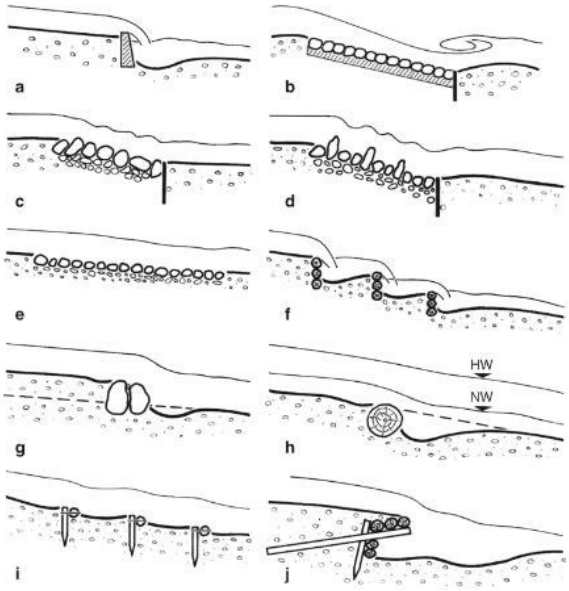

Figure 22 Bed supporting structures [6]

3.1.3 Channel widening

Channel widening is done to promote sedimentation. Due to a wider channel the water depth decreases and the stresses as well. This leads to increased transport capacity. Attention has to be put on the downstream end of the widened channel where the channel bed becomes narrow. This part prone to erosion and has to be protected, if necessary.

4. Numerical modelling

A numerical model is a simplified mathematical copy of a real system and its processes. In hydraulic engineering, numerical models are used to recreate steady or transient flow phenomena and subsequently put it into graphs. Examples for common fields of application are determination of retention effects, wave calculations or determination of hydraulic impacts of river training measures. Concerning the spatial characteristics, hydrodynamic-numerical models (HN-models) are divided into one-, two- and three-dimensional models.
Nowadays, in river engineering one- and two-dimensional hydrodynamic simulations are commonly used. Which system is applied is a question of available data and of the problem that has to be solved. Additionally, it is a question whether neglecting of processes is acceptable or not. One-dimensional calculations only consider processes in x-direction (main flow direction) and deliver the mean velocity of a profile. This fact may give inaccurate results for heavily meandering rivers or problems such as flooding. Therefore, two-dimensional calculations are more precise for such kind of problems since they consider lateral processes and show mean velocity over depth. Three-dimensional models record spatial distribution of al quantities.

4.1 Hydrodynamic principles

Numerical calculations consist of conservation of mass and momentum in a defined system.
Conservation of mass and momentum is expressed by equation of continuity and the Navier-Stokes equation.

- Navier-Stokes equation

$$\underbrace{\frac{\partial u_i}{\partial t}}_{\text{local \& convective acceleration}} + \underbrace{u_j \frac{\partial u_i}{\partial x_j}}_{\text{local \& convective acceleration}} = \underbrace{\frac{-1}{\rho}\frac{\partial p}{\partial x_i}}_{\text{pressure}} + \underbrace{\nu \frac{\partial^2 u_i}{\partial x_j \partial x_j}}_{\text{friction}} + \underbrace{\frac{1}{\rho} f_i}_{\text{mass forces}} \quad (15)$$

Where

u_i is the three dimensional flow vector

p is the hydrostatic pressure

v is the kinematic viscosity

ρ is the density of water

f_i are the mass forces as Coriolis force or gravitational force

The condition of inflowing mass is equal to outflowing mass is fulfilled by the equation of continuity. [9]

- Equation of continuity

$$\frac{\partial u_i}{\partial x_i} = 0 \tag{16}$$

4.2 Saint-Venant equation

One way to simplify the before mentioned flow equations is the depth averaged shallow water equation which is applied in two-dimensional simulation software. It is the result of integration over the vertical axis that is based on the following assumptions:

- Vertical extent of the system is much smaller than the horizontal
- The length of a wave is much longer than its height
- Velocity and in turn momentum in vertical direction is neglected
- Hydrostatic pressure
- Velocities in x and y direction are considered
- Velocity is averaged over height

Finally, the equations for shallow water applications are expressed as follows:

$$\frac{\partial h}{\partial t} + \frac{\partial q}{\partial x} + \frac{\partial r}{\partial y} = 0 \tag{17}$$

$$\frac{\partial}{\partial t}q + \frac{\partial}{\partial x}\left(\frac{q^2}{h} + \frac{gh^2}{2}\right) + \frac{\partial}{\partial y}\left(\frac{q \cdot r}{h}\right) = gh(I_{Sx} - I_{Ex}) \quad (18)$$

$$\frac{\partial}{\partial t}r + \frac{\partial}{\partial y}\left(\frac{q \cdot r}{h}\right) + \frac{\partial}{\partial x}\left(\frac{r^2}{h} + \frac{gh^2}{2}\right) = gh(I_{Sy} - I_{Ey}) \quad (19)$$

Where
h is the water height
I_S is the bed slope
I_E is the energy slope
q is the specific discharge in x-direction
r is the specific discharge in y-direction
The indices x and y describe the directions.
[16] [9]

4.3 Modelling of turbulences

Most of the flow processes in nature are turbulent and transient processes. Turbulences occur in very small spatial and temporal scales and are usually not of interest for most of the problems in hydraulic engineering. Dimension of the smallest vortex in an open channel is approximately 10^{-3} to 10^{-4} times the water depth. Solution methods for turbulent flow are presented in Figure 23.

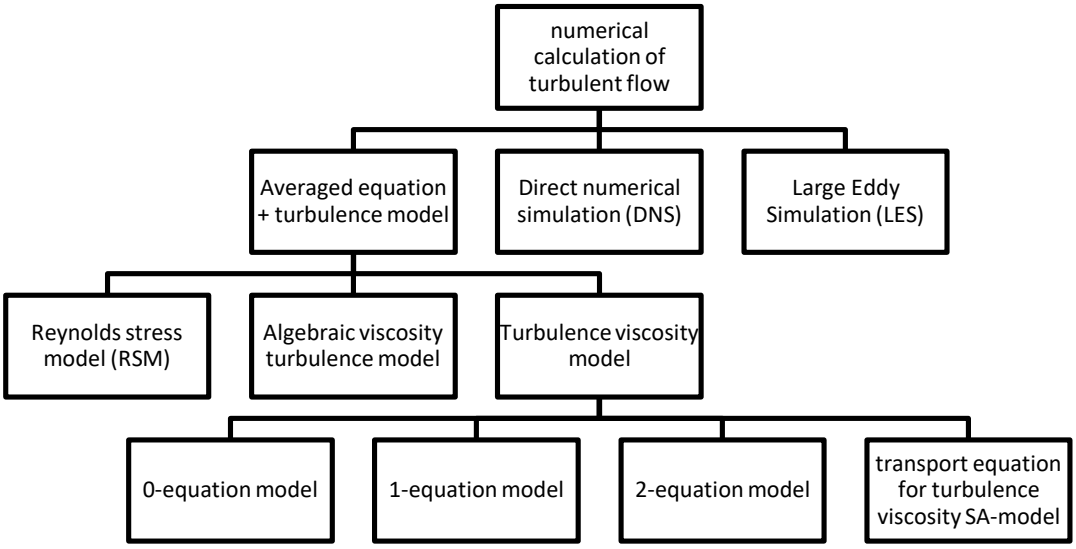

Figure 23 Overview of possible turbulent flow calculation [17]

The method of Direct Numerical Simulation (DNS) is based on the empirical approach of Navier-Stokes and describes the complex turbulence phenomena. To apply this method, one requires a fine subdivision of the study area and in turn an enormous volume of computing power.

The Large Eddy Simulation works with coarser meshes and thus does not represent small vortexes but needs less computational effort. [17] The Reynolds-equation enables the determination of turbulences by averaging the Navier Stokes equation over a period of time. The so-called Reynolds Averaged Navier Stokes equation (RANS) is a statistical method to describe turbulent flows. The current flow vector u_i and the current pressure p are divided into average values $\overline{u_i}$ and $\overline{p}$ and fluctuation values u_i' and p'. This is considered in the momentum equation due to the additional term $\rho\overline{u_i'u_j'}$. [9]

$$u_i = \overline{u_i} - u_i' \tag{20}$$

$$p = \overline{p} - p' \tag{21}$$

- Reynolds-equation

$$\frac{\partial \overline{u_i}}{\partial t} + \overline{u_j}\frac{\partial \overline{u_i}}{\partial x_j} = -\frac{1}{\rho}\left[\frac{\partial \overline{p}}{\partial x_i} - \rho\frac{\partial}{\partial x_j}\left(v\frac{\partial \overline{u}_i}{\partial x_j} - \overline{u_i' u_j'}\right)\right] + \frac{1}{\rho}\overline{f}_i \tag{22}$$

The overbar indicates average values.

This leads to several unknown factors in the equation and has to be eliminated by turbulence models. Turbulence models describe the relation between fluctuation values and averaged flow parameters. [17] [9]
In algebraic viscosity turbulence models turbulence viscosity v_t depends on averaged friction velocity $\overline{u_\tau}$ and water depth $\overline{h}$. Algebraic approaches do not consider flow-transported turbulence. This requires turbulence transport models. The following turbulence viscosity models are based on the assumption that the flow conditions are influenced by Reynolds stress as well as by inner friction. The turbulence viscosity principle of BOUSSINESQ implies turbulence viscosity vt as a proportional factor and thus links Reynolds stress to velocity.

$$-\overline{u_i{}' u_j'} = \nu_t\left(\frac{\partial \overline{u_i}}{\partial \overline{x_j}} + \frac{\partial \overline{u_j}}{\partial \overline{x_i}}\right) - \frac{2}{3}k\delta_{ij} \tag{23}$$

δ_{ij} ensures that the sum of normal stresses is equal to turbulent kinetic energy k.

$$k = \frac{1}{2}\left(\overline{u_i{}' u_i'}\right) \tag{24}$$

A complete turbulence model requires a velocity and length scale which is proportional to the turbulence viscosity. This is expressed by Prandtl-Kolmogorov-Equation. Prandtl-Kolmogorov describes velocity scale as the square root of kinetic energy k.

$$v_t \sim L\sqrt{k} \tag{25}$$

Classification of turbulence models depends on the numbers of differential equations additionally applied. There are plenty of models available but still no generally valid model is available. 0-equation models calculate viscosity in relation to hydraulic parameters. One-equation models determine one additional transport equation that characterizes the characteristic velocity scale. Two-equation models solve additional transport equation for the characteristic length scale. It supposes an isotropic turbulence viscosity (turbulence is portable but independent in direction) and thus prevents secondary flow caused by turbulences. The most used turbulence model in hydraulic engineering is the k-ε model. It is a two-equation model that applies the turbulent kinetical energy *k as* velocity scale and dissipation *ε* as length scale. This gives the following equation, where c_μ identifies an empirical constant.

$$\nu_t = c_\mu \frac{k^2}{\varepsilon} \tag{26}$$

Reynolds-Stress-Model (RSM) is based on anisotropic assumptions of turbulence viscosity. It consists of six transport equations that describe the Reynolds stresses and one equation that characterizes dissipation ε. It constitutes all turbulence phenomena but since it presents high computational effort it is hardly used. [9]

In a river momentum exchange predominantly occurs on the channel bottom. Turbulences caused by inner forces, as gravity or shear stresses between single layers are negligible small compared to the stresses caused by outer forces. Furthermore, turbulences generated by outer forces as wind close to the water surface hardly influence the flow conditions. Thus, the focus is given to bottom shear stresses that are determined by a quadratic law of velocity.

$$\tau_{b,i} = \rho\, c_f\, U_i U \tag{27}$$

Where U is the averaged velocity over depth. c_f is a shear stress coefficient, which includes the drag coefficient λ and in turn surface roughness. The connection between these values is expressed as follows:

$$c_f = \frac{\lambda}{8} = \frac{g\, n^2}{h^{-1/3}} = \frac{g}{C^2} \tag{28}$$

4.4 Discretization

The partial differential equation can be solved by using numerical methods. For this discretization of time and space is required. The latter is done by dissection of the area into points, areas or volumes. The methods are the finite difference method (FDM), finite volume method (FVM) and finite element method (FEM). Their advantages and disadvantages are depicted in Figure 24. [18] [9]

- FDM

  Conservation equation is used as differential equation while the derivation is replaced by differential quotient. Results are given on the nodes of the mesh. FDM provides very accurate results. Meshes are structured and the number of neighbor elements is fixed.
- FVM

  The conservation equation is an integral equation while the integral is displaced by summation, results given at the nodes are averaged over the volume. Meshes can be structured or unstructured. Conservatism of mass for each element.
- FEM

  Differentials are expressed by linear or parable equations and Results express the whole area. FEM is very flexible but less accurate. Conservation of mass for the whole model area but not for every single element.

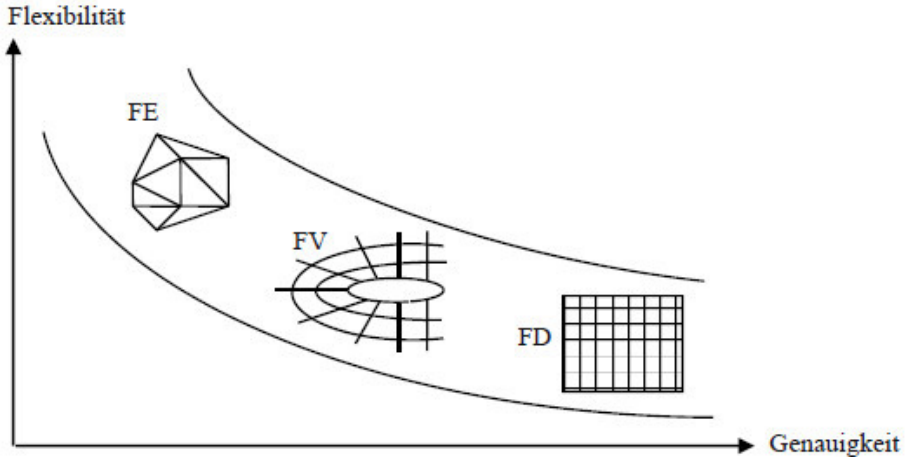

Figure 24 Methods for discretization [18]

As already mentioned above two different meshes are used- structured and unstructured meshes (Figure 25). Structured meshes are commonly used for FDM and unstructured meshes are applied for FEM.

Constant number of cells in one direction may identify structured meshes. Structured meshes are further subdivided into regular, orthogonal and curvilinear meshes. The advantages of structured meshes are less time effort and less needed memory space. A disadvantage is less flexibility of geometry. Unstructured meshes enable the representation of complex geometries but require more computational effort. Unstructured mesh data consist of nodes information, which include the exact coordinates. Moreover, elements are described with all nodes that are creating the element.

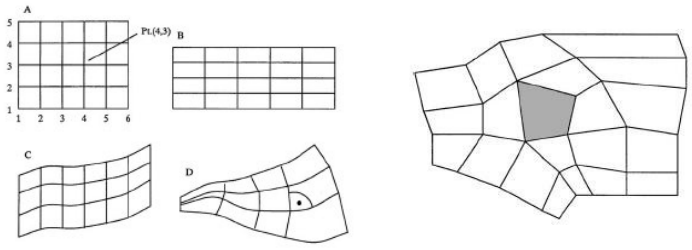

Figure 25 Structured (left) and unstructured (right) mesh [16]

Differential equations can be solved explicit or implicit. One is talking about an explicit method if the unknown quantities as velocity or water level are calculated by considering only the results of neighbor elements at the previous time step. In

implicit methods, all unknown values of the previous time steps are used to determine the quantities of the current time step. In explicit methods, the time step is restricted by the Courant criteria to ensure stable results.

$$\boldsymbol{Cr} = \frac{\boldsymbol{v}\,\boldsymbol{\Delta t}}{\Delta s} \leq \mathbf{1} \tag{29}$$

Where
v is the flow velocity
Δt is the time step length
Δs is the distance between the nodes
The Courant criteria implies that the length of a time step should not be bigger than the time a water particle needs to move from one node to the next node. [17]

4.5 Model definition

For solving the partial differential equation, a system has to be defined by setting boundaries. One has to give boundaries for every time step. For time-dependent differential equations (transient flow) additional initial conditions have to be set. Within a flow the boundary types are inlet and outlet cross section, water level as variable boundary and fixed boundaries as geometry data. The model area is defined by setting the location of the inlet and outlet cross section. The boundary condition on the inlet cross section is usually the velocity in normal direction. In that case it is not allowed to set the velocity as the outlet boundary. The variable boundary (water level) is determined from the flow equation.

Data required for 2d-numerical calculations are:

- Digital area model including the channel geometry
- Location and geometry of barriers (dams, roads, bridge piers, buildings, etc.) and its hydraulic parameters
- Surface roughness of the channel and the surrounding area
- Inflow location and its hydrograph

- Outflow location and its rating curve
- Tributaries its location and hydrographs

For transient simulations, additional initial conditions are required. Results are influenced significantly by boundary conditions and thus have to be chosen carefully. Initial conditions do not affect the results as much as boundary conditions but they may accelerate the duration of the simulation. [16]

4.6 Mesh quality

Results of numerical models contain uncertainties that are of great importance for all involved parties. Calibration, validation and sensitivity analysis are important steps to quantify the accuracy of a numerical model.

4.6.1 Model errors

A numerical model is a simplified presentation of natural conditions and phenomena described by mathematical equations. [9] Simplifications lead to errors, which should be eliminated as good as possible. Sources of errors in numerical models are measurement errors, errors in model results and mathematically caused errors. Reference values taken for calibration are either measured in nature or taken from laboratory tests and already contain errors. Errors in model results are caused by several assumptions and simplifications made in the generation process of the model. It includes errors developed when choosing an equation or input data errors as in geometry on boundary conditions. Additional errors are mathematical errors. Errors of discretization are created when solving the differential equation. In good computer software, this error is negligible as long as an appropriate mesh exists. Besides that, rounding errors present a source of errors. Usually mathematically caused errors are small compared to that mentioned before.

4.6.2 Calibration

For evaluation of the ability to reproduce a certain phenomenon a calibration is required. This means that various tests are made which vary in empirical parameters. The process of calibration includes several simulation tests with different empirical parameters. Empirical parameters mainly cover resistance values. In two-dimensional and three-dimensional models, turbulence plays a significant role and influences the position of water level. Consequently, turbulent viscosity is a parameter to calibrate as well as the surface roughness. Suitable data for comparison are flow velocity, water level at certain discharge, flood line, etc. from in situ measurement, gauging stations, previous calculations or physical models.

4.6.3 Validation

The next step in mesh quality assessment is validation. It is the process of improving and verifying forecast ability. The empirical values that are already calibrated are used for further simulations and compared with other measured values. Ideally these values should originate from measuring independently taken from the data used for calibration. Therefore, additional flood events are suitable. Success of validation is closely related to the quality of the measured values.

Beside calibration and validation a sensitivity analysis is made. It is an assessment of the confidence of the model by observing its behavior when parameters changes. Many times sensitivity analysis is done within the calibration process. Which deviations of the measured data are acceptable depends on the problem that has to be modelled. [9]

5. Assessment methodology

In the present chapter the procedure of a hydromorphological survey is explained. It shows the processes which are subsequently applied for the case study in chapter 6. The target of this survey is the identification of hydromorphological conditions and trends. The survey is supported by an HN-model and thus its outcomes strongly depend on the reliability of the HN-model.

Now the individual processes and steps that lead to the desired goal are listed. The chapter is divided into a collection of data, HN-model generation and finally the survey of hydromorphological conditions.

5.1 Collection of data

5.1.1 General information of the study area

First of all, an overview of the study area and the edited river should be established. Historical development of the catchment area and the channel, anthropogenic interventions and its effects are presented to understand the current channel behavior and the source of problems. In case of any intervention projects planning documents or reports provide beneficial information. Previous projects may give data essentially for creating the HN-model.

5.1.2 Input data

The following paragraph describes required data one has to collect for running a HN-model.

- Hydrology

Hydrological data consists of discharges with different recurrences and rating curves on installed measurement stations. Besides several extreme flow events which might be required to calibrate and validate the numerical model the channel forming discharge plays an important role. For the presented assessment the channel forming discharge is assumed to be the discharge with a recurrence of

two to five years. In case of tributaries within the section their hydrological parameters should be known as well.

- Topography

Geometry is the basis for hydrodynamic simulations. Depending on the applied software the volume of topographical data varies.

1-D calculations require at least the profile data and the distance between each profile. For 2-D calculations data should be given as 3-D-Points. The distance between the profiles depends on how strongly the channel changes its physical characteristics. Bed steps or artificial installations such as wires, bridges, and culverts have to be measured in more detail. Besides the channel the foreland has to be surveyed. It includes marked ground breaks, roads, trenches, etc.

- Surface roughness

Nowadays, most of the programs require roughness coefficients in form of Strickler value k_{St} [$m^{1/3}/s$] or its inverse which is known as Manning´s value $n=1/ k_{st}$. Surface roughness influences the results enormous and is the main error source in hydraulic calculations. Data collection is done on-site and needs a lot of experience.

5.2 HN-model generation

Working with an HN-model requires knowledge of the basics the software is based on. For that, the applied software is introduced.

5.2.1 Software

For this work the software TELEMAC-2D and BlueKenue is used. BlueKenue is a pre- and post-processing software which enables preparing of input data and analysis of results. It is developed by the *Canadian Hydraulics Centre of the National Research Council of Canada* and provides the import of results from TELEMAC. The solver TELEMAC-2D is an open source software for two-dimensional hydrodynamic simulations developed by *Electricité de France*. It solves the

2D-shallow water equation using the finite-element method. It works with unstructured grids composed of triangular elements for which it calculates depth and two velocity components at each point of the mesh. TELEMAC-2D is mainly used for free-surface maritime and river hydraulics.

A simulation performed with TELEMAC-2D requires various data:

- Data which contain physical and numerical parameter for the simulation in text format
- Binary data in Seraphin format (*.ser) which is the specific TELEMAC format. It contains for example bathymetry and initial conditions

TELEMAC-2D provides four turbulence models:

- Constant viscosity
- Elder model
- Model of Smagorinsky
- k-ε model

Friction approaches used by the software are:

- without friction
- Chezy
- Strickler
- Manning
- Colebrook-White
- Haaland
- Nikuradse

Variables solved and printed by TELEMAC-2D can be set by the user as well as the listing and graphic printout period. The variables are water depth, water level, velocity, Courant number, Froude number, bottom height and friction velocity. [19]

Name der Software:	TELEMAC-2D
Hersteller:	Laboratoire d'Hydraulique der EDF – DER, Chatou, Paris
Webpage:	www.telemacsystem.com
Kosten:	keine Angaben
Betriebssysteme:	UNIX, Windows
Raumdiskretisierung:	Finite Elemente
Gittertypen:	Unstrukturiertes Dreiecksgitter
Numer. Methoden:	Streamline Upwind Petrov-Galerkin-Verfahren
Turbulenzmodelle:	• konstante Wirbelviskosität • k-ε-Modell • Ansatz von Elder
Projektreferenzen:	• Design von Hochwasserdurchlässen unter einer Autobahn (Sauvaget et al., 2002) • Modellierung von Dammbrüchen in urbanen Bereichen (Hervouet et al., 2000)
Literaturreferenzen:	Anderson et al. (2000)

Figure 26 Information about TELEMAC-2D [16]

5.2.2 Quality control of the model

Special attention is given to the process of quality control. The aim of this step is to optimize the HN-model and finally obtain the settings that enable natural presentation of flow phenomena.

Quality control includes:

- Calibration
- Validation
- Sensitivity analysis

For that, several simulations with different settings are performed and subsequently its results are compared with comparative values. Comparative values are ideally gained from on-site measurings. Comparative values are for example velocities, water levels or water depths on a certain point. It is recommended to use values which source from different measurings for calibration, validation and sensitivity analysis.

5.3 Assessment

5.3.1 Identification of incipient motion

The identification of morphological processes requires the identification of incipient motion and thus a characteristic grain size diameter. Therefore, a soil sample of the cover layer is taken and the grain size distribution curve obtained.
The grain size distribution curve delivers characteristic grain size diameters that are subsequently used for describing incipient motion. According to the used approach different characteristic grain size diameters are applied. Beside d_{50} or d_{90} - which present the diameter 50% or 90% of the sediments fall below- the effective diameter d_m in a common value for determining incipient motion. Latter one is used in the formula of MEYER-PETER-MÜLLER and presents the arithmetic average of all occurring grain size diameters. d_m is obtained with the following formula:

$$\boldsymbol{d_m} = \frac{\sum \boldsymbol{d_k}\ \boldsymbol{p_{b,k}}}{\sum p_{b,k}} \tag{30}$$

Where
d_k is the grain size diameter
$\boldsymbol{p}_{b,k}$ is the fraction of grain size diameter group in percentage
In the present work the formula of MEYER-PETER-MÜLLER is applied.

5.3.2 Analysis

Now the HN-model with its proven settings, that are gained in 5.2.2 is applied. Several simulations are performed with different discharges. Telemac-2D delivers friction velocity for each node of the mesh. To obtain long term hydromorphological changings special attention is given to the bed forming discharge which is described either as bank full discharge, discharge with recurrence interval between two to five years or as the effective discharge that mobilizes the largest amount of sediments.

Post processing is as well done in BlueKenue. It includes further processing of results and preparing of graphics. Since shear stresses are more descriptive for the subsequent comparison, friction velocities are applied to calculate shear stress τ.

5.3.3 Results and conclusion

The processed results are compared with the critical shear stresses according to MEYER-PETER-MÜLLER. Out of it one asses if erosion or sedimentation takes place.
Dynamic processes derived from the comparison are additionally compared with results of an on-site survey. On-site survey is a qualitative assessment of current channel conditions. Therefor a field visit is done where physical parameters of the banks or beds or the condition of applied protection methods are noted. To make sure that conditions are well visible the current flow condition and the vegetation period have to be considered.

6. Case study Sulm / Heimschuh

Within this master thesis a hydromorphological assessment supported by an HN-model is performed in south-west of Styria. In this chapter, the processes implemented for the assessment are explained. First, the study area is described. Second, the input data and processes which are required for establishing a reliable HN-model are explained. Finally, an analysis is performed and subsequently results and experiences discussed.

6.1 Study area

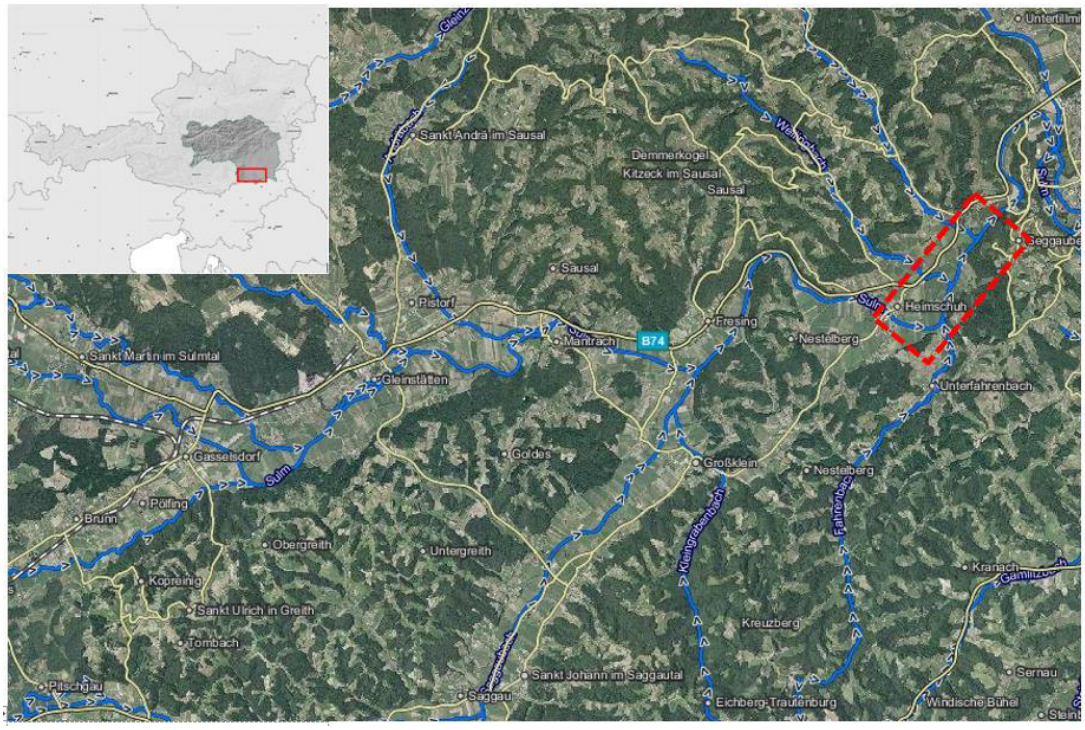

Figure 27 Map of the Sulm valley [20]

The treated stretch is on the river Sulm in south-west of Styria as it is depicted in the map in Figure 27. The river is a right side tributary of the river Mur. Its headstreams are the Schwarze Sulm und Weiße Sulm. Both streams have their source on the east side of the Koralpe at sea level of 1660m and 1560m and are combined in Prarath upstream of Gleinstätten. From there on the river is called Sulm. It is 29km long and finally leads into the river Mur in Obervogau, where its catchment area is about 1113km^2.

The study area starts in Heimschuh where L604 Arnfelserstraße crosses the Sulm and reaches downstream of the Sulm lakes to Eisernersteg. Except of two meanders, within this stretch the river bends smoothly and has a bottom slope of about 1‰. Historical maps show the river as a meandering river (Figure 28) but in the last decades several anthropogenic interventions were done and the channel course got heavily modified [21].

Figure 28 Historical map [15]

From 1961 to 1966 the river Sulm was regulated close to the village Heimschuh to enable a hazard-free discharge of HQ_{25} which corresponded to 173m³/s. After 1966, several anthropogenic changes in the catchment area and the upper reach leaded to significant changes in its flood behavior. In 1998, the discharge of a HQ_{25} correlated to a flood with a recurrence interval of 5 years (HQ_5) and flood control was not guaranteed anymore. In the following two years another flood protection project was developed with a stretch of 3.5km between Heimschuh and the Sulm lakes. The project objectives were:

- Flood protection up to HQ100 for Heimschuh, this should be realized with help of widening one side of the channel downstream from the village
- Minimal maintenance effort, due to oversized profiles

- Elimination of the narrow section at Eiserner Steg, due to a flood channel
- Bioengineering construction methods to protect the channel banks (except the methods applied in Heimschuh)
- Increasing the length of the stretch by creating of two meanders in dependence on the historical natural stream course (Figure 28)

Within the project which was concluded in 2000, 69 bioengineering constructions are applied in the study area to structure aquatic habitats and protect banks. Applied bioengineering constructions include rootstocks, tree groynes, tree spurs, triangular groynes and stones. Additionally, bank pile walls, rock layering, crib walls and brush mattress constructions protect the banks from erosion. Figure 29 shows the study area with all bioengineering construction methods applied in this stretch. [22]

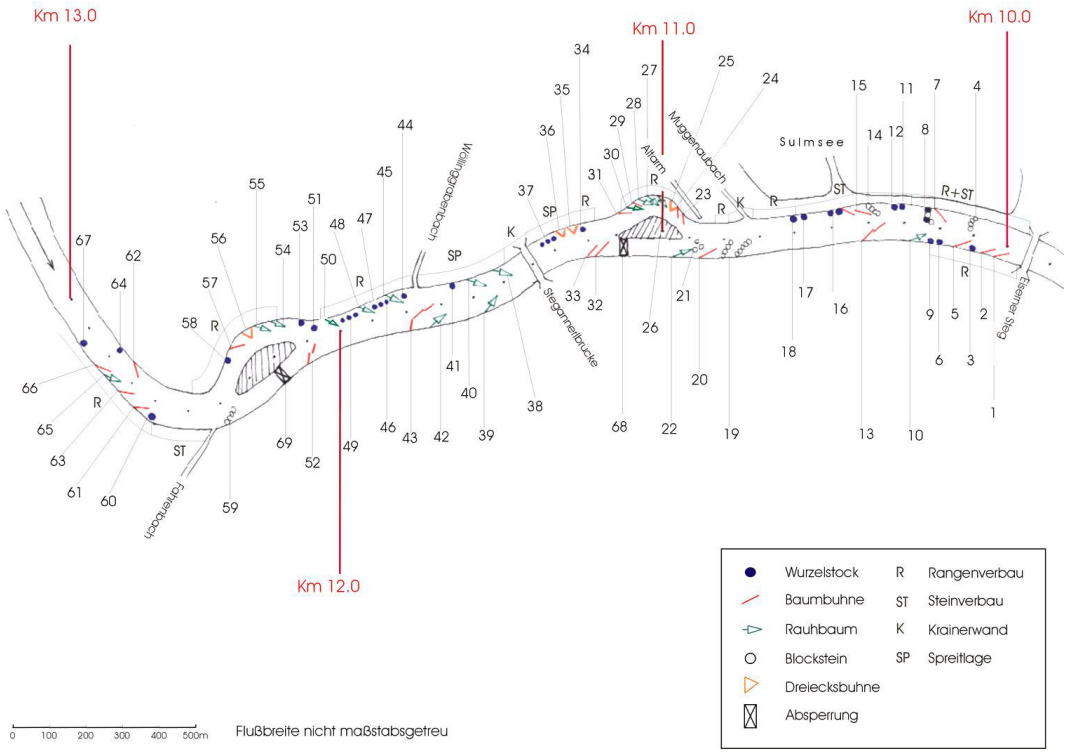

Figure 29 Location of bioengineering construction methods [21]

root stocks (●) tree groynes (／) tree spurs (▻) triangular groynes (▷) stones (○) pile walls (R) rock layering (ST) crib walls (K) brush mattress (SP)

The study area reaches from river kilometer 13.806- bridge in Heimschuh to river kilometer 10.012 -Eisernersteg and presents the area of the flood protection project. To identify the location within the stretch the profile designation of [23] is copied. The side map including the profiles is given in Figure 31.

Within the study area, two new meanders were developed which are named as meander 1 and meander 2. Meander 1 is the one located downstream of Stegannerlbrücke between P104 and P100, while meander 2 identifies the upstream meander between P115 and P112. For the meanders a new main channel is trenched. The new main channel is shifted to the left side. The old channel bed now acts as a bypass channel, which is flushed at a certain discharge and thus releases the main channel. According to engineering documents, the dam is overtopped from HQ1. A dam on the upstream end separates the bypass channel from the main channel. It is passable and connects the right river bank with the island which arises between the main channel and the bypass channel. The dam core is a construction of piles and panels filled with loos material, a fleece layer prevents washing out the material. The outside is covered with stones. A schematically presentation of the cross section of the dam is given in Figure 30 [15]

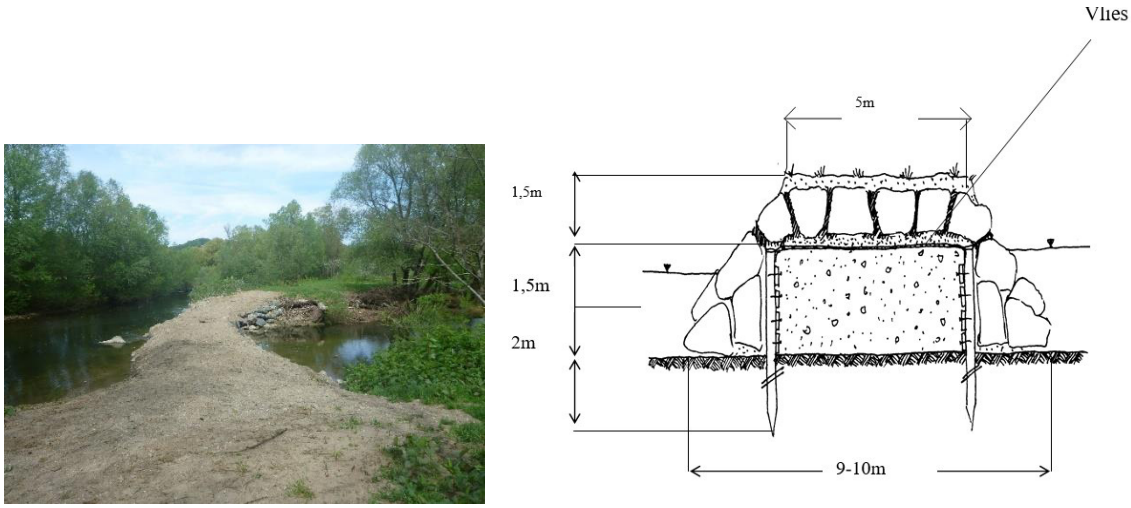

Figure 30 Dam of meander 1

6.2 Numerical model

For the following hydromorphological assessment several simulations are performed on a before created model. The input data and its preparation that are required for establishing a HN-model are explained in this chapter.

6.2.1 Geometry and mesh

Between 2006 and 2008 on behalf of Land Steiermark a 2-D flood analysis of several streams and rivers in South-west Styria was performed by Hydroconsult GmbH. This analysis provides many data for this case study. In the following document, this analysis is referred as flood analysis.

The HN-model reaches from P125 to P81 and thus presents only a small section of the flood analysis. It should be noted that the HN-model presents a river stretch of 5.1km but the subsequently performed hydromorphological analysis is only applied on a 3.8km long section. This is justified by uncertainties of boundary conditions and explained in 6.2.2.

Geometry data are filtered from the mesh of this flood analysis. Thus, a short introduction of the software applied for the flood analysis is given.
The programs applied are Hydro_AS-2d and SMS. Hydro_AS-2d is a hydrodynamic-numerical solver software developed by Dr. Nujic and Hydrotec. Hydro_AS-2d uses SMS as user interface. SMS is used to set model parameters, generate the mesh and for post-processing. The method for spatial distribution is the finite volume method. Hydro-AS-2d works with unstructured triangular and rectangular elements. For modelling turbulent processes, it applies the k-ε model.

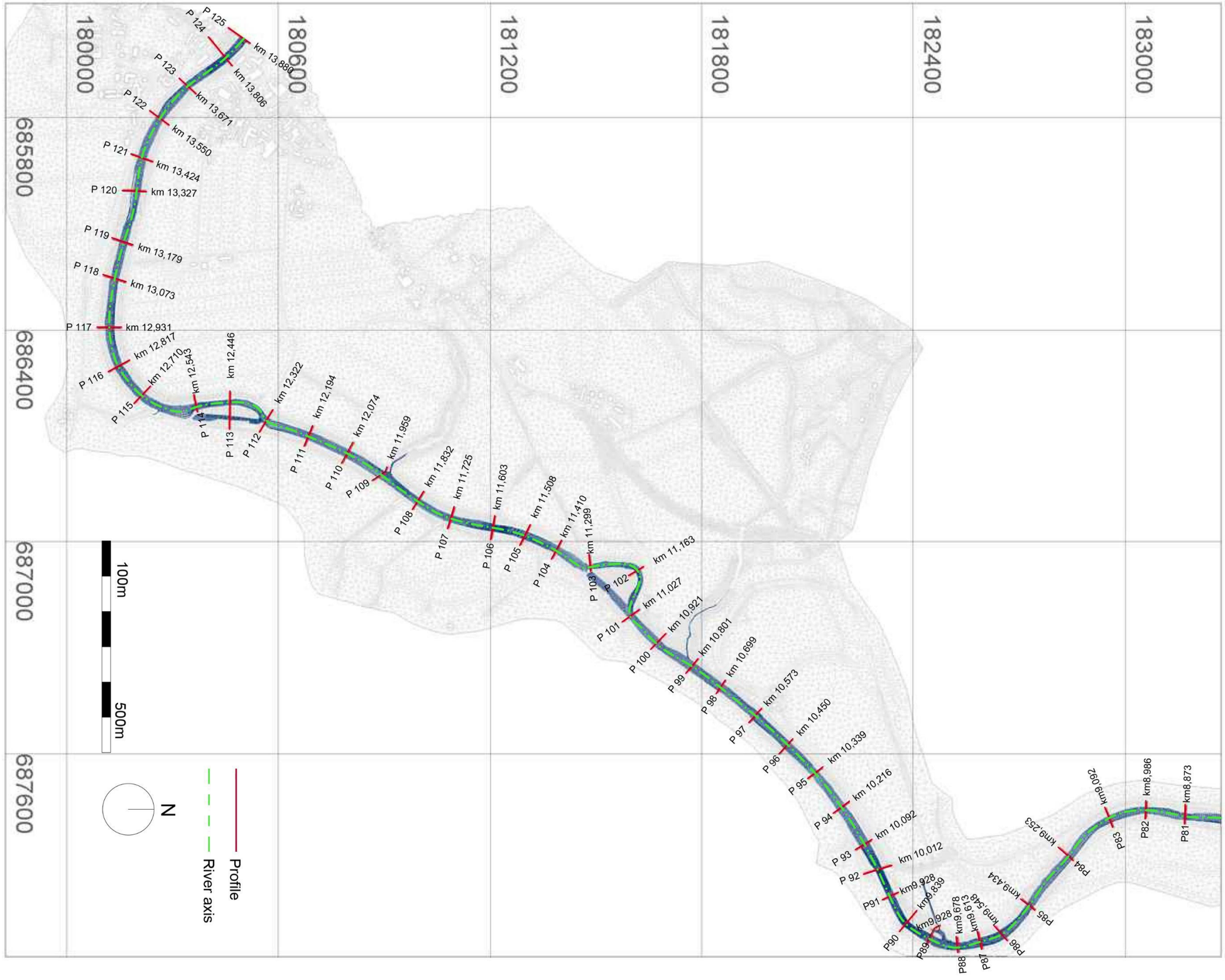

Figure 31 Site map of the river Sulm

The channel geometry is based on terrestrial surveys and the foreland is measured with laser scan. Depending on the width of the channel the profile distances vary between 65 meter to 185 meter. Additional surveys were done to record islands, constructions or bottom steps. Between the profiles, the slope and breaking edges are adopted from the laser scan survey. [23] Bioengineering methods applied within the flood protection project are not considered in the survey.
The mesh of the flood analysis is given as *.2dm-file, which is the 2D-Mesh file created by SMS. This file includes the following information:

- 4-noded quadrilateral elements (E4Q) and 3-noded triangular elements (E3T); consists of ID of the element, ID of the nodes that form the element and the ID of the material that is attached to the element

```
E4Q    297    333    285    283    331      6
E4Q    298    332    284    286    334      6
E4Q    299    335    287    285    333      6
E4Q    300    286    324    336    334      6
E4Q    301    337    288    287    335      6
E3T    302    290    338    289      6
E3T    303    289    338    291      6
E3T    304    292    339    290      6
E3T    305    339    338    290      6
E3T    306    293    291    338      6
```

- ID and location of each node given as x, y and z coordinated of the point (ND)

```
ND   9461 6.73697656e+005 1.78217670e+005 3.05696618e+002
ND   9462 6.73698138e+005 1.78217916e+005 3.05793258e+002
ND   9463 6.73695401e+005 1.78222445e+005 3.05747091e+002
ND   9464 6.73693079e+005 1.78227186e+005 3.05797448e+002
ND   9465 6.73690761e+005 1.78231927e+005 3.05851140e+002
ND   9466 6.73688620e+005 1.78234283e+005 3.05636993e+002
ND   9467 6.73689333e+005 1.78234595e+005 3.05804993e+002
ND   9468 6.73686074e+005 1.78239321e+005 3.05654263e+002
ND   9469 6.73683511e+005 1.78244351e+005 3.05671533e+002
ND   9470 6.73680928e+005 1.78249370e+005 3.05688803e+002
```

- Material (MAT) includes the name and the ID. The name of the material in form of Strickler values.

```
MAT   10        15        0
MAT   11        29        0
MAT   12        29        0
MAT   14        29        0
MAT   16        29        0
MAT   20        29        0
MAT   21        29        0
MAT   22        15        0
MAT   23        25        0
MAT   26        25        0
MAT   28        15        0
```

For this simulation two meshes are used. Mesh 1 is equal to the mesh of the flood analysis. The *.2dm is imported in BlueKenue which automatically splits quadrilateral elements into triangular elements. Mesh 2 is a completely new generated mesh based on the node coordinates given in the *.2dm file. The default edge length for the mesh in the model area is set to 15m while several areas of the mesh are denser. In BlueKenue, the opportunity is given to mesh the channel separately. This process takes left and right banks into account as well as thalweg. Separate channel meshing is not made for Mesh 2 due to a lack of data. Instead of that, areas with denser mesh are defined. The maximum edge length in the channel is set to 3m and in the area of the Sulm See to 10m. Buildings, which are within the flood plains are considered as barriers and in the vicinity of barriers the mesh get refined.

The new developed mesh, mesh 2, shows less smooth channel banks. Due to interpolated bottom elevation, BlueKenue creates broken channel banks, which generate additional roughness. A selection of the two meshes in the area of meander 1 is presented in Figure 32 and Figure 33.

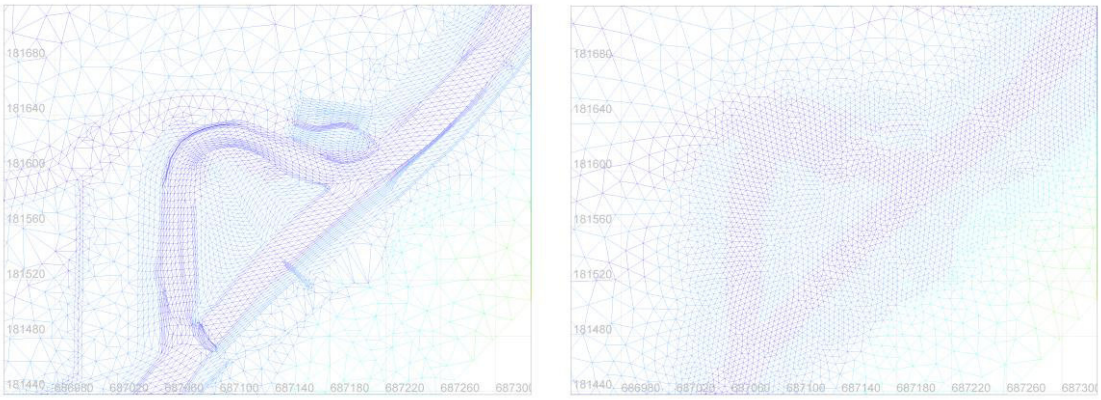

Figure 32 2d - Meander 1 - mesh 1 (left) and mesh 2(right)

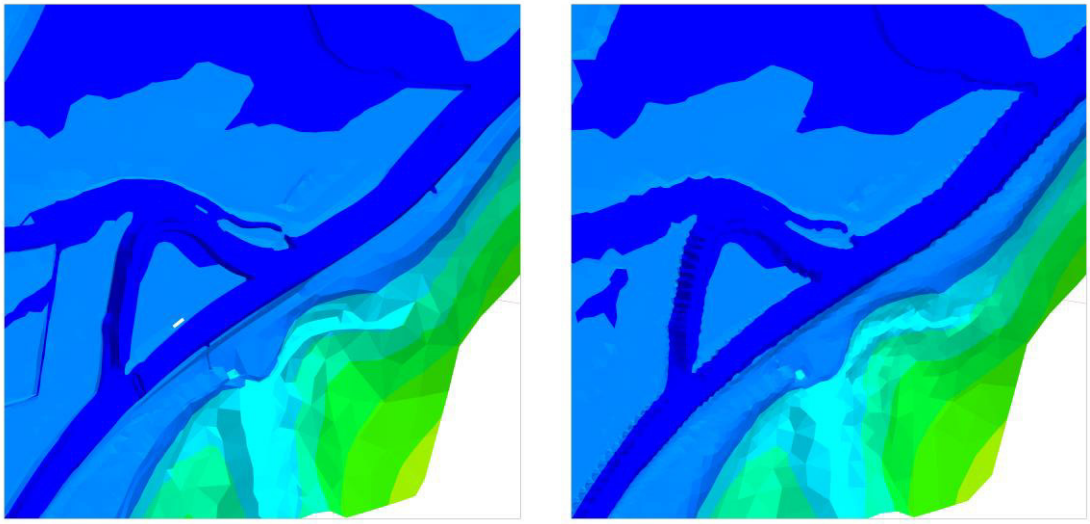

Figure 33 3d - Meander 1 – mesh 1 (left) and mesh 2(right)

6.2.2 Hydrology and boundary conditions

The conditions of the HN-model boundaries have to be defined. The current model consists of three different kinds of boundaries. While the edges of the model and all barriers (as houses) are defined as closed boundaries, the upstream and downstream end of the channel are set as opened boundaries. Closed boundaries prevent the flow of water masses.

The upstream boundary is defined as inflow with prescribed discharge and the downstream boundary, named as outflow, is set as boundary with prescribed height. These settings enable the specification of a hydrograph for the inflow boundary and a rating curve for the outflow boundary.

Due to lack of a gauging station within the study area no current data are available. Thus, discharge data are taken from previous projects and are summarized in Table 3. Within the stretch three tributaries join the river Sulm. For the sake of convenience, in this work tributaries are not considered. However, additional discharge of Muggenaubach is considered by applying two different values for HQ30 and HQ100. This is done for getting comparable results for calibration and validation. The discharge of Muggenaubach is 5m³/s in case of HQ30 and 6m³/s for HQ100. [23] Thus, in the following work the terms HQ30 and HQ100 are complemented by the value of the specific discharge.

Table 3 Hydrological data

Flow event	Discharge $[m^3/s]$	Reference
HQ100_348	348 m^3/s	[23]
HQ100_342	342 m^3/s	
HQ30_283	283 m^3/s	
HQ30_278	278 m^3/s	
HQ10	205 m^3/s	[22]
HQ5	160 m^3/s	
HQ1	95 m^3/s	
MQ	8,85 m^3/s	

All simulations performed in this master thesis are transient. Their quantitative description is made in *.txt-file which serves as input file for TELEMAC-2D. Each starts from steady MQ conditions, increases for twelve or fifteen hours until it reaches a predetermined value and afterwards becomes steady for minimum further twelve hours. An example is given in Figure 34.

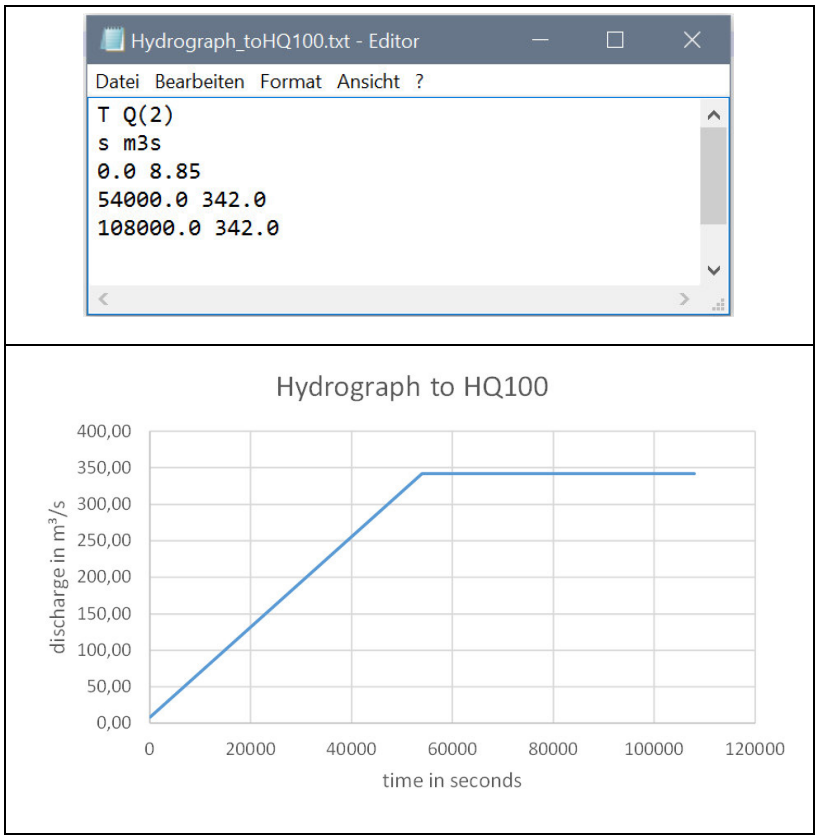

Figure 34 Inflow hydrograph for HQ100

The outflow boundary condition is quantified in an *.txt file. Rating curve is obtained from a software called Bed Load Analyzer. The software enables the determination of hydraulic and sedimentological parameter by entering geometry data of the profile and surface roughness of the channel, the left and right bank. Bed Load Analyzer uses the Strickler formula to calculate steady uniform flow and considers one dimensional flow. [14]

The outflow boundary is consciously set further downstream, where discharge occurs just in the channel stream. There the river is more or less straight, which minimizes errors occurring due to one dimensional water level calculations or incorrect assumptions (as roughness). Therefore, the outflow is located more than 1km downstream of P92, which represents the downstream end of the hydromorphological analysis.

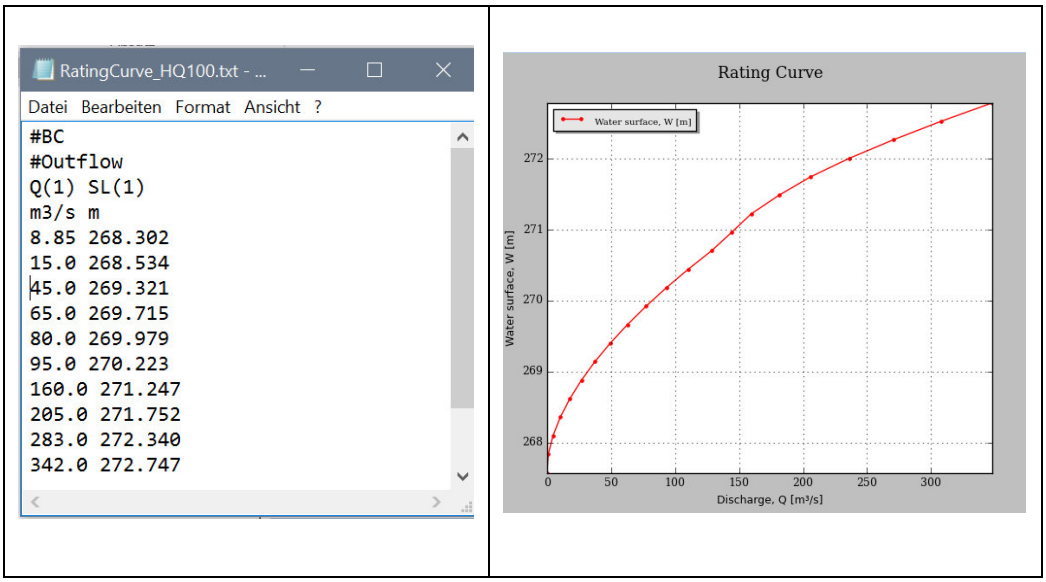

Figure 35 Outflow rating curve for HQ100

6.2.3 Surface roughness

Surface roughness is described by Strickler values k_{St}. One assumes that foreland conditions have not changed significantly for the last years thus values are extracted from the flood analysis (Table 4). Values are obtained from field visits done in spring 2007 or experienced in previous projects. For channel roughness two approaches are made. In approach 1 k_{St} is set to $k_{St} = 29\ \frac{m^{1/3}}{s}$ upstream of P94 at river km 10,216 and to $k_{St} = 30\ \frac{m^{1/3}}{s}$ downstream of P94. [23] In approach 2 channel roughness is uniformly set to $k_{St} = 25\ \frac{m^{1/3}}{s}$. This value is taken from Table 2 (flat channel bottom with rough gravel). A value of $25\ \frac{m^{1/3}}{s}$ corresponds as well to the conditions which predominate in meander 1. Surface roughness of approach 1 is mapped in Figure 36.

Table 4 Foreland Strickler values k_{st}

Surface	Roughness k_{st} [$m^{1/3}/s$]
Foreland	10
Grassland	15
Forest	8
Acre	10
Channel without vegetation	20
Channel with weak vegetation	17
Channel with average vegetation	12
Channel with high vegetation	8
Unpaved surface	30
Paved surface	22
Bank forestation	8
Settlement area	8

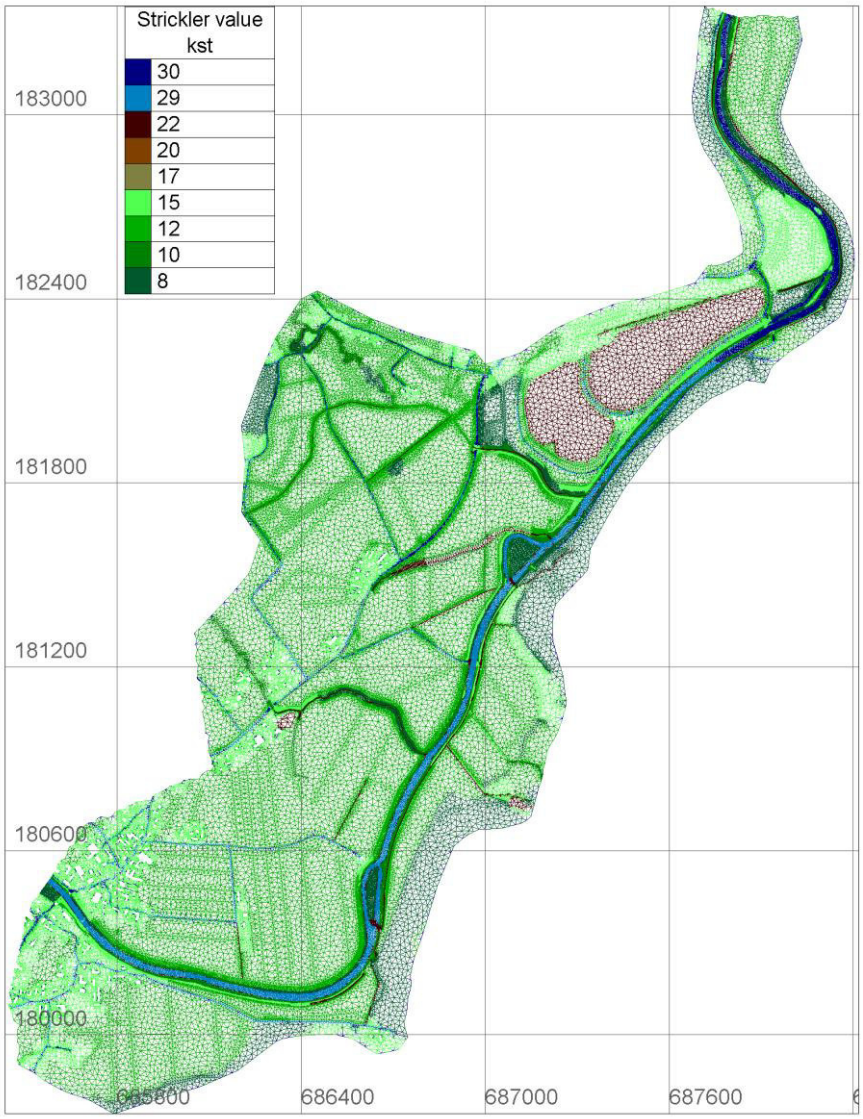

Figure 36 Surface roughness distribution in the study area (approach 1)

6.2.4 Turbulence model

Two turbulence models are applied; Elder Model and Constant Viscosity Model. The approach of constant viscosity requires a prescribed viscosity, which presents molecular and turbulent viscosity and dispersion. Turbulent viscosity is not a material property but depends on velocity distribution. Hence, turbulent viscosity cannot be constant. The model of constant viscosity might be a satisfying approach for turbulence structures, which are temporally and spatially homogeneous. For the selection of constant viscosity value, it should be considered that

turbulent viscosity is many times larger than molecular viscosity, which is about $10^{-6}\ \frac{m^2}{s}$ for water at 20 degrees Celsius.

In the present work, one chose viscosity of $0{,}5\,\frac{m^2}{s}$. The value is explained below.

Elder model, also known as depth-averaged parabolic Eddy viscosity model is based on the well-known vertical velocity distribution and assumes a main flow direction in x-axis. It considers a parabolic velocity profile and a specific mixing length and integrates turbulent viscosity over depth. Formula (31) and (32) present how friction velocity is obtained when applying the Elder model.

$$\overline{v_t} = \alpha_t u_* h \tag{31}$$

$$u_* = \sqrt{c_f U^2 V^2} \tag{32}$$

u_* is the friction velocity and α_t is an empirical coefficient which commonly set to $\kappa/6$. c_f is the coefficient of surface roughness , U and V indicates velocities in x and y direction. This leads to turbulent viscosity where quantities as water depth and friction are high. For areas where the vertical velocity profile differs from the logarithmic velocity profile (with additional horizontal velocity gradients) this model presents insufficient results.

6.2.5 Advection scheme

For advection of water depth two different assumptions are made. The applied schemes are the N-Edged based Residual Distributive scheme (NERD) and the Method of characteristics. NERD scheme is the less diffusive one. Both of them are applied for calibration and their effect on the results analysed.

6.3 Model quality

To get a model that presents flow phenomena as real as possible many different simulations are performed. Their nomination is chosen in accordance to their settings as it is mentioned in the previous subchapter. An overview of the executed simulations is given in Table 5.

Table 5 Performed simulations

Chapter	Name	Flood event	Discharge in m^3/s	Tubulence model	Viscosity in m^2/s	Advection scheme	Mesh	Roughness
6.3.3 Constant Viscosity	HQ30_278_CV_0.5_NERD_1_app1	HQ30	278	CV	0.5	NERD	1	app1
	HQ30_278_CV_0.1_NERD_1_app1	HQ30	278	CV	0.1	NERD	1	app1
	HQ30_278_CV_0.01_NERD_1_app1	HQ30	278	CV	0.01	NERD	1	app1
	HQ30_278_CV_0.001_NERD_1_app1	HQ30	278	CV	0.001	NERD	1	app1
6.3.4 Calibration	HQ30_278_Elder_NERD_1_app1	HQ30	278	Elder		NERD	1	app1
	HQ30_278_CV_NERD_1_app1	HQ30	278	CV	0.5	NERD	1	app1
	HQ30_278_CV_MoC_1_app1	HQ30	278	CV	0.5	MoC	1	app1
	HQ30_278_Elder_MoC_1_app1	HQ30	278	Elder		MoC	1	app1
	HQ30_283_Elder_NERD_1_app1	HQ30	283	Elder		NERD	1	app1
	HQ30_283_CV_NERD_1_app1	HQ30	283	CV	0.5	NERD	1	app1
	HQ30_283_CV_MoC_1_app1	HQ30	283	CV	0.5	MoC	1	app1

	HQ30_283_Elder_MoC_1_app1	HQ30	283	Elder		MoC	1	app1
6.3.5 Sensitivity analysis	HQ30_278_Elder_NERD_1_app1	HQ30	278	Elder		NERD	1	app1
	HQ30_278_Elder_NERD_1_app2	HQ30	278	Elder		NERD	1	app2
	HQ30_278_Elder_NERD_2_app1	HQ30	278	Elder		NERD	2	app1
	HQ30_283_Elder_NERD_1_app1	HQ30	283	Elder		NERD	1	app1
	HQ30_283_Elder_NERD_1_app2	HQ30	283	Elder		NERD	1	app2
	HQ30_283_Elder_NERD_2_app1	HQ30	283	Elder		NERD	2	app1
0 Validation	HQ100_342_Elder_NERD_1_app1	HQ100	342	Elder		NERD	1	app1
	HQ100_342_CV_NERD_1_app1	HQ100	342	CV	0.5	NERD	1	app1
	HQ100_348_Elder_NERD_1_app1	HQ100	348	Elder		NERD	1	app1
	HQ100_348_CV_NERD_1_app1	HQ100	348	CV	0.5	NERD	1	app1

6.3.1 Basis of quality control

The provided documents of the flood analysis deliver comparative values for the following quality assessment of the established model. These values are water levels at HQ30 and HQ100 and are measured at certain bridges in the study area. Two bridges are chosen – Stegannerlbrücke and Eisernersteg. Stegannerlbrücke is located between the two meanders at river km 11,603 and corresponds to profile P106. Eisenersteg is directly downstream of the Sulm See at river km 10,012. Its location is equal to profile P92. The comparative water levels are obtained from steady simulations and measured directly upstream of each bridge, hence the location of measurement may differ slightly from the mentioned profiles. [23]

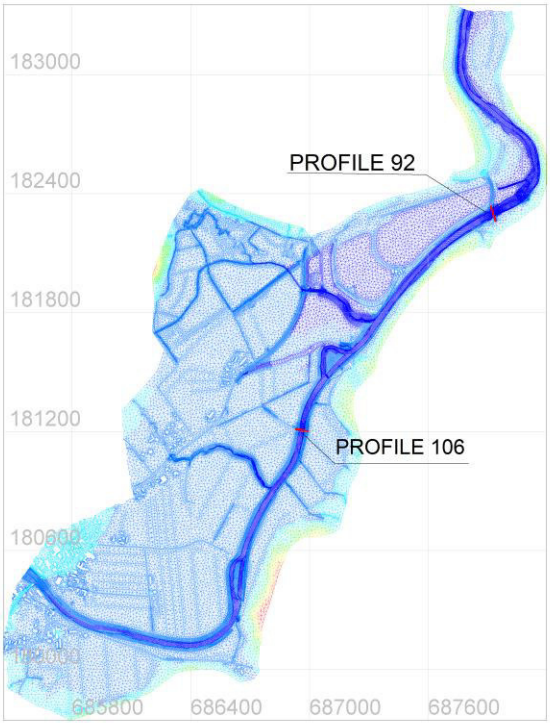

Figure 37 Location of control profiles

Between these two control profiles, P106 and P92, tributary Muggenaubach joins the river Sulm. Thus, the comparative discharge for P106 is 5m³/s or 6m³/s less than for P92. The valid discharges for comparison at P106 are HQ30 = 278 m³/s and HQ100 = 342 m³/s and at P92 are $HQ30_{P92}$ = 283 m³/s and $HQ100_{P92}$ = 348 m³/s. Comparative values are presented in Table 6.

Table 6 Comparative values - Water level at P92 and P106

	$H_{fa, HQxx, P92}$ **Water level at P92 [m.a.s.l.]**	$H_{fa, HQxx, P106}$ **Water level at P106 [m.a.s.l.]**
HQ 30	274,16	275,20
HQ100	274,66	275,48

6.3.2 Examination of steady conditions

All hydrographs applied for the simulations listed in Table 12 are of the same characteristics and aim to archive steady conditions. If these conditions occur are checked by observing the velocity course at certain control points in the channel and the floodplain. An example for simulation HQ30_278_Elder_NERD_1_app1 is given in Figure 38. The hydrograph set for this simulation gives increasing discharge for twelve hours until it reaches HQ30 of 278m³/s. After these twelve hours discharge remains constant for further sixteen hours. It takes approximately ten hours after discharge remains constant until conditions in the whole study area become steady. This is caused by the retention effect of the floodplain.

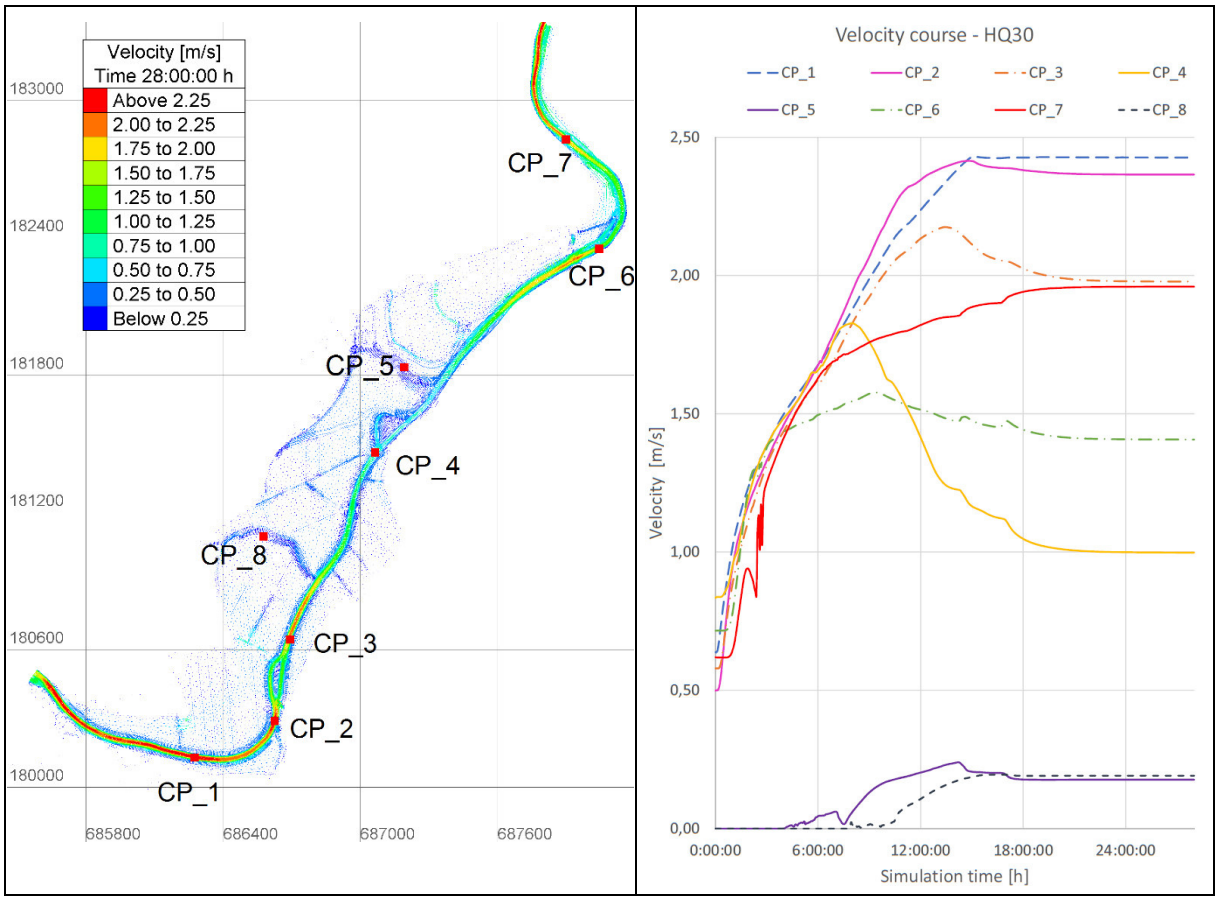

Figure 38 HQ30 - Control of steady conditions

6.3.3 Constant Viscosity

Before analyzing several simulations, the choice of the constant velocity is explained. As already mentioned above a viscosity has to be prescribed for the turbulence model of Constant Viscosity. The set value is assumed for the whole study area and includes molecular and turbulent viscosity. Four HQ30 simulations with different values for viscosity are conducted. The set viscosity values are $0{,}5\,\frac{m^2}{s}$, $0{,}1\,\frac{m^2}{s}$, $0{,}01\,\frac{m^2}{s}$ and $0{,}001\,\frac{m^2}{s}$. Its results are compared qualitatively with the floodplains of the flood analysis implemented between 2006 and 2008. Floodplains of each simulation are depicted in Figure 40.

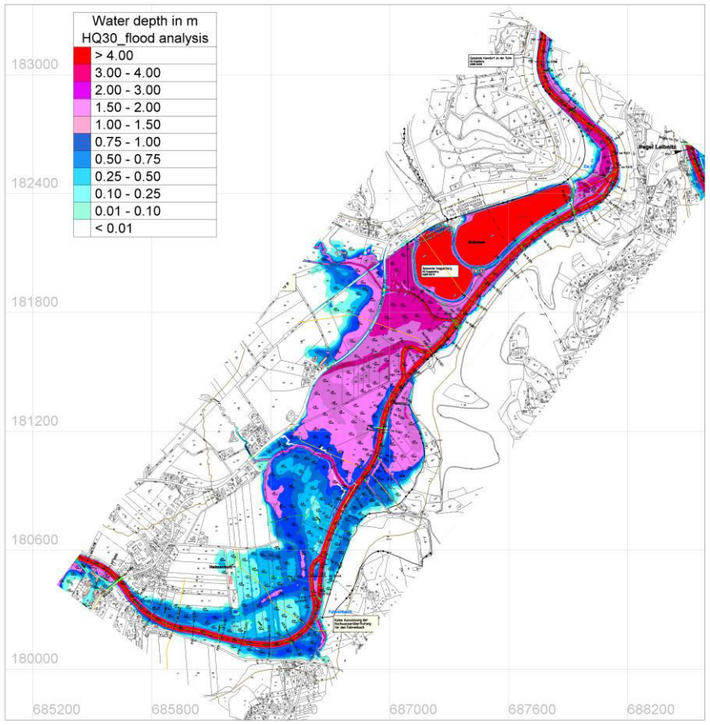

(a)

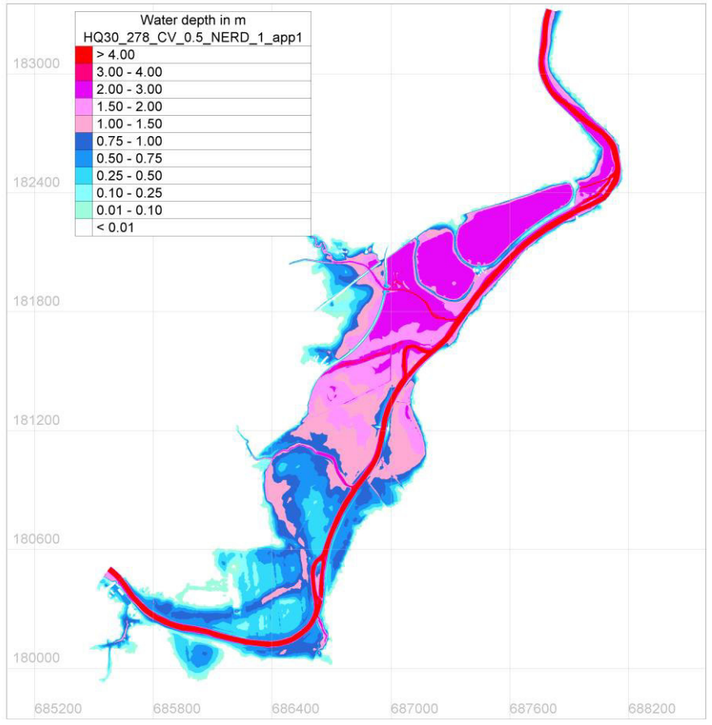

(b)

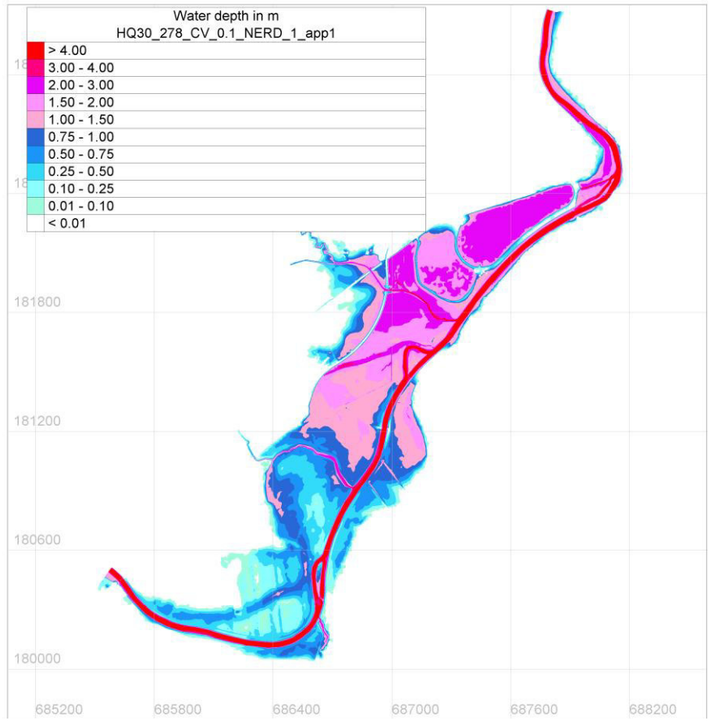

(c)

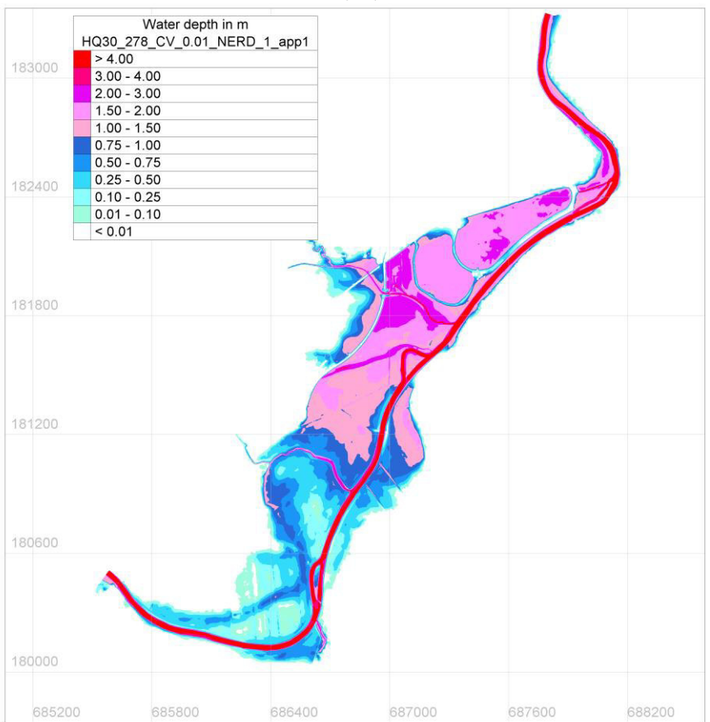

(d)

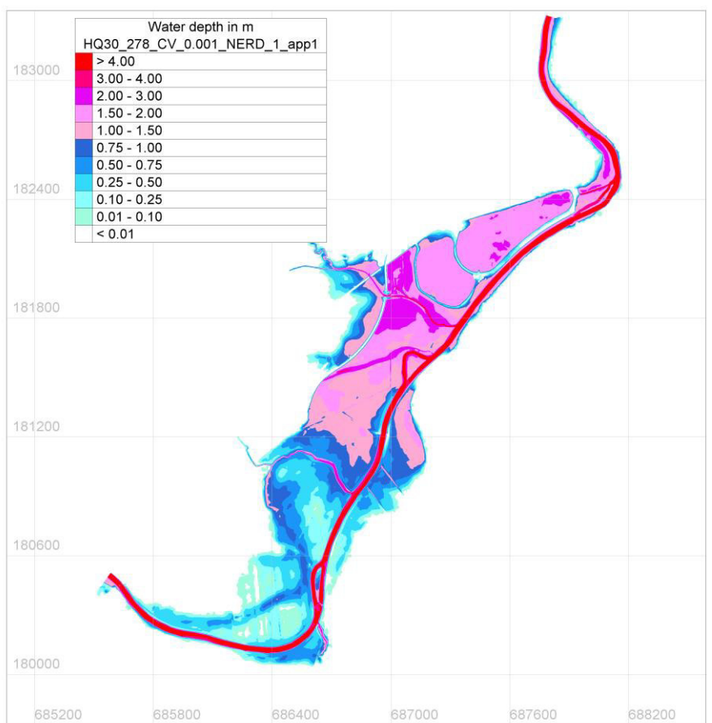

(e)

Figure 39 Comparison of floodplain of (a) flood analysis (b) $v = 0{,}5\ m^2/s$ (c) $v = 0{,}1\ m^2/s$ (d) $v = 0{,}01\ m^2/s$ (e) $v = 0{,}001\ m^2/s$

As seen in Figure 39 floodplain area and water depths decrease with small viscosity values. As (d) and (e) give smaller water depths than (a). Viscosity of $0{,}1\frac{m^2}{s}$ (c) gives the most similar results to flood analysis, whereas in (b) water depths are bigger. Especially upstream of meander 2, on the right side of the channel, where additional areas are flooded. Nevertheless, due to the fact that tributaries are not considered and the set discharge is higher, bigger water depths upstream of Fahrenbach are realistic. Fahrenbach is a right side tributary and joins river Sulm between P114 and P115.

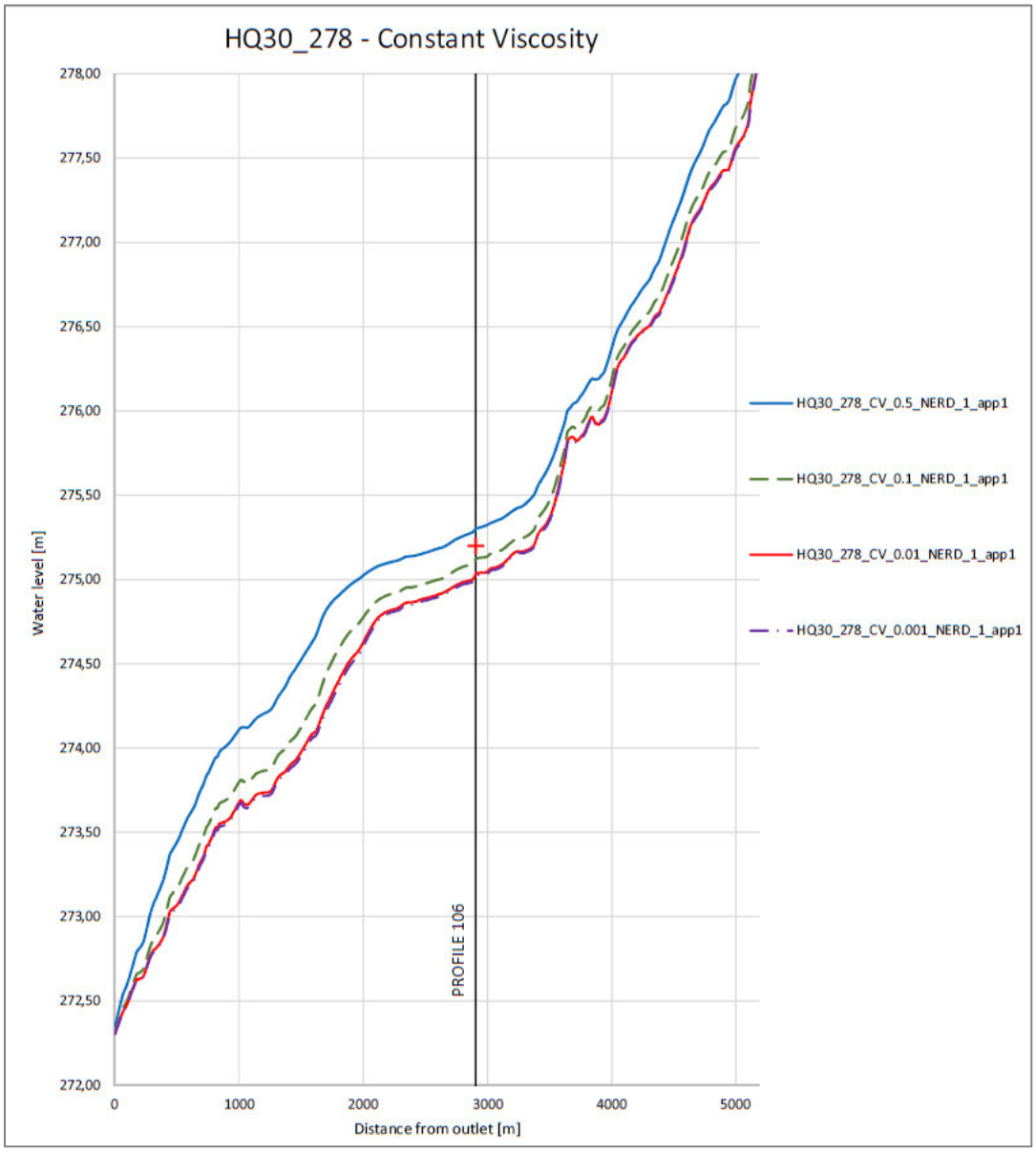

Figure 40 Comparison of water surface profile of simulations with different constant viscosity

Big differences of water levels are depicted in Figure 40. Water level at P106 and its deviation to $H_{fa,HQ30,P106}$ are given in Table 7.

Table 7 Water level HQ30- Turbulence Model Constant viscosity

Simulation	H_{CVxx} [m.a.s.l.]	$\Delta H = H_{CVxx} - H_{fa,HQ30,P106}$ [m]
HQ30_278_CV_0.5_NERD_1_app1	275,297	0,094
HQ30_278_CV_0.1_NERD_1_app1	275,116	-0,084
HQ30_278_CV_0.01_NERD_1_app1	275,028	-0,172
HQ30_278_CV_0.001_NERD_1_app1	275,015	-0,185

Simulations with $v = 0{,}01\frac{m^2}{s}$ and $v = 0{,}001\frac{m^2}{s}$ deliver similar results but set values are too low to describe the turbulent processes in a channel. $v = 0.1\frac{m^2}{s}$ delivers too low values as well, thus for the following simulations a value of $0.5\frac{m^2}{s}$ is assumed. Higher values as it is obtained with $v = 0.5\frac{m^2}{s}$ can be explained by the increased discharge which already includes the discharge of Muggenaubach.

6.3.4 Calibration

For a calibration a steady HQ30 is simulated. Water level is measured on both profiles and subsequently compared with comparative values.
Simulations executed for calibration are based on mesh 1 and roughness approach 1. In addition, the two turbulence models and two advection schemes are tested.

Settings are summarized below:

- Turbulence model – Elder Model (Elder) and Constant Viscosity Model with $v = 0{,}5\frac{m^2}{s}$ (CV)
- Advection scheme – NERD and Method of Characteristics (MoC)
- Mesh 1
- Roughness approach 1

Hence, the conducted simulations are:

- HQ30_278_Elder_NERD_1_app1
- HQ30_278_CV_NERD_1_app1
- HQ30_278_CV_MoC_1_app1
- HQ30_278_Elder_MoC_1_app1

- HQ30_283_Elder_NERD_1_app1
- HQ30_283_CV_NERD_1_app1
- HQ30_283_CV_MoC_1_app1
- HQ30_283_Elder_MoC_1_app1

The figures above (Figure 41 to Figure 43) determine the simulation with Elder model and NERD scheme delivers results closest to the flood analysis. The measured water levels and the difference between the comparative and the measured value are listed in Table 8. Differences in profile 92 are quite large compared to profile 106. Possible reason for this could be ground steps and bridge piers which leads to wave formation. Additionally, the description of the location of measurement is inaccurate.

Figure 41 Calibration - HQ30 - Water surface profile

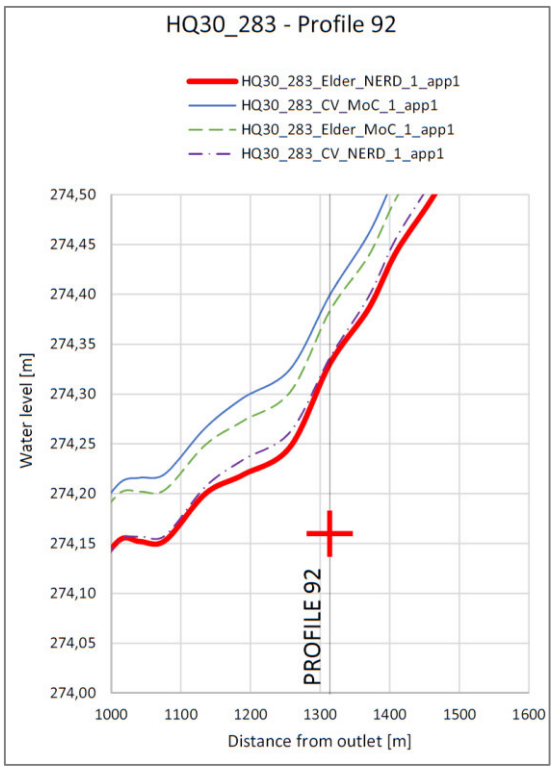

Figure 42 Calibration- HQ30 - Water surface profile in Profile 92

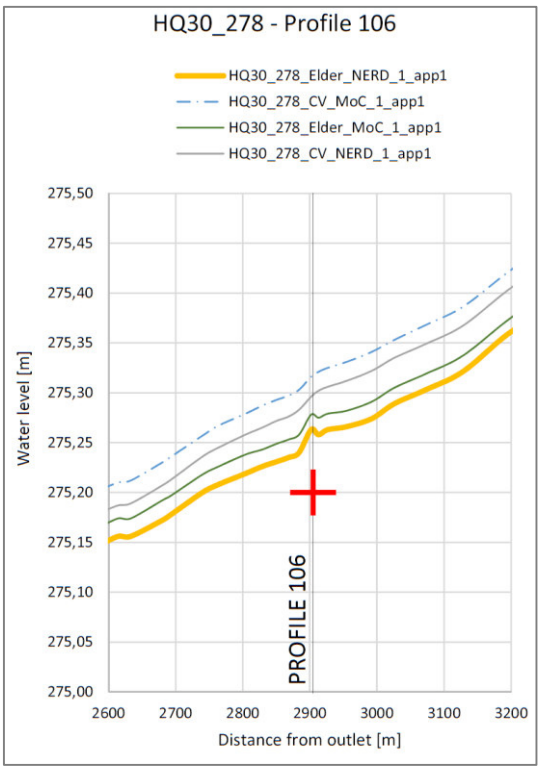

Figure 43 Calibration - HQ30 - Water surface profile in Profile 106

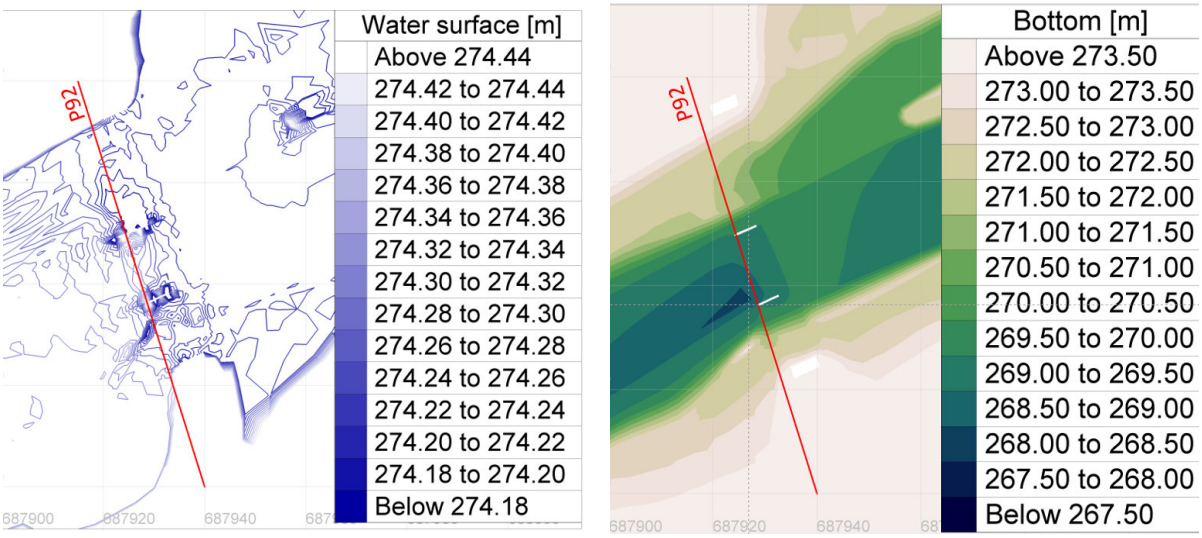

Figure 44 Water and bottom surface at P92

Table 8 Calibration – comparison of water level HQ30

Measuring location	Simulation	H [m.a.s.l.]	ΔH [m]
PROFILE 106	HQ30_278_CV_MoC_1_app1	275,317	0,117
	HQ30_278_Elder_MoC_1_app1	275,277	0,077
	HQ30_278_CV_NERD_1_app1	275,297	0,097
	HQ30_278_Elder_NERD_1_app1	**275,262**	**0,062**
PROFILE 92	HQ30_283_CV_MoC_1_app1	274,400	0,24
	HQ30_283_Elder_MoC_1_app1	274,384	0,224
	HQ30_283_CV_NERD_1_app1	274,337	0,177
	HQ30_283_Elder_NERD_1_app1	**274,331**	**0,171**

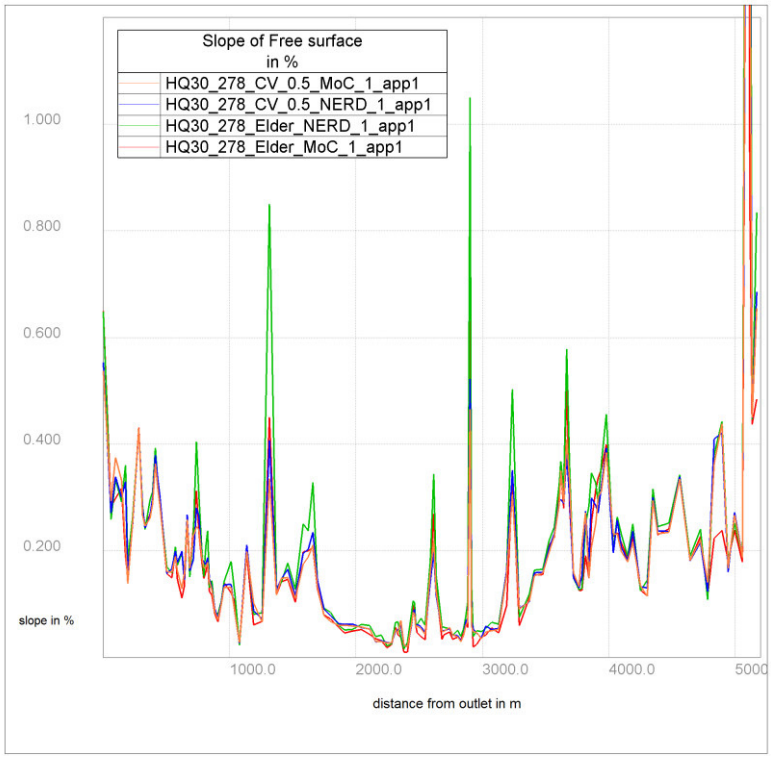

Figure 45 Slope of water surface profile along the channel

Elder model combined with the NERD scheme delivers water levels with steeper and faster changing slopes than others. In general, with NERD scheme water level slope changes faster, this confirms the less diffusive behavior of the scheme. This is presented in Figure 45. Figure 45 additionally contains the average slope of water surface along the channel.
One assumes that turbulence model of Elder in combination with advection scheme NERD delivers the best results (HQ30_278_Elder_NERD_1_app1 and HQ30_283_Elder_NERD_1_app1). Thus, further investigations are based on that findings.

6.3.5 Sensitivity analysis

Due to the results of calibration roughness approach 2 and mesh 2 were applied in combination with the proven turbulence model and advection scheme. These settings are chosen to observe changes of results and in turn assess the sensitivity of the model.

- HQ30_278_Elder_NERD_1_app1
- HQ30_278_Elder_NERD_1_app2
- HQ30_278_Elder_NERD_2_app1

- HQ30_283_Elder_NERD_1_app1
- HQ30_283_Elder_NERD_1_app2
- HQ30_283_Elder_NERD_2_app1

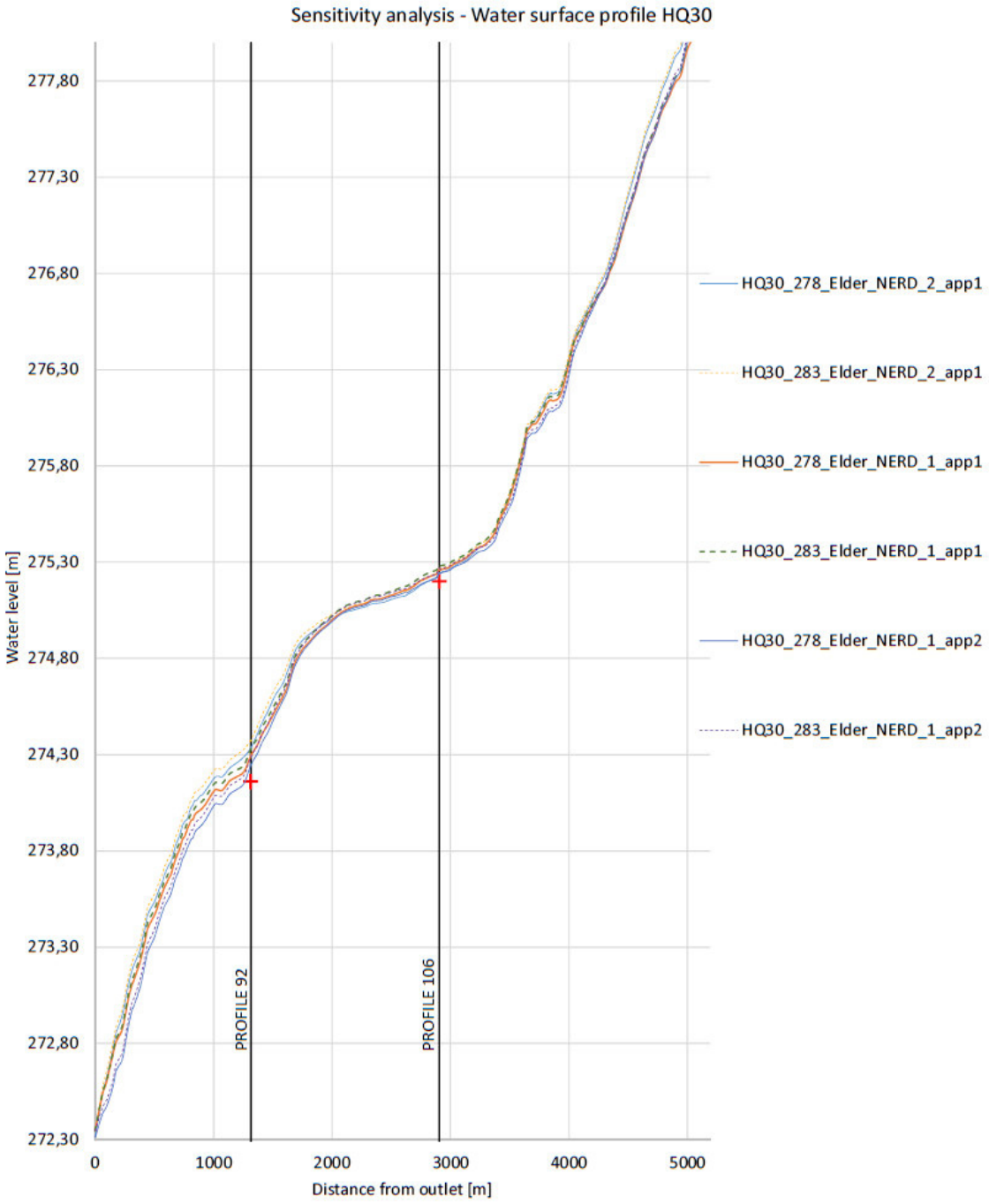

Figure 46 Sensitivity analysis – HQ30 – Water surface profile

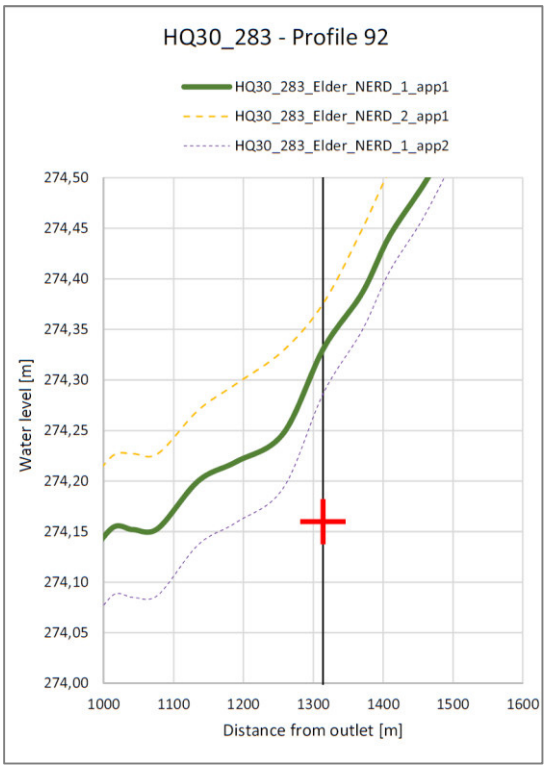

Figure 47 Sensitivity analysis - HQ30 – Water surface profile in P92

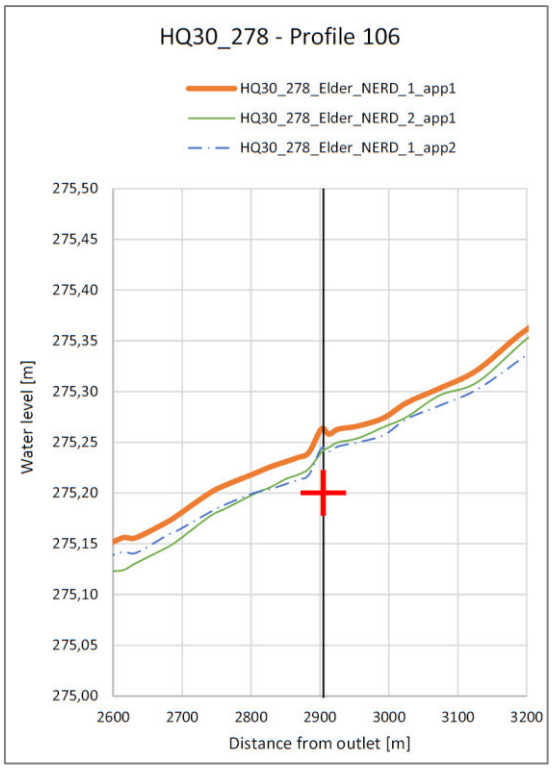

Figure 48 Sensitivity analysis - HQ30 – Water surface profile in P106

In Table 9 water levels and deviations from simulation HQ30_278_Elder_NERD_1_app1 are listed. Approach 2 with Strickler Value of $25\frac{m^{1/3}}{s}$ gives very similar results. Water surface profile along the channel is constantly below the surface profile of approach 1. Except between P95 and P102 and P117 and P122 approach 1 and approach 2 brings very similar results. This is because of the increased cross section due to overstepping of the channel edges and flooding of foreland. Thus, channel roughness hardly influences the water surface.

Comparing mesh 1 and mesh 2, that results of the two meanders are again very similar. In the area where water is more restricted to the channel the rough banks have greater influence. This causes higher water level in the simulation with mesh 2. However, differences between the results are very low and thus the proven model and scheme remains valid.

Table 9 Sensitivity analysis– comparison of water level HQ30

Measuring location	Simulation	H [m.a.s.l.]	$\Delta H = H_{Elder\_NERD\_1\_app1} - H_{Elder\_NERD\_x\_appx}$ [m]
PROFILE 106	**HQ30_278_Elder_NERD_1_app1**	**275,262**	
	HQ30_278_Elder_NERD_1_app2	275,243	-0,019
	HQ30_278_Elder_NERD_2_app1	275,241	-0,021
PROFILE 92	**HQ30_283_Elder_NERD_1_app1**	**274,331**	
	HQ30_283_Elder_NERD_1_app2	274,287	-0,044
	HQ30_283_Elder_NERD_2_app1	274,376	0,045

Even the water level with roughness approach 2 is closer to the comparative values, one continues with Strickler value of $k_{St} = 29\frac{m^{1/3}}{s}$ or $k_{St} = 30\frac{m^{1/3}}{s}$. This is justified by the fact meander 1 does not represent whole study area well. In addition, the slope in meander 1 is less steep than in the rest of the area. This is caused most likely by sediments with greater diameter.

Mesh 2 is not an option since it falsifies real ground conditions.

6.3.6 Validation

HQ100 is chosen for validation. Just one advection scheme with the following settings.

- Turbulence model – Elder Model (Elder) and Constant Viscosity Model (CV)
- Advection scheme – NERD
- Mesh 1
- Roughness approach 1

The analyzed simulations are:

- HQ100_342_Elder_NERD_1_app1
- HQ100_342_CV_NERD_1_app1
- HQ100_348_Elder_NERD_1_app1
- HQ100_348_CV_NERD_1_app1

Figure 49 to Figure 51 presents the water surface profiles at HQ100. The measured values at the relevant profiles are given in Table 10 Validation – comparison of water level HQ100Table 10.

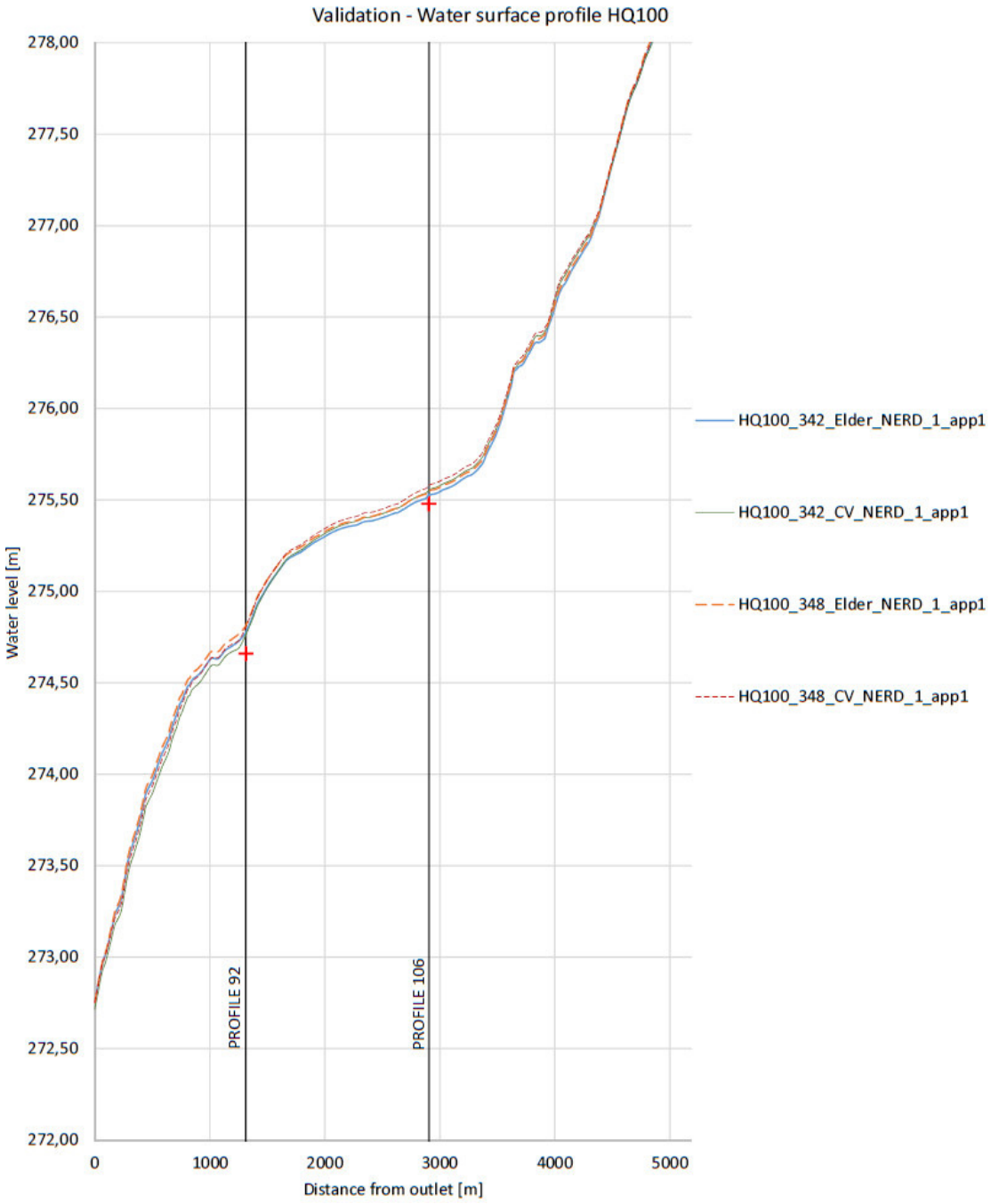

Figure 49 Validation – HQ100 – Water surface profile

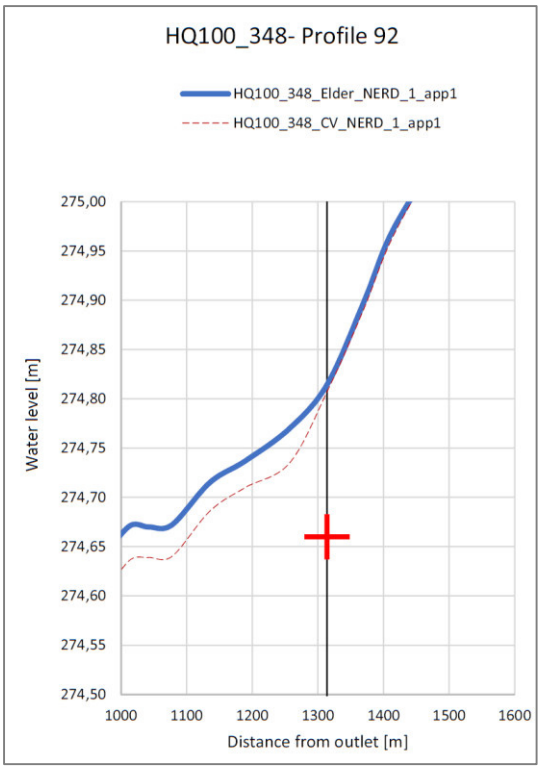

Figure 50 Validation – HQ100 – Water surface profile in P92

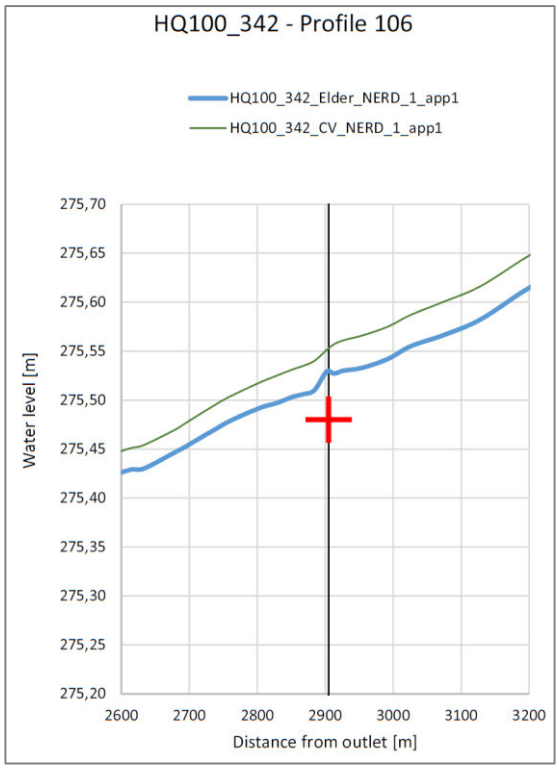

Figure 51 Validation – HQ100 – Water surface profile in P106

Table 10 Validation – comparison of water level HQ100

Measuring location	Simulation	H [m.a.s.l.]	ΔH [m]
PROFILE 106	**HQ100_342_Elder_NERD_1_app1**	**275,529**	**0,049**
	HQ100_342_CV_NERD_1_app1	275,552	0,072
PROFILE 92	**HQ100_348_Elder_NERD_1_app1**	**274,815**	**0,155**
	HQ100_348_CV_NERD_1_app1	274,808	0,148

In case of HQ100 simulation with Elder Model and NERD scheme show water levels closer to the comparative values than Constant Viscosity Model. That leads to the assumption that calibrated parameters might give sufficiently accurate results.

6.3.7 Summary

Results of simulations executed for calibration, sensitivity analysis and validation presents small differences in profile P92 and P106. Which settings are chosen for the subsequent analysis depend only on water level at that profiles. The simulation settings, which deliver the result values closest to the comparative value is taken for further simulations.

The results of calibration, sensitivity analysis and validation are seen as adequate and allow further morphological investigations. However, the quality of the comparative values used for the calibration and validation is questionable because the used values stem from a previous simulation. The simulations´s results in the study area are not compared with field measurements. The nearest comparative values are given by the measuring stations Gleinstätten and Leibnitz. To use these values, the study area would have to be expanded. This would lead to an enormous additional expense and data requirement.
Therefore, the available data are taken and the following simulation settings are recommended:

- Mesh 1
- Roughness approach 1
- Elder Model
- Nerd scheme

6.4 Hydromorphological survey

Now the hydromorphological impacts of several flow events are analyzed. Simulations are based on the settings listed in 6.3.7. Due to simplification, simulations are named according to the simulated flow event. The name of the applied turbulence model, advection scheme, mesh and roughness approach are not mentioned anymore.
The area for the hydromorphological analysis extends from the bridge in Heimschuh (P124) where L604 Arnfelserstraße crosses the Sulm to Eisernersteg (P92). For the assessment, the study area is divided into four sections. The section which presents meander 1 is assessed qualitatively. Therefor critical shear stresses are obtained as explained in 6.4.1.

6.4.1 Identification of incipient motion

To determine the grain size distribution, the line pebble counting method is chosen and supplemented subsequently by the Fuller line to obtain the full grain size distribution curve. Within this case study nine samples were implemented at four locations to get a representative grain size distribution curve for meander 1. The locations of sampling are marked in Figure 52. Six linear sediment samples were taken at location 1 in June 2016 within the lecture “River and Sediment hydraulics”. During the lecture, an Acoustic Doppler Current Profiler (ADCP) was used to measure velocity conditions, at a profile immediately downstream of Stegannerlbrücke (P106). The obtained discharge on that day was about $6\,{}^{m^3}/_{s}$ and thus is below the medium flow rate MQ. Sample VII to IX where taken on location 1,2 and 3 in July 2016, while discharge was not measured on that day.

Figure 52 Location of sample collection

Out of the evaluated distribution curves (Figure 53), characteristic grain size diameters are obtained for each location (Table 11).

Table 11 Characteristic grain sizes

Location	d_m [mm]	d_{50} [mm]	d_{90} [mm]
1	18,3	19,3	42,3
2	22,3	22,5	49,5
3	22,7	18,2	48,5
4	20,2	20,2	54,1

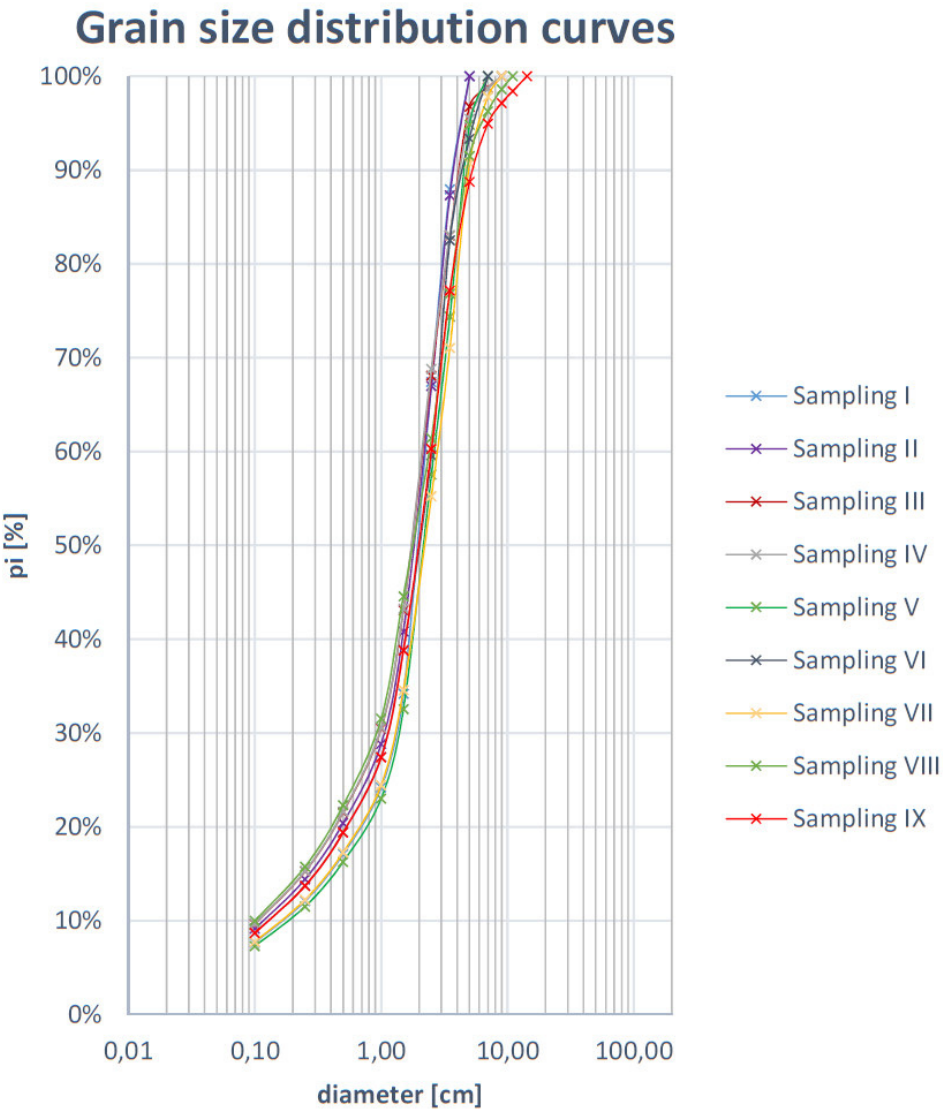

Figure 53 Grain size distribution curves

Since the curves slightly differ from each other, the decision to create an average characteristic diameter $d_{m,m}$ has been choosen. This value represents the effective grain size diameter for the area of meander 1 and is subsequently applied to calculate critical shear stresses. In this master thesis the incipient motion is described by SHIELDS approach. Critical shear stress τ_{crit} and critical friction velocity u^*_{crit} are obtained by the following formula.

$$\tau_{crit} = \theta_{crit}(\rho_s - \rho_W) g d_{m,m} \tag{33}$$

$$u^*_{crit} = \sqrt{\frac{\tau_{crit}}{\rho_W}} \tag{34}$$

The set value for the non-dimensional critical shear parameter θ_{crit} is 0,047 as recommended by MAYER-PETER-MÜLLER. The results of the mentioned formulas in shown in Table 12.

Table 12 Incipient motion in meander 1

$d_{m,m}$ [mm]	T_{crit} [N/m²]	u_{crit}^* [m/s]
19,5	14,80	0,12

6.4.2 Analysis

To make it more clear the study area is divided into four sections as depicted in Figure 54. Except meander 1, analysis of the study area is done qualitatively, as there is lack of information concerning channel resistance and bed material. Zones with relatively high or low shear stresses are identified and subsequently compared with on-site conditions. On-site conditions are recorded within several field visits in spring 2016. Particular attention was given to visible erosion or sedimentation processes since this are characteristics for morphological changes. For the section of meander 1 (P104 to P101) the obtained effective grain size diameter enables a more detailed statement about hydromorphological processes. An additional tool that supports the assessment are orthophotos provided by Land Steiermark [24].

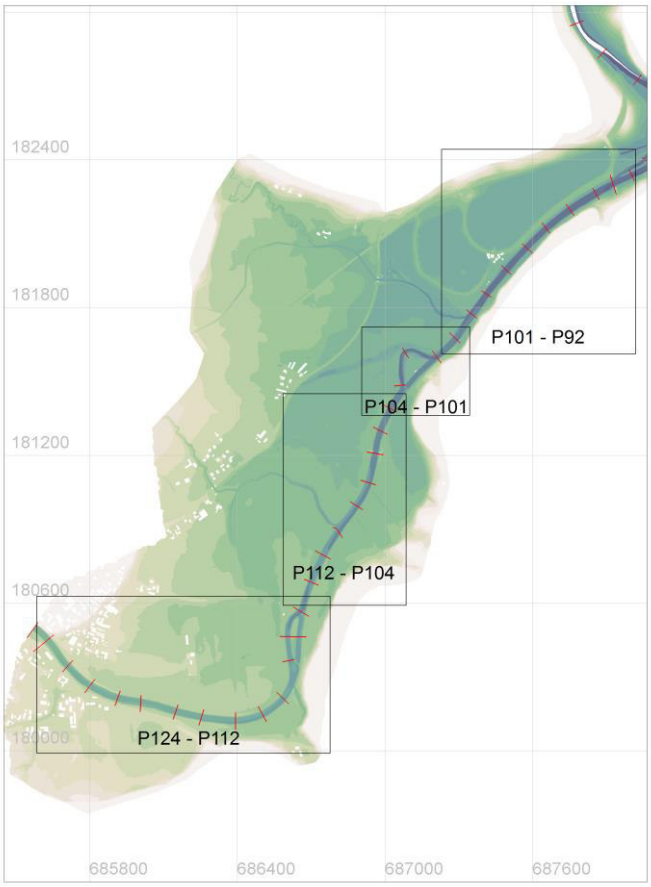

Figure 54 Sections of analysis

The simulations and their settings that are performed and analyzed within this master thesis are given in Table 13.

Table 13 Simulation of the analysis

Flood event	Discharge	Tubulence model	Advection scheme	Mesh	Roughness
MQ	8,85	Elder	NERD	1	app1
HQ1	95	Elder	NERD	1	app1
HQ5	160	Elder	NERD	1	app1
HQ10	205	Elder	NERD	1	app1
HQ30	278	Elder	NERD	1	app1

Special attention is given to channel forming discharge. It is the most relevant discharge for hydromorphological changes. According to literature [7] channel forming discharge is between HQ2 and HQ5. HQ2 is not given for this study area, hence, discharges between HQ1 and HQ5 are taken as channel forming discharge.

6.4.3 Results and conclusion

In the following paragraphs, the results of each section are examined and discussed separately from upstream to downstream. The location description is indicated with profiles as given in Figure 31. For the assessment made on-site, the location is well described by the before mentioned profiles but since the profiles are not exactly localized, deviations from the exact profile locations may arise.

It has to be mentioned that the simulation refers to morphological conditions of 2007. Now, nine years later it is assumed that dynamic processes identified of simulations are already taking place. Thus, the on-site assessment is an evidence if predicted processes as they are derived from numerical results occur.

Shear stress distribution over the whole study area are attached in appendix A. The descriptive terms -left and right- always apply the view in current direction. For better clarity, assessments made in field survey are written in *italics*.

<u>Section P124 to P112</u>

This section starts at the bridge in Heimschuh and ends directly downstream of meander 2.

According to numerical results, bed shear stresses are higher between Heimschuh (P124) and meander 2 (P114) compared to the rest of the study area. Remarkable high bed stresses are between P124 and P123, P120 and P119 and at P115. These are caused by steeper slopes.

In Heimschuh the river turns right. Between P124 and P123 the river becomes straight before bending to the left. Thalweg is shifting from the left to the right side of the channel. The bend causes increased shear stresses at the left side, which is the outer bank. During and field survey in April 2016 a gravel bank on the right side of the river bed at P124, is noticed (Figure 55). The gravel bank extends downstream of the bridge and is a result of decreased shear stresses in the inner side of a bend.

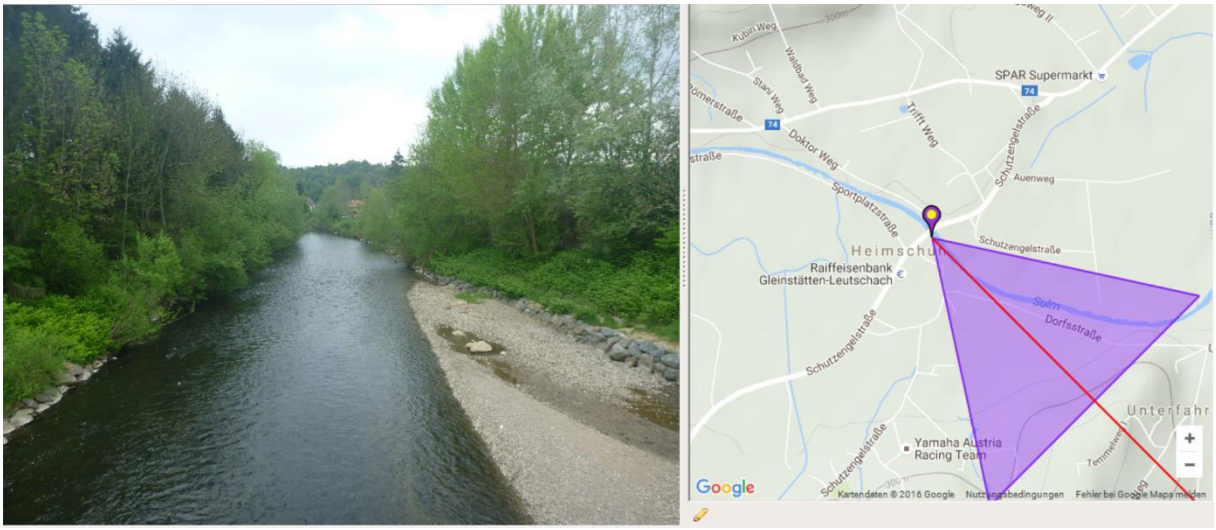

Figure 55 View downstream of P124

In the area of Heimschuh banks are protected with stones to prevent erosion. Between P120 and P119 an additional constriction of the channel generates increased shear stresses at bed and banks. *Steep banks on both sides are observed (*Figure 56*). Increased bottom level is identified on the left side of the channel between P121 and P120 (Figure 57) and on the right side downstream of P119 (Figure 58) where the channel becomes wider again.*

Figure 56 Steep bank between P120 and P119

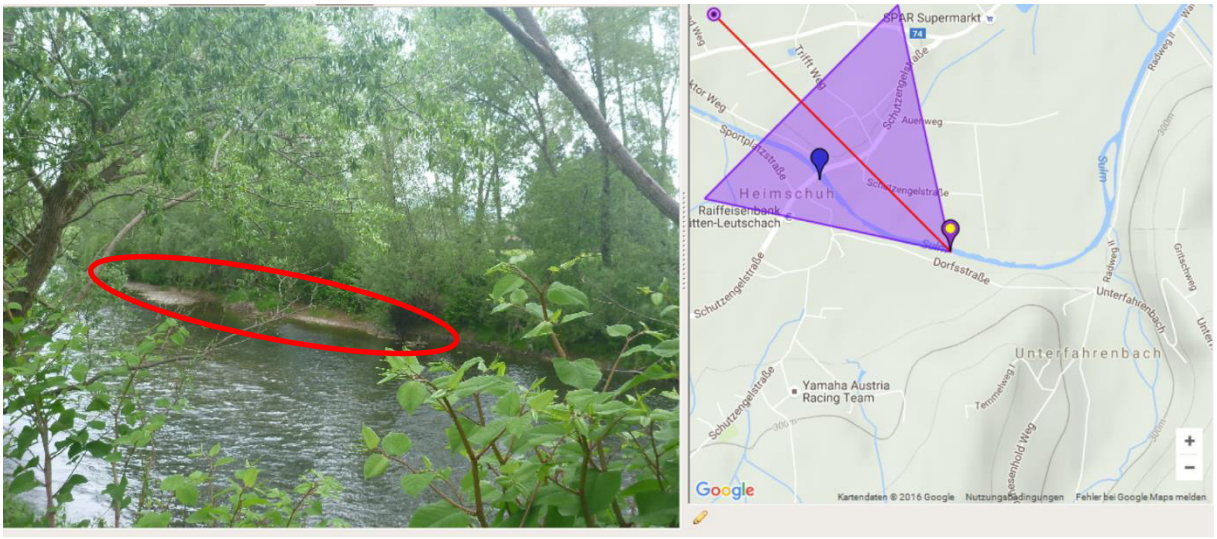

Figure 57 Sedimentation between P121 and P120

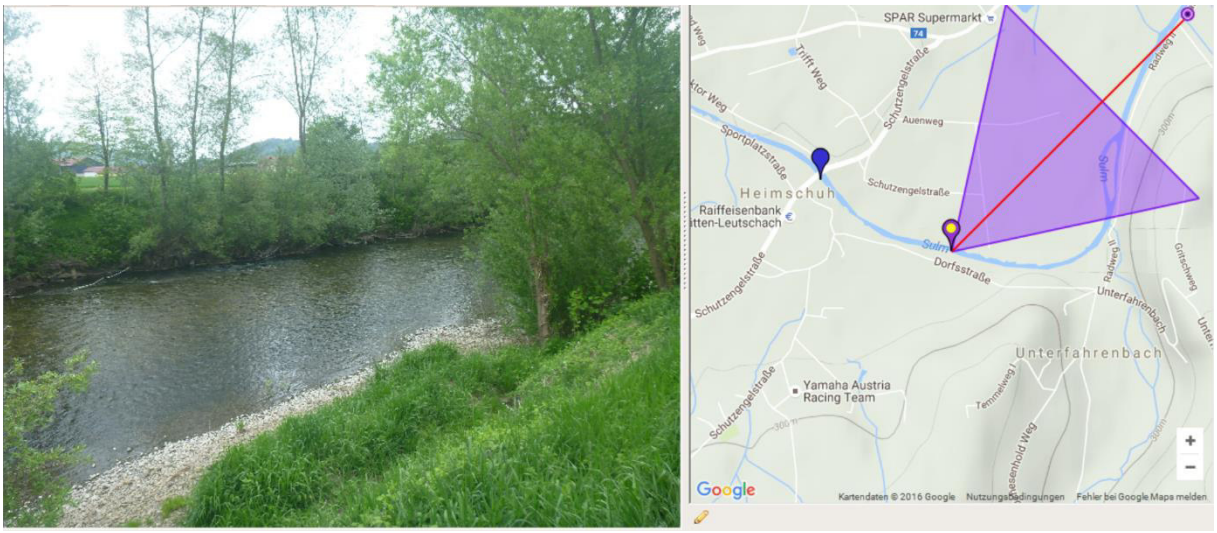

Figure 58 Sedimentation immediately downstream of the narrowing at P119

Increased bank shear stresses are calculated along the complete outer bank of the left bend between P117 to P115. High values are given at P115 in special. *Steep banks are observed on the right side, sedimentation on the left side and substantiate the numerical results. Steep banks are protected by pile walls and stones, which limit dynamical processes.*

Figure 59 Steep outer banks and smooth inner banks at between P117 an P116

Relatively low values of shear stresses are observed immediately upstream of meander 2 between P115 and P114. This let assume deposition of sediments. *A big gravel island with partial vegetation is observed in the field survey (Figure 61). Orthophotos show the development of meander 2 (*Figure 60*).* Comparison of the model with the latest orthophoto proves ongoing sedimentation.

Recording period 2008-2011	Recording period 2011-2013	Recording period 2013-2015

Figure 60 Development of meander 2 [24]

Sedimentation might be promoted by a stone groyne that is located upstream the deposition zone. It directs the stream to the left bank. A discharge is concentrated on the left side and causes steep banks. Downstream the groyne on the right side, zones with decreased velocities occur and lead to sinking the sediments.

Figure 61 Gravel island and the upstream located stone groyne between P115 and P114

At MQ water does not leave the main channel, hence, no water overflows the dam and the bypass channel shows no shear stresses. Instead, water masses are accelerated downstream the gravel island (P114) due to constriction of the channel. This effects high shear stresses and in lead to scour on the left side.

At higher discharges, the upstream end of the meander island is extremely exposed, due to current and high shear stresses, that occur where the channel is separated. From HQ1 the bypass channel is flushed and water flows over parts of the dam. In the main channel the right bank is prone to erosion.

From discharge of HQ5, the whole dam is overflowed. Due to increased water depths, the meander island becomes flooded more and more and the location of stream separation is shifted downstream. Areas of high shear stresses on the island extend downstream. Bank shear stresses on the right side in the main channel decrease since the main channel is released by the bypass channel. Shear stresses on the left bank remain increasingly even if the bypass channel is flushed.

The outer bank of the meander presents steep banks protected by pile walls and dense vegetation.

Shear stress tau [N/m²]
Above 200.00
150.00 to 200.00
125.00 to 150.00
100.00 to 125.00
75.00 to 100.00
50.00 to 75.00
40.00 to 50.00
30.00 to 40.00
20.00 to 30.00
10.00 to 20.00
0.01 to 10.00
Below 0.01

MQ

HQ1

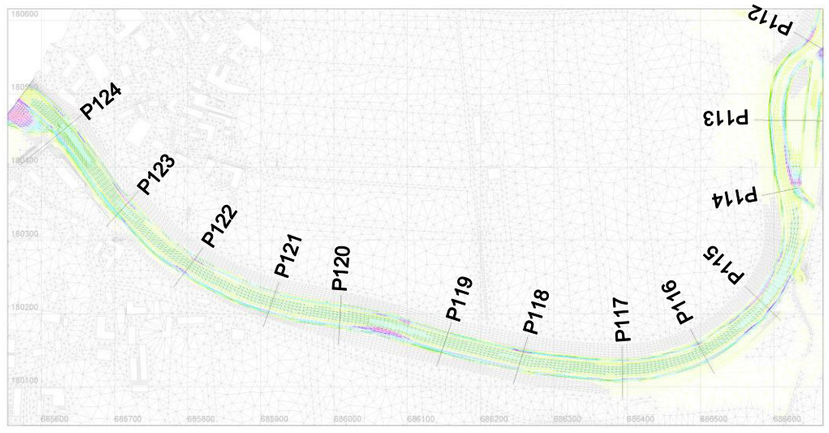

HQ5

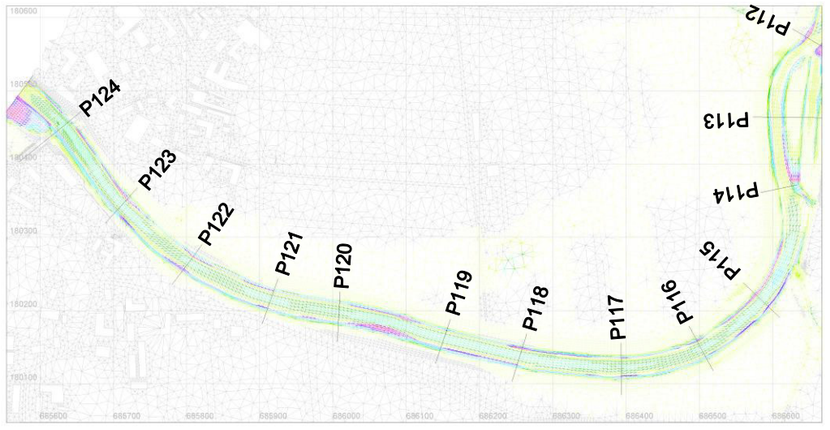

HQ10

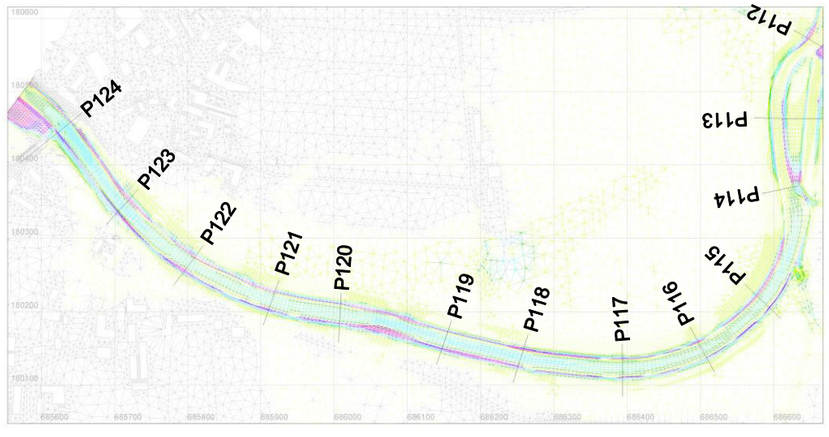

HQ30

Figure 62 Shear stresses between P112 and P124

Section P112 to P 104

The section P112 to P104 starts downstream of meander 2 and ends immediately upstream of meander 1.

Downstream the meander island (P112), the water of the main channel and bypass channel reunites again and continue in a tighter channel. Constriction causes increased velocities and shear stresses. Numerical simulation from HQ5 shows increased shear stresses on the right side of P112. *There the bottom level is higher due to deposited material.* The calculated shear stresses indicate a flood with a recurrence interval bigger than 5 years might washes away this island.

The raised channel elevation is caused by sedimentation. Upstream of junction point of the two channels, backwater is generated and lead to lower velocities. The material, which is transported through the bypass channel is deposited. *Furthermore,* d*eposition is observed in the field visits as well and presented in Figure 63.*

Figure 63 Deposition downstream of the bypass channel

Between P112 and P111 an inclined tree groyne (Figure 64) redirects the stream to the center of the channel and promotes sedimentation upstream.

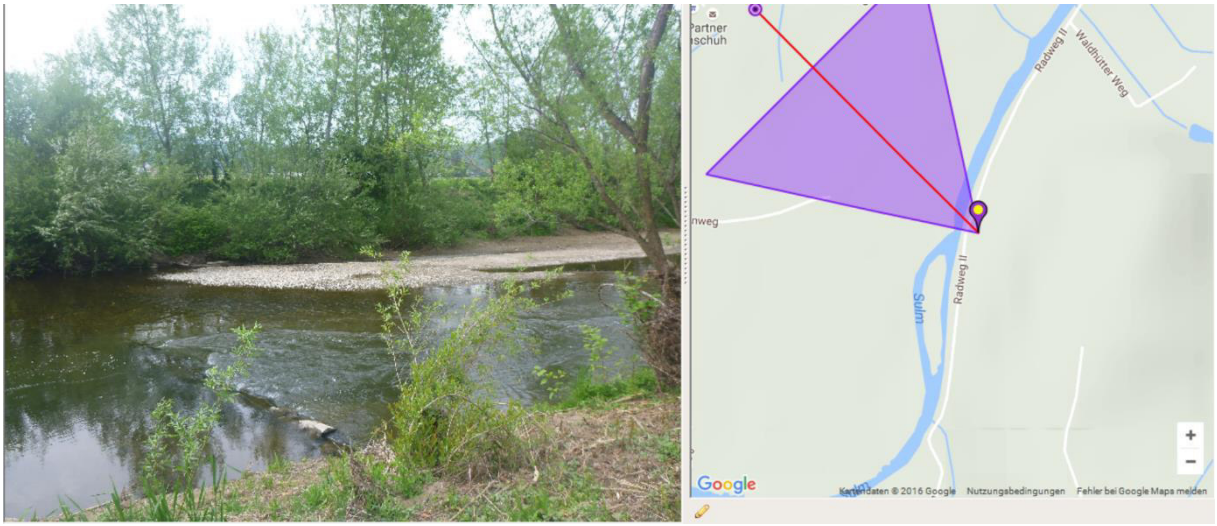

Figure 64 Tree groyne between P112 and P111

Between P109 and P108 the Wöllinggrabenbach joins the river Sulm. *In the field survey deposition of sediments is observed at the mouth of tributary. According to* [15] *upstream located tree groynes should redirect the stream at low discharges to the left. This would lead to concentrated current on the left and hence, minimize sedimentation at the mouth of the tributary. At the time of the field survey, the profile was clogged by woody debris which created a small vertical drop (*Figure 65*).*

Figure 65 Mouth of tributary Wöllinggrabenbach P109

Figure 66 shows the development of the island, which currently occurs at the mouth of the tributary. Even if it shows that before the flood in 2014 the sedimentation area was denser vegetated the orthophotos present the trend to sedimentation. Numerical re-

sults show low shear stresses as well, which increase with higher discharge. But results directly at the mouth of a tributary are treated with caution since in the present simulations discharges of tributaries are not considered.

		
Recording period 2008-2011	Recording period 2011-2013	Recording period 2013-2015

Figure 66 Development of a deposition zone downstream of P109

According to simulation results, the left bank between P109 and P108, which is the outer bank of a big winding shows risk of erosion. The biggest values are calculated at HQ5 and HQ10. *In this area the lower part of the banks is protected by pile walls and not any visible bank erosion is noticed.*

Downstream of P108 the highest bed shear stresses are obtained at HQ5 and HQ1. This is justified by increased velocities in case of the mentioned discharges, since water masses are restricted to the channel and do not leave the stream channel. At higher discharges, the river starts to overtop the channel edges and the channel is released. Groynes between P107 and P106, located on both sides, promote shear stresses in the center of the channel.
At P106 a small ground step causes increased velocities directly downstream of Stegannerlbrücke. The biggest influence is visible at HQ1. Additionally, high shear stresses are given downstream the bridge pier at right river bank. *Therefore*, s*parse vegetation is observed in the field survey and indicates increased shear stresses.*

Numerical results show, the right bank at P104 is prone to erosion at HQ1 and HQ5. *Within the flood protection project several construction measures were applied to protect the left and right banks. These construction measures influence the stream at low discharges.*

Shear stress tau [N/m²]
Above 200.00
150.00 to 200.00
125.00 to 150.00
100.00 to 125.00
75.00 to 100.00
50.00 to 75.00
40.00 to 50.00
30.00 to 40.00
20.00 to 30.00
10.00 to 20.00
0.01 to 10.00
Below 0.01

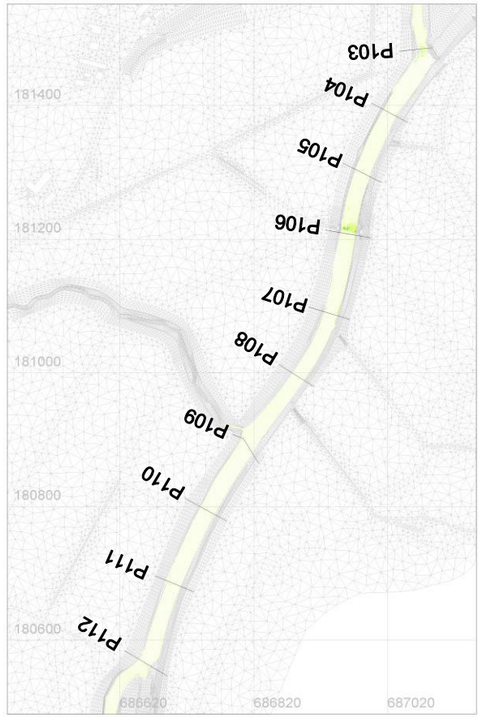

MQ

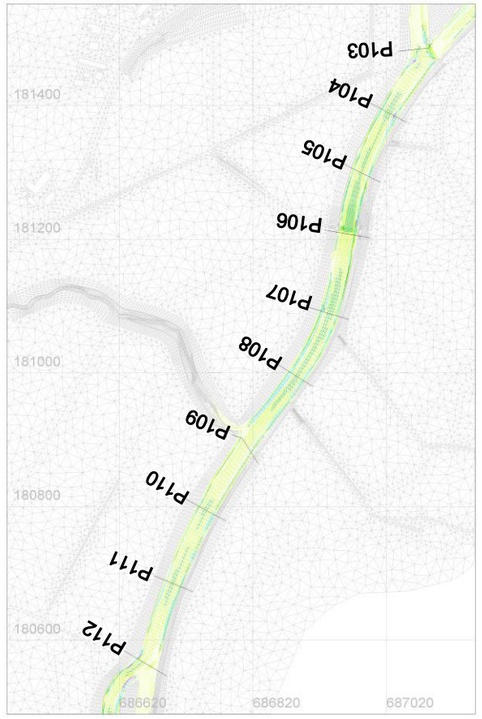

HQ1

HQ5

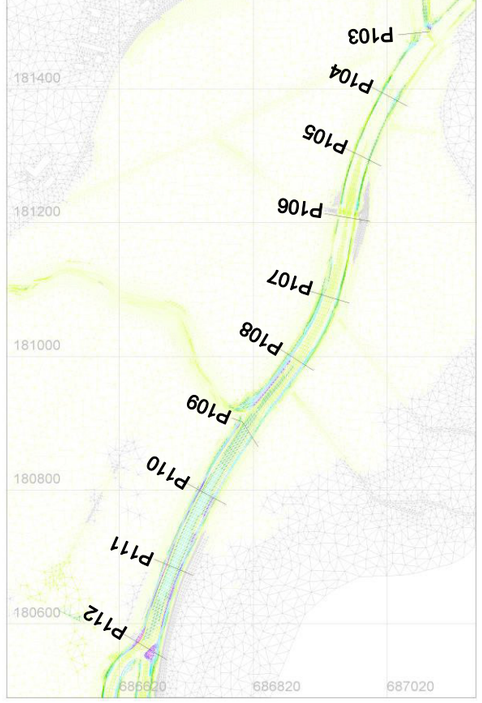

HQ10

HQ30

Figure 67 Shear stresses between P112 and P104

Section P104 to P100 – Meander 1

This section starts approximately 100m upstream and reaches 30m downstream of meander 1. In this section, shear stresses are compared to the critical values obtained in 6.4.1. In Figure 73 the zones where $\tau > \tau_{crit}$ are highlighted. To demonstrate the influence of other hydraulic parameters, water depths and velocities are depicted for each flow event in Figure 74.

The remarkable low bed shear stresses obtained in meanders 1 result from a flatter slope in that area. In meander 1, the channel bed got shifted and extended for about 100m. Consequently, the bed slope decreases. According to numerical results, the bed shear stresses for all flood events are below the critical value τ_{crit} while upstream and downstream the bed shear stresses are higher. This leads to bed aggregation in the meander and to a deficit of a bed load downstream the meander. The increased shear stresses are obtained on the banks. It has to be mentioned that banks are vegetated or covered with construction methods for which τ_{crit} is not valid.

Between P104 and P103 landed up pile walls (Figure 68) indicate sedimentation of fine material on the left banks. This could result from flooding. In the area of overflowing velocities and shear stresses are very low and promote fine materials, that are transported close to the water surface, to sink.

Figure 68 Landed up pile walls

Upstream the meander island at P103 the left bank is prone to erode. This indicates that the increased bottom level on the point bar is washed away by higher discharges.

The developed point bar generates areas of backflow downstream of P103 and supports sedimentation. Beside the g*ravel bank on the left side in P103 two declined tree groynes are observed on-site. The groynes are located between P104 and P103 and intend to direct the current at low discharges from the right to the left side and keeps it away from the dam. At the time of taking samples in June 2016 the groynes where already flooded at a discharge of about* $6\,{}^{m^3}/_{s}$. It is assumed that the influence of the groynes can be neglected for HQ1 and HQ5 and thus have no impact on dynamic processes.

High shear stresses are determined downstream of P103 on the right bank which present the cut-off bank of the left bend.
The result of high shear stresses on the right side downstream of P103 can be seen on-site where slope failure occurs.

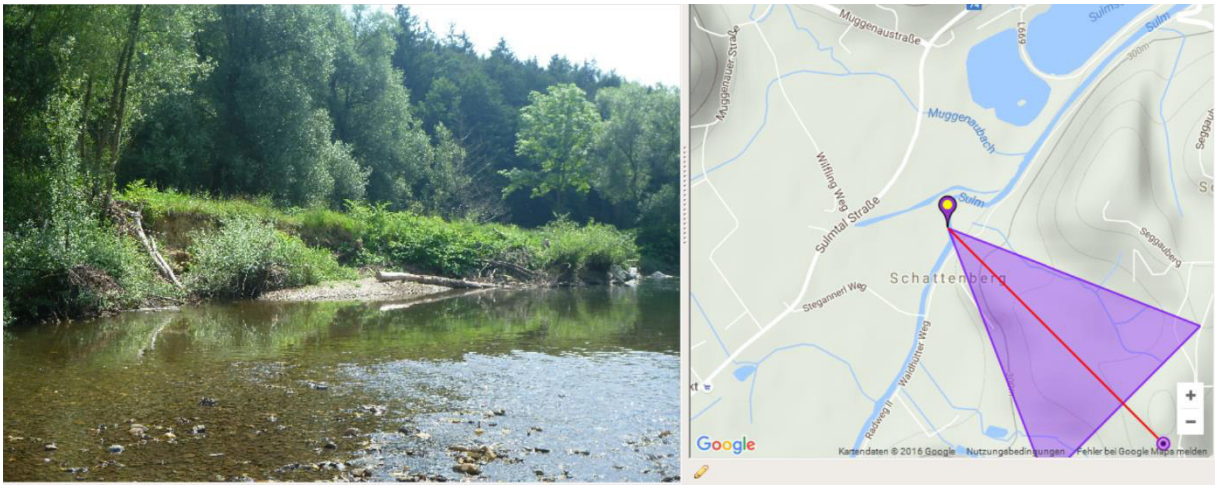

Figure 69 Eroded bank at the meander island

Between P103 and P102 the thalweg moves from the right to the left side of the channel. *The left bank, between P103 and P102 is protected with pile walls, dense vegetation protects the upper part of the banks as depicted in Figure 70. It shows current concentrated on the left side and* increased bottom level in the center of the stream.

Figure 70 Protected outer bank at P102

Further downstream, between P102 and P101, numerical results deliver increased values for the cut-off bank of the right bend. *The erosion is prevented by pile walls. At some of them outflanking is observed (Figure 71). This might be caused by back flowing water masses.*

Figure 71 Outflanking of pile walls at P102

*In the field survey big morphological changes of the meander island are realized. Directly downstream P102 deposition is observed at the right bank followed by slope failure (*Figure 72*)*. It proves the calculated results of HQ1 and HQ5 are right. In the section between P102 and P101 thalweg moves from the left side to the right side of the channel.

Figure 72 Slope failure on the meander island between P102 and P101

From HQ1 the dam is overflown and the bypass channel is flushed. Thus, the dam and the bypass channel are exposed to shear stresses.

Like at meander 2, the area of current separation (right side of P103) is heavily prone to erosion. From HQ5 meander island becomes flooded and the main channel is released. In addition, in the main channel the river oversteps the left channel edge and thus velocity decreases.

Downstream the meander where the bypass channel joins the main channel, low shear stresses cause a deposition of material.

According to numerical results, narrowing of the profile leads to increased shear stresses on the inner and outer banks. *Dense vegetation and stones on the right side protect the banks.*

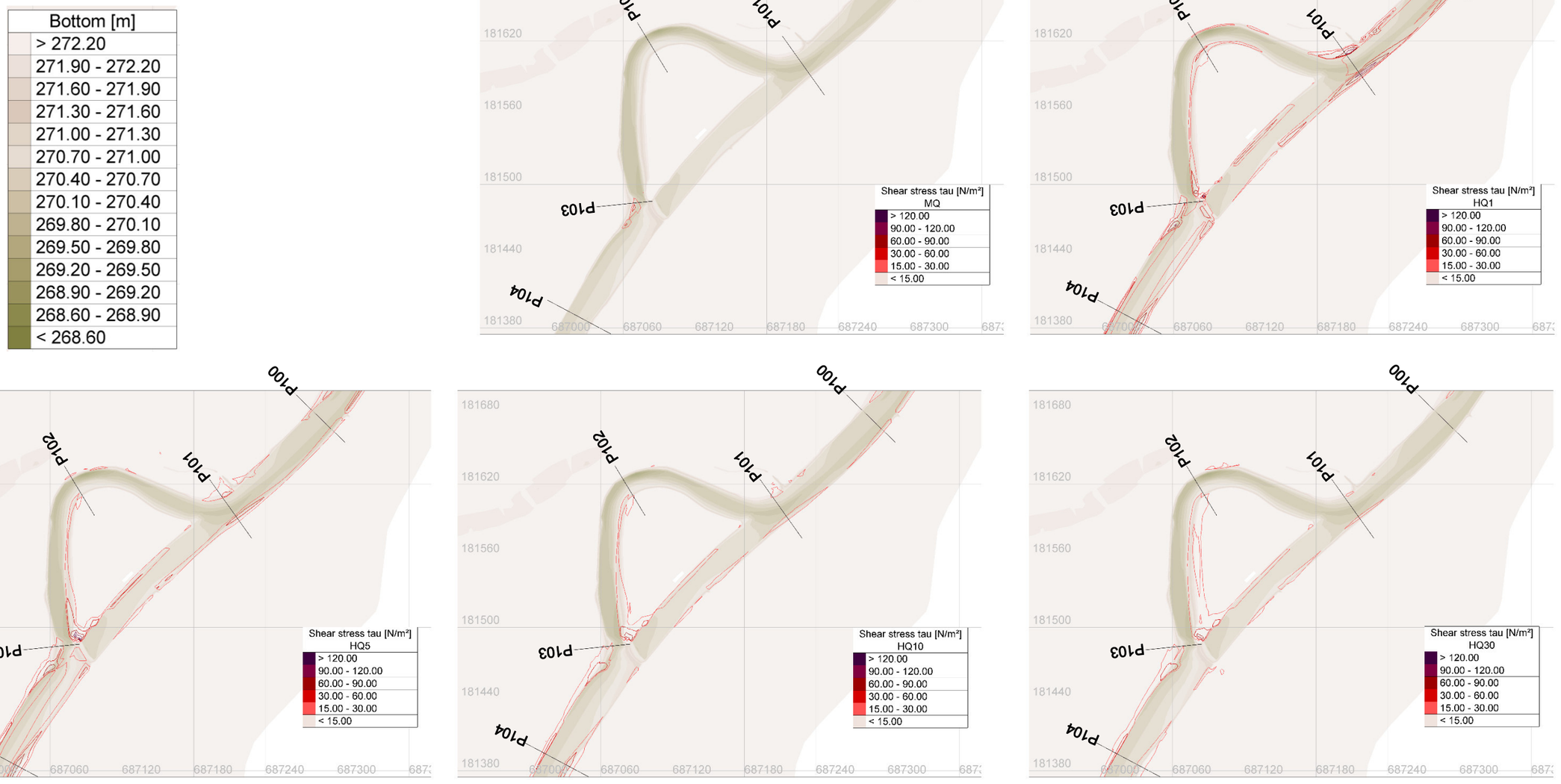

Figure 73 Shear stress in meander 1

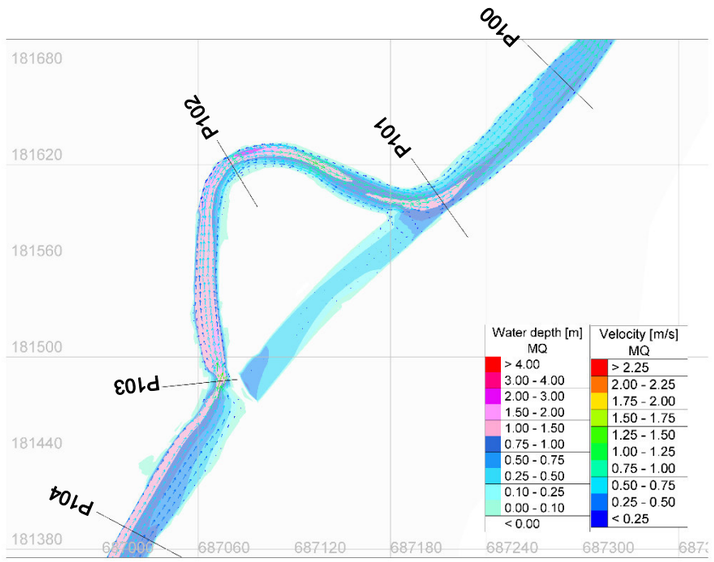

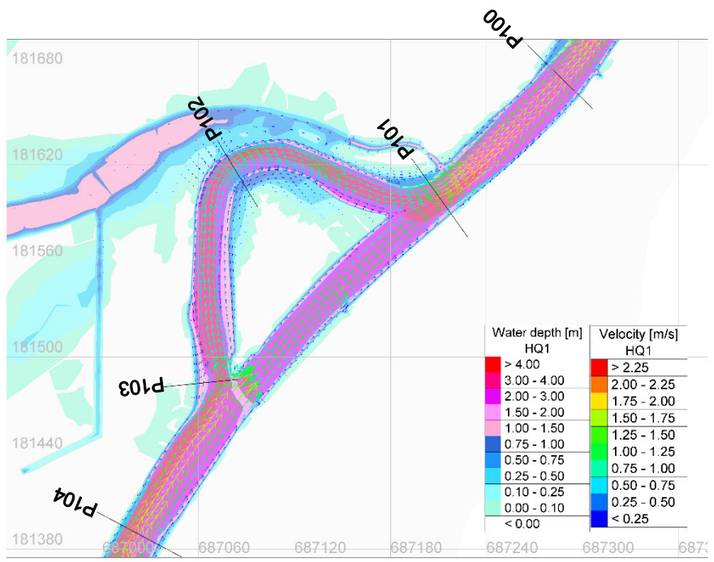

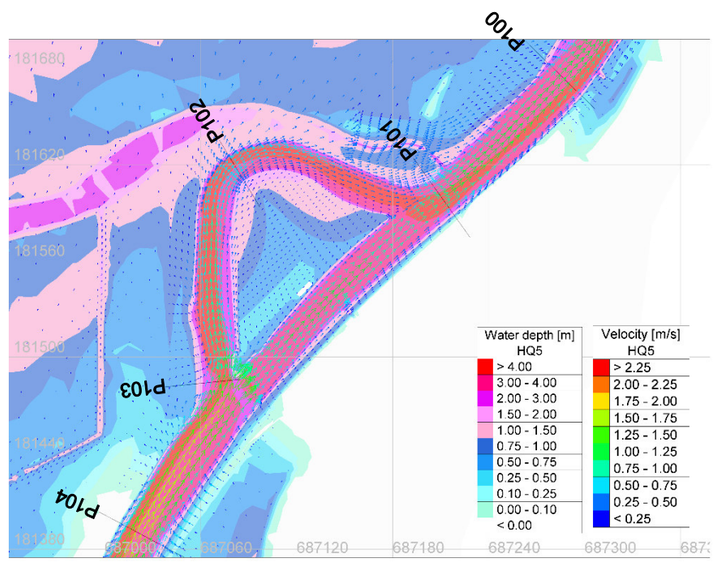

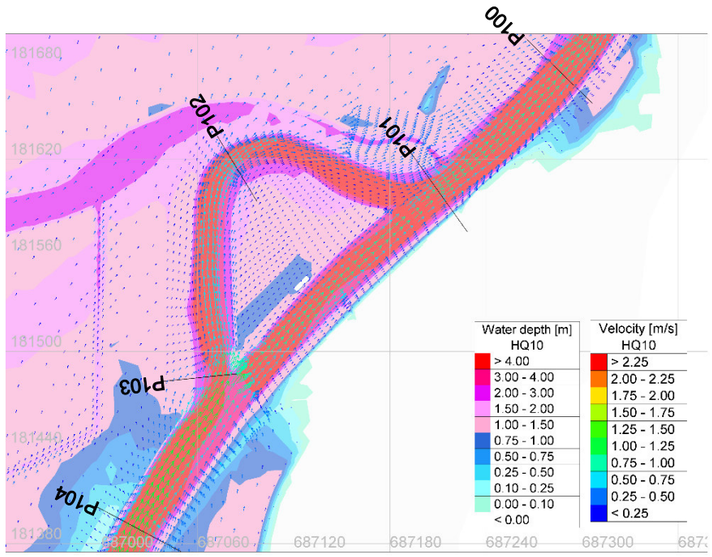

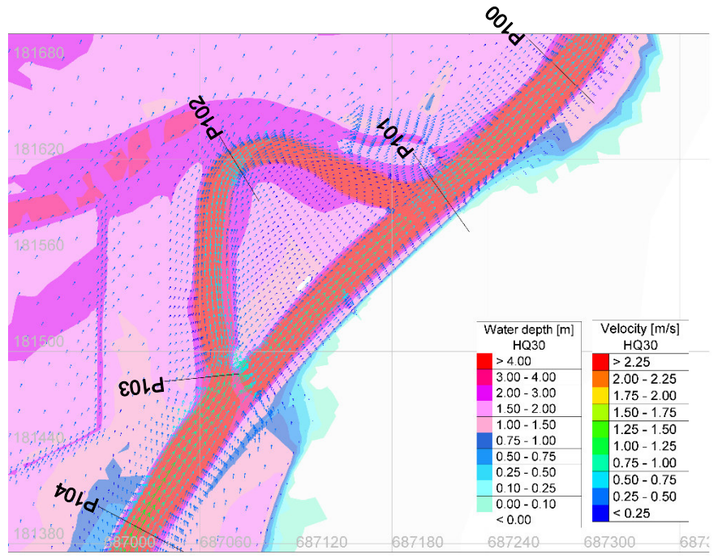

Figure 74 Velocity and water depth in meander 1

Section P101 to P92

This section reaches from meander 1 to Eisernersteg and presents an upstream located left bend between P101 and P98 which merges in a big right bend.
According to numerical results, shear stresses between P101 and P99 are relatively low for discharges greater HQ5. This is caused by overtopping of the channel edges and a big adjacent floodplain area. Downstream P99, the bed shear stresses rise since water masses are restricted to the channel. At HQ1, the water does not overtop the channel edge between P101 and P99 and thus generates highest shear stresses at bed and banks.
Left and right bending of the channel justifies the high shear stresses calculated by TELEMAC 2d. Between P101 and P99 the right bank is more liable to erode, while between P99 and P92 the left bank is affected. *Local erosion is observed on the right bank between P100 and P99 in the field survey. Downstream the meander the right toe of the bank is covered with stones. Where the stone cover ends, local slope failure is noticed. Eroded toes of the bank could be the reason for sliding of the banks.*

Figure 75 Slope failure downstream of meander 1

After a small widening between P97 and P96, the water is restricted to a tighter channel. Geological conditions prevent overbank flow on the right side and thus discharge is forced to the stream channel. Local acceleration of water masses causes higher shear stresses. *Along this section, the toes of the banks are protected by stones, piles or crib walls. Additionally, groynes are installed on the channel´s left and right side thus, induces local narrowing of the channel. At some locations, the banks present*

*poor vegetation. For example, between P97 and P96 (*Figure 76*). This could be an indicator of high shear stresses.*

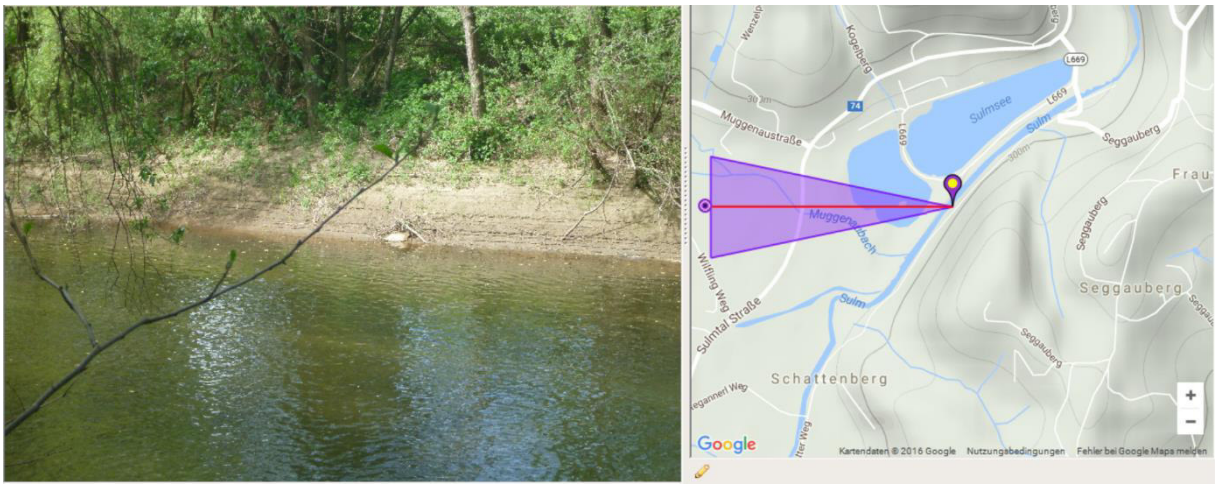

Figure 76 Poor vegetated river bank between P97 and P96

Shear stress tau [N/m²]
Above 200.00
150.00 to 200.00
125.00 to 150.00
100.00 to 125.00
75.00 to 100.00
50.00 to 75.00
40.00 to 50.00
30.00 to 40.00
20.00 to 30.00
10.00 to 20.00
0.01 to 10.00
Below 0.01

MQ

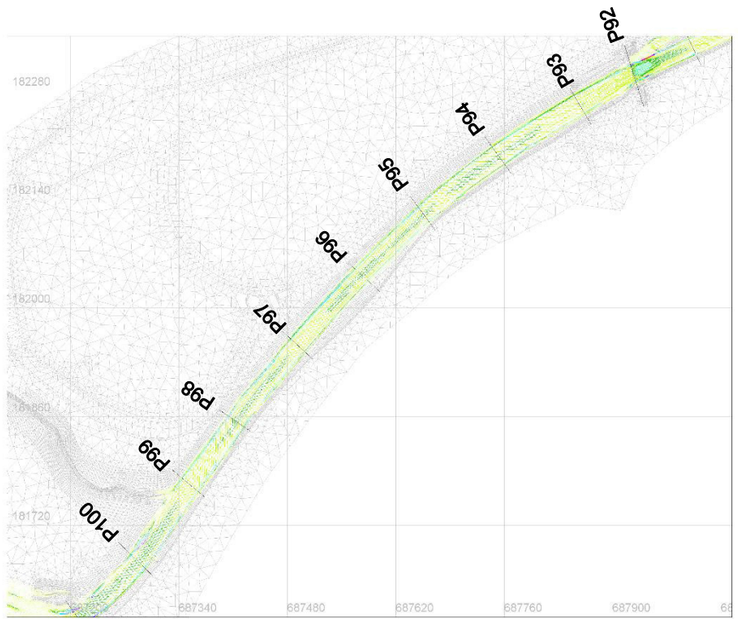

HQ1

HQ5

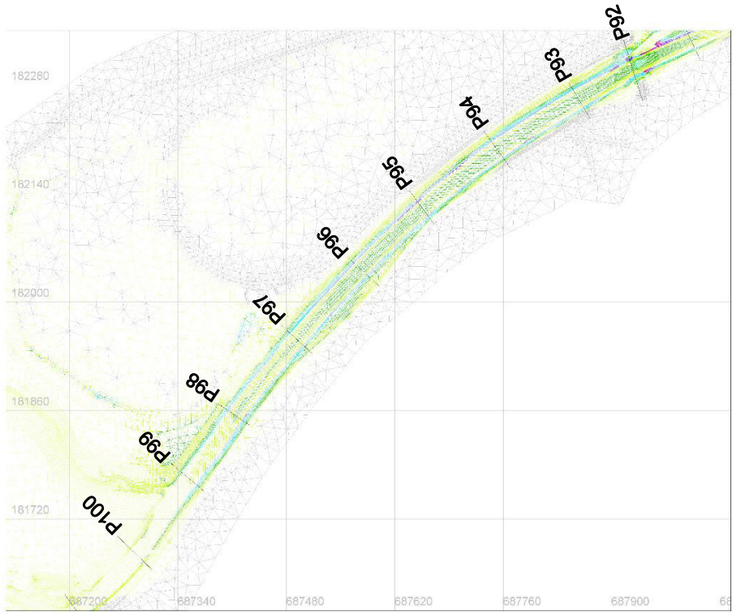

HQ10

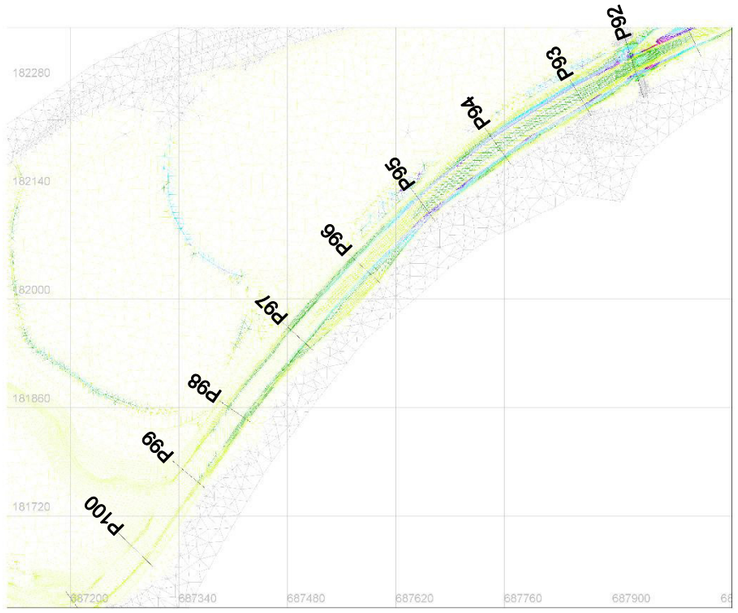

HQ30

Figure 77 Shear stresses between P101 and P99

Conclusion

The shear stresses obtained in the numerical calculations are locally high enough to cause erosion but in almost all locations protection measures or intensive vegetation seems to be sufficient to prevent erosion. Even if it is intendent that the river is free to move and modify, the river hardly has any opportunities to do that. That's why from today's view no changes of plan view are expected.

The monitoring program performed between 2000 and 2003 showed that within the first three years of existence, the channel bottom increased over the whole stretch. This behavior was expected after channel widening. Additionally, the water surface wide decreased. [22] According to the results gained in this master thesis it is assumed that stretch-wide sedimentation processes are completed. A shear stress between 10N/m² and 30 N/m², as it predominantly occurs at HQ1 and HQ5 corresponds to an effective diameter d_m of 1.31cm to 3.94cm. It is quite conceivable that the effective diameter lays in this range hence, neither erosion nor sedimentation occurs as a predominant process. This would mean that sedimentation processes as they occurred in the first three years after completion stopped.

If the channel now is in equilibrium or not cannot be assessed without a survey of current channel conditions.

Sedimentation, which occurs at the mouth of Wöllinggrabenbach is rated critically since it possibly leads to a backflow in the tributary in case of flood and may promotes flooding conditions. Except the mentioned location and meander 1 and 2, all other areas of sedimentation are assumed to be temporary and are reshaped or washed away during floods.

It is striking, that shear stresses are very low in meander 1 compared to the rest of the stretch. It is alarming that not any discharge produces shear stresses, which are high enough to generate erosion. On a long-time perspective it leads to silting up.

Due to flushing of the bypass channel the profile area of discharge increases and thus, the velocities and shear stresses in the main channel decrease with an increasing discharge. Of hydromorphological point of view the bypass is flushed too early but a later start of flushing involves negative effects on flood protection.

In addition to silting up of the main channel in meander 1, lower shear stresses even occur right in front of the dam which lead to an increasing bottom level. As a result, the dam already gets flooded by low discharges. A greater fear regarding to sedimentation is given upstream of meander 2 where already a big gravel island has developed. Generally, it can be said that the mentioned problems of meander 1 are valid for meander 2 as well but there they are less significant.

The morphological change of the meander 1 can be observed in series of orpthophotos taken in the period between 2003 and 2015 (Figure 78).

Recording period 2003-2007

Recording period 2008-2011

Recording period 2011-2013

Recording period 2013-2015

Figure 78 Morphological change of meander 1 [24]

Recording period 2003-2007 approximately shows the conditions which the simulations are based on. Recording period 2013-2015 more or less presents current conditions. A flood occurred in September 2014 could be the reason for modification. The gravel island, which is noticeable on the downstream side of the meander island, captured in the recording period 2011-2013 disappeared. In the latest orthophoto the meander island is poorer vegetated and it seems that sediments cover parts of the surface. This indicates the settlement of fine material which might has remained of the flood in 2014.

The erosive potential that exists on the left bank in the main channel indicates that the river tends to morphologic modification. But this is prevented due to bank protection measures. From today's view, except of the outflanked bank in P102 protection is guaranteed along this section.

The big modifications that occur on the meander island within the last years present the natural dynamic processes and are welcome. Due to the erosive processes between P102 and P101 which can be observed in the orthophotos as well as in the numerical results, sediments are transported downstream. This may prevent sediment deficit downstream meander 1. From today´s view, poor vegetation on the downstream pointing side of the island let assumed that erosive processes will continue.

7. Experiences and discussion

To conclude the present work, the experiences gained while working with the numerical model in this case study are summarized and discussed.

The present HN-model contains uncertainties due to the quality of comparative values used for calibration and validation. According to the results of this processes the model is assumed to be satisfying. But values taken from previous simulations are already containing errors and thus present an additional source of error for the current simulation. **For future projects it is recommended to use comparative values obtained from field measuring.**

In case of any hydraulic investigations the sensitivity of a HN-model should be examined with hydraulic parameters that influence the results one is interested in. In case of hydromorphological survey, velocity is an appropriate parameter since it influences shear stresses significantly. For the present work, besides water depth additional applications of velocity would increase the value of the sensitivity analysis.

In addition, better results can be achieved by **setting additional boundary conditions for tributaries**. Additional hydrographs for tributaries would influence local flow conditions especially in flooding situations and influence the spreading area of floodplain.

An additional survey of profiles which presents current conditions would enable a more precise statement about long term changings. Without this information no assessment of the channel bed can be done. A monitoring over several years would give the best conditions for identifying long term changes.

The dimension of an HN-model should be appropriate to the issue. For instance, the application of an 1D model for hydromorphological issues in meandering channels would provide insufficient results. Transversal velocities are not considered in a 1D model but have great impact to erosion processes. However, the data required for a 2D simulation and the effort which is connected to its collection have to be considered and set in relation to its outcome.

Finally, it can be said, that unless the modeler has a profound knowledge a hydrodynamic-numerical software definitely presents a perfect tool to improve the outcome of any river engineering project. To ensure reliable results of an HN-model the modeler has to have the knowledge about the theoretical basis on which the solver software is based on. Generation of a HN-model and the subsequent processing of results need a lot of experience in working with pre-and post-processing software. Nevertheless, the effort which is required has to be set in relation with the desired outcome.

This master thesis gives an inside view in working with hydraulic modelling software. Its results show the complexity of generating a suitable HN- model and gives an idea about the variety of potentials of improvement.

It should serve as an assistance for establishing hydrodynamic-numerical models and may set the modeler of future projects thinking about the importance of processes to improve quality of a model.

Bibliography

[1] H. Patt, P. Jürging und W. Kraus, Naturnaher Wasserbau-Entwicklung und Gestaltung von Fließgewässern, Springer Verlag, 2011.

[2] H. Mühlmann, Leitfaden zur hydromorphologischen Zustandserhebung von Fließgewässern, Vienna: Bundesministerium für Land- und Forstwirtschaft, Umwelt und Wasserwirtschaft, 2013.

[3] „Wasserwirtschaft Land Steiermark," [Online]. Available: http://www.wasserwirtschaft.steiermark.at/cms/ziel/4651916/DE/. [Zugriff am 1 August 2016].

[4] U. Maniak, Hydrologie und Wasserwirtschaft, Springer Verlag, 2010.

[5] H. Kulisch und A. Malcherek, „Experimentelle Hydromechanik," 02 August 2016. [Online]. Available: https://www.unibw.de.

[6] H. Patt und P. Gonsowski, Wasserbau - Grundlagen, Gestaltung von wasserbaulichen Bauwerken und Anlagen, Berlin: Springer Verlag, 2011.

[7] D. Biedenharn, R. Copeland, C. Thorne und R. Hey, „Effective Discharge Calculation: A Practical Guide," US Army Corps of Engineers, Washington, 2000.

[8] J. Miller und C. Kochel, „Assessment of channel dynamics, in-stream structures and post-project channel adjustments in North Carolina and its implications to effective stream restoration," *Environ Earth Science,* 2009.

[9] DVWK, Numerische Modelle von FLüssen, Seen und Küstengewässern, Bd. 127, Bonn: Wirtschafts- und Verlagsgesellschaft Gas und Wasser mbH, 1999.

[10] H. Herrmann und H. Bucksch, Dictionary Geotechnical Engineering, Berlin: Springer Verlag, 2013.

[11] H. Knoblauch und J. Schneider, „Fluss- und Sedimenthydraulik," Institute of Hydraulic Engineering and Water Resources Management, Graz, 2009.

[12] R. Fehr, „Geschiebeanalyse in Gebirgsflüssen," ETH Zürich, Zürich, 1987.

[13] H. Habersack, M. Tritthart, P. Lalk, F. Schöberl, M. Hengl, B. Huber, H. Knoblauch, D. Rieckenmann, B. Schober, M. Klösch, H. Gabriel, M. Haimann, M. Moser, U. Stephan, H. Badura, C. Hauer und N. Krouzecky, „Fließgewässermodellierung – Arbeitsbehelf Feststofftransport und Gewässermorphologie," Bundesministerium für Land- und Forstwirtschaft, Umwelt und Wasserwirtschaft, Österreichischer Wasser- und Abfallwirtschaftsverband, Vienna, 2011.

[14] C. Dorfmann und R. Fleißner, *BED LOAD ANALYZER - Referenzhandbuch,* Graz, 2013.

[15] AMT DER STEIRISCHEN LANDESREGIERUNG, „Sulm," AMT DER STEIRISCHEN LANDESREGIERUNG, Graz, 2016.

[16] H. Habersack, M. Hengl, H. Knoblauch, G. Reichel, P. Rutschmann, B. Sackl und M. Tritthart, Fließgewässermodellierung – Arbeitsbehelf Hydrodynamik, Wien: Bundesministerium für Land- und Forstwirtschaft, Umwelt und Wasserwirtschaft, Österreichischer Wasser- und Abfallwirtschaftsverband (ÖWAV), 2007.

[17] H. Martin, Numerische Strömungssimulation in der Hydrodynamik, Springer, 2011.

[18] S. Lecherler, Numerische Strömungssimulationen - 3.Auflage, Springer Verlag, 2014.

[19] R. ATA, C. Goeury und J. Hervouet, TELEMAC MODELLING SYSTEM - 2D hydrodynamics TELEMAC- 2D Software -Release 7.0 - USER MANUAL, EDF, 2014.

[20] „Hydrographischer Dienst Österreich," [Online]. Available: http://ehyd.gv.at/. [Zugriff am 11 08 2016].

[21] A. Eisner, Monitoring flussbaulicher Maßnahmen an der Sulm - Gewässerlebensraum und Fischfauna, Wien: Universität für Bodenkultur Wien, 2001.

[22] I. Novak, Monitoring von Hochwasserschutz- und Restrukturierungsmaßnahmen an der Sulm, Vienna: Universität für Bodenkultur Wien, 2003.

[23] Hydroconsult, „Technischer Bericht - Hochwasserabflussuntersuchungen Sonderprogramm 2005 -Teil 1 - Sulm - Laßnitz," Land der Steiermärkischen Landesregierung - FA 19A, Graz, 2006.

[24] L. S. -. A. d. s. Landesregierung, „Geoportal GIS Steiermark,“ [Online]. Available: http://www.gis.steiermark.at/. [Zugriff am 30 September 2016].

[25] Dittrich, „Hydraulische Belastbarkeit ingenieurbiologischer Bauweisen,“ 1995.

[26] L. Landesanstalt für Umweltschutz Baden-Württemberg, „Naturnahe Bauweisen im Wasserbau. Dokumentation und Bewertung am Pilotprojekt Enz / Pforzheim 1990-1995,“ Bd. 25, Nr. Handbuch Wasser, 1996.

[27] Gerstgraser, „The Stability of Engineering Biological Bank Stabilization Structure,“ Springer Verlag, Austria, 2000.

[28] D. Muschalla, „Hydrology,“ Institute of Urban Water Management and Landscape Engineering, Graz, 2015.

[29] P. Downs and G. Kondolf, "Post-Project Appraisals in Adaptive Management of River Channel Restoration," no. 29, 2002.

List of figures

List of tabels

Appendix

A

Attached are the shear stresses as they occur at MQ, HQ1, HQ5, HQ10 and HQ30.

Shear stress MQ

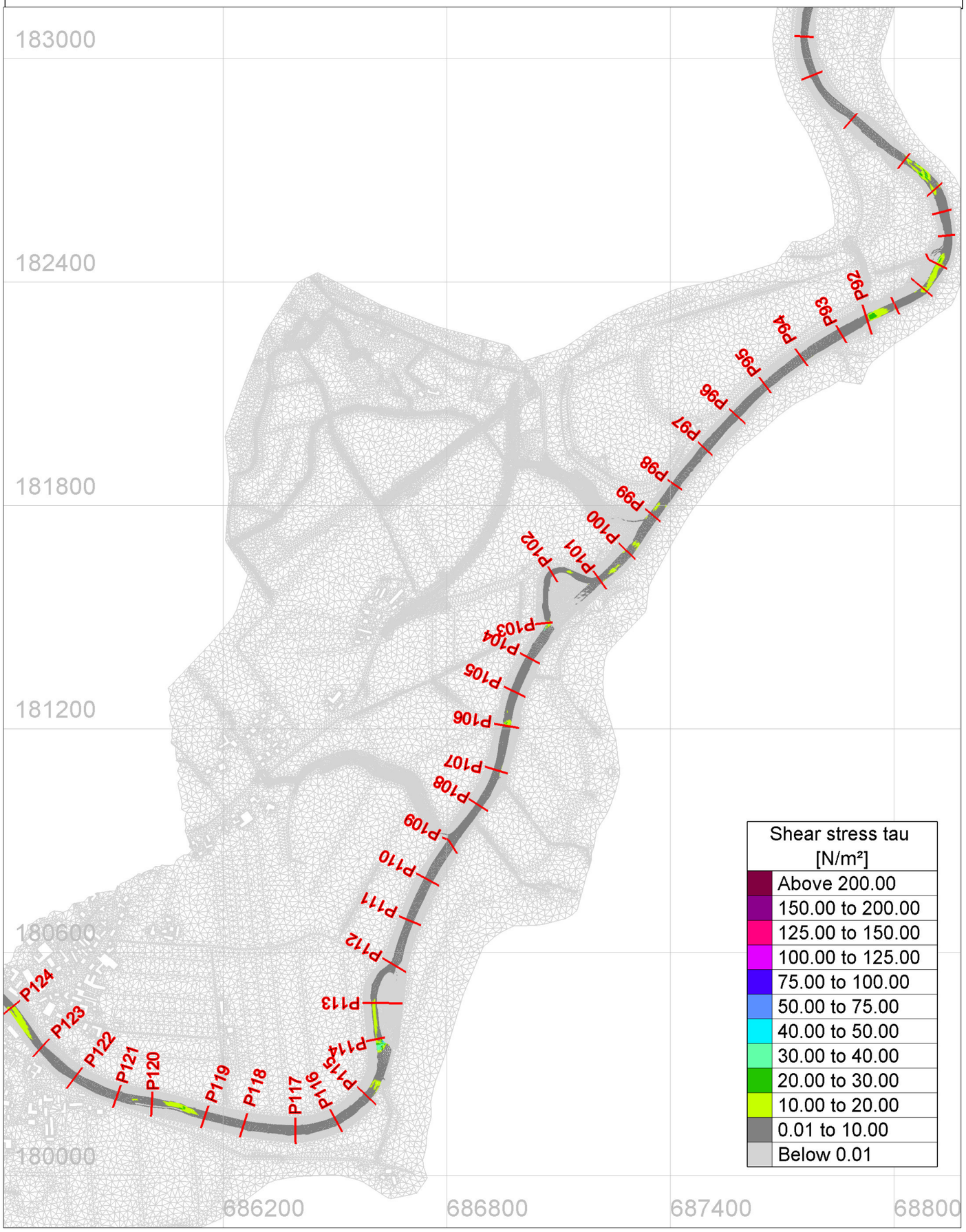

Shear stress HQ1

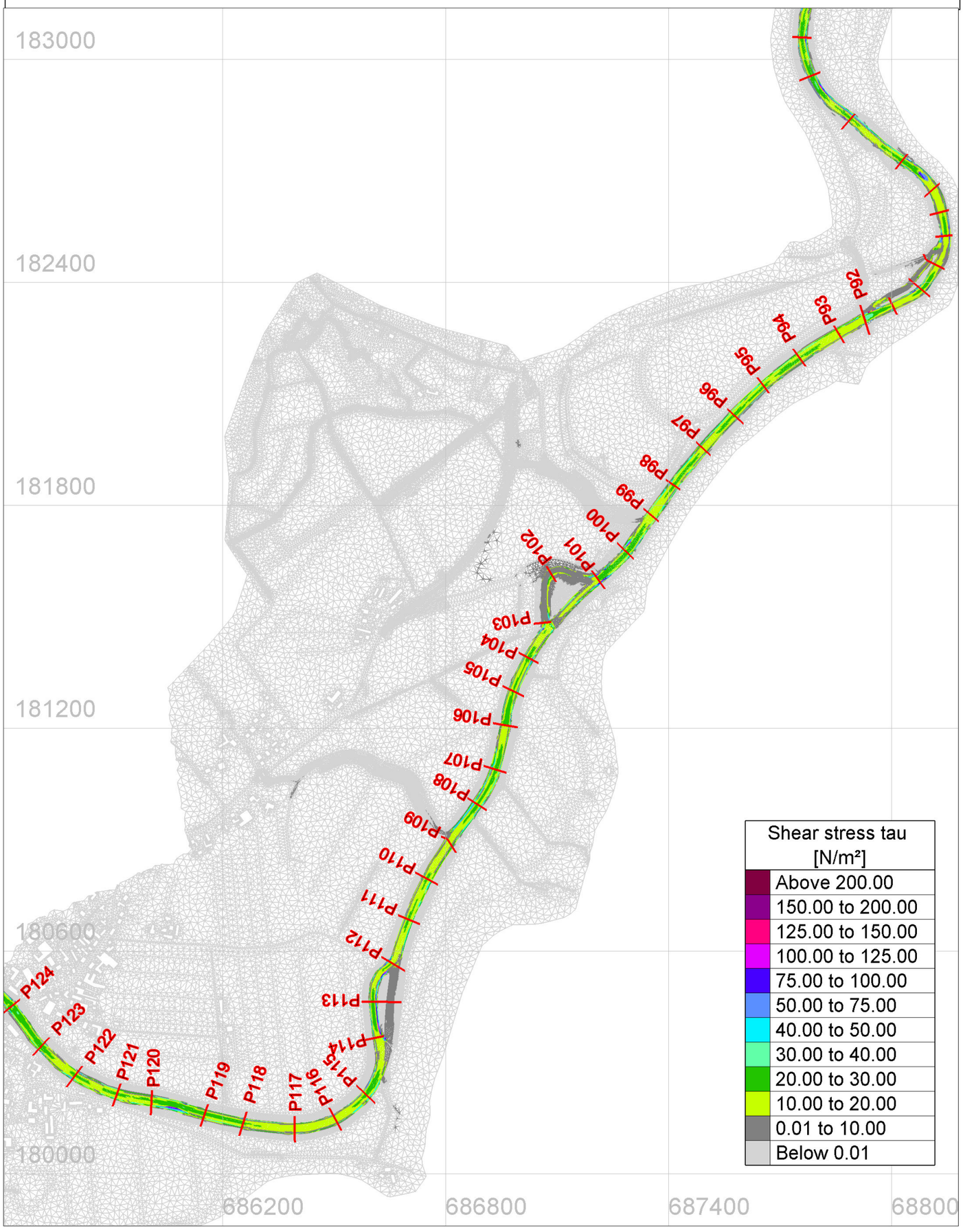

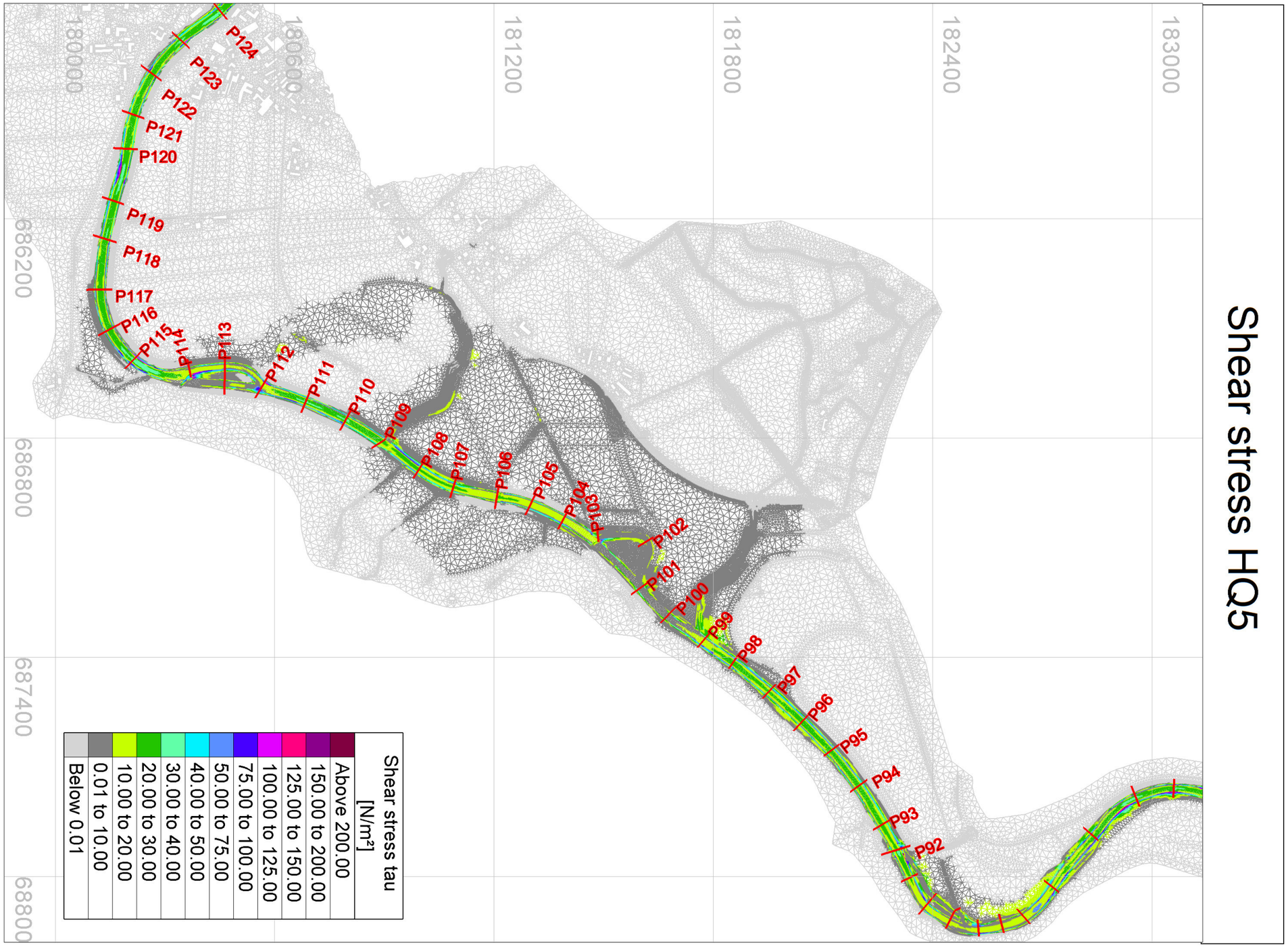
Shear stress HQ5
180000
180600
181200
181800
182400
183000
686200
686800
687400
688000
P124
P123
P122
P121
P120
P119
P118
P117
P116
P115
P114
P113
P112
P111
P110
P109
P108
P107
P106
P105
P104
P103
P102
P101
P100
P99
P98
P97
P96
P95
P94
P93
P92
Shear stress tau [N/m²]
Above 200.00
150.00 to 200.00
125.00 to 150.00
100.00 to 125.00
75.00 to 100.00
50.00 to 75.00
40.00 to 50.00
30.00 to 40.00
20.00 to 30.00
10.00 to 20.00
0.01 to 10.00
Below 0.01

Shear stress HQ10

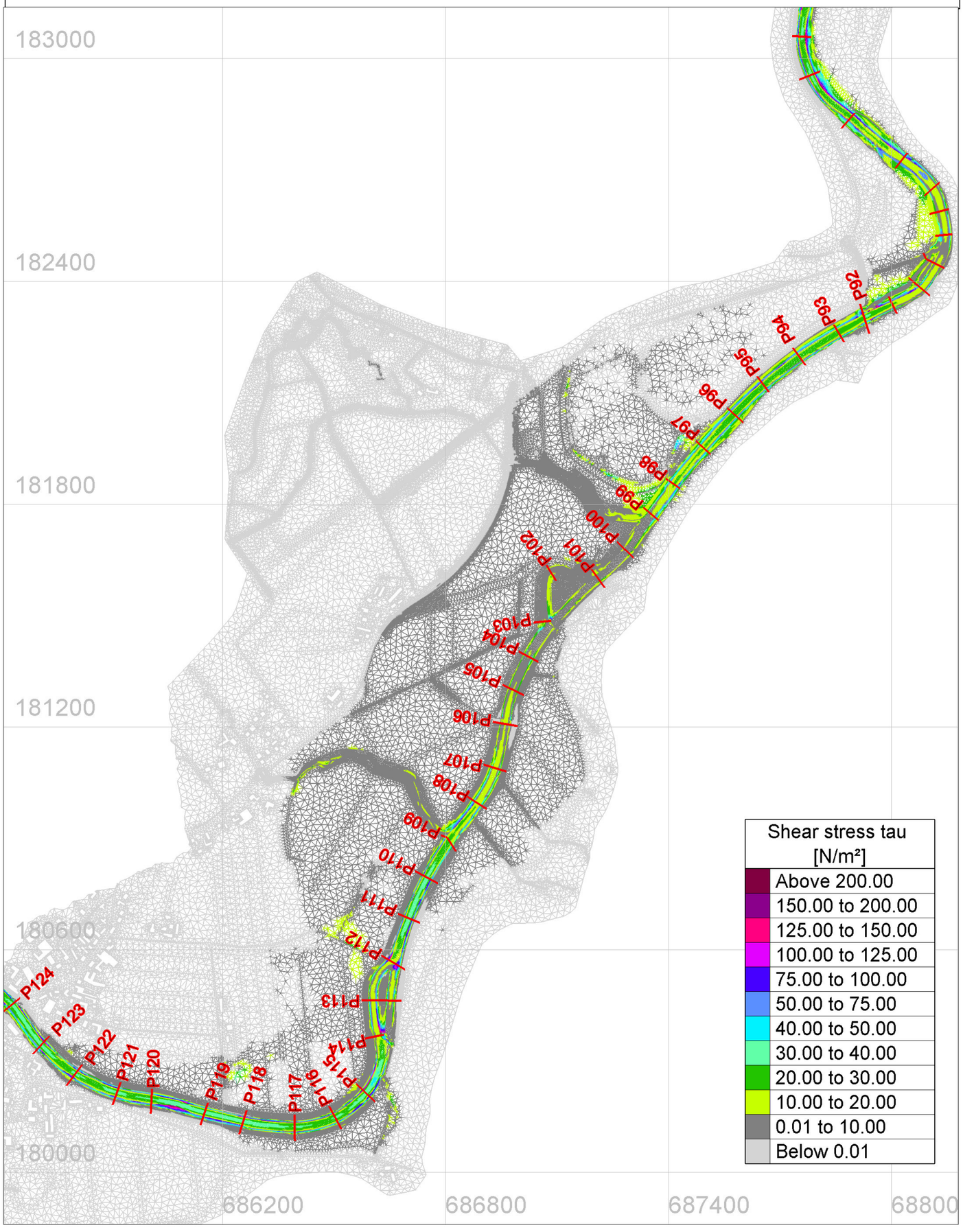

Shear stress HQ30

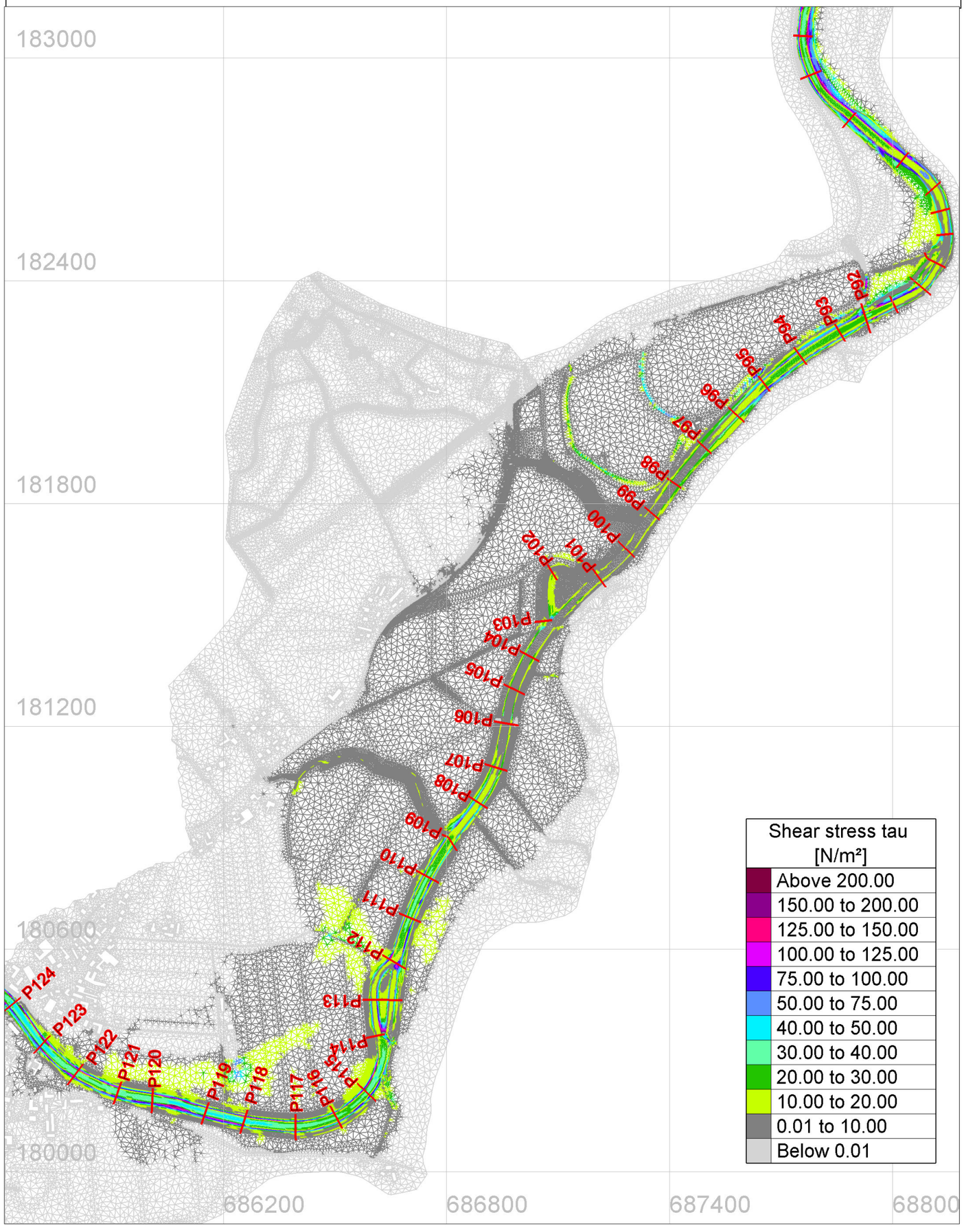

B

The enclosed CD contains all simulations used for the analysis. All results given in chapters 6.4 can get obtained from this CD and enable further processing.